

**Clonal Analysis of Growth Behaviors  
During *Drosophila* Larval Tracheal  
Development**

**Inauguraldissertation**

Zur

Erlangung der Wuerde eines Doktors der Philosophie

Vorgelegt der

Philosophisch-Naturwissenschaftlichen Fakultaeet

Der Universitaet Basel

Von

**Li Lin**

aus

Wuhan, Hubei

CHINA

Basel, Juni 2009

Genehmigt von der Philosophisch-Naturwissenschaftlichen Fakultät

Auf Antrag von

Prof. Dr. Markus Affolter (Dissertationsleiter)

Prof. Dr. Rolf Zeller (Koreferent)

Basel, den 26.05.09

Prof. Dr. Eberhard Parlow

(Dekan der Philosophisch-

Naturwissenschaftlichen Fakultät)



# Index

## Index

## Acknowledgements

## Summary

|  |           |
|--|-----------|
| <b>I. Introduction.....</b>  | <b>9</b>  |
| <b>1. Thoracic air sacs – an old structure newly discovered.....</b>                     | <b>12</b> |
| 1.1 Embryonic development of <i>Drosophila</i> tracheal system                           |           |
| 1.2 Discovery of thoracic air sacs   |           |
| 1.3 Discovery of “repopulation”  |           |
| 1.4 Development of thoracic air sacs during the 3 <sup>rd</sup> instar larval stage (L3) |           |
| <b>2. FGF signaling in development.....</b>  | <b>24</b> |
| 2.1 Overview of FGF signaling pathways   |           |
| 2.2 FGF signaling in animal development  |           |
| <b>3. Cell behaviors during development.....</b>   | <b>29</b> |
| 3.1 Overview: What does it take to make a multi-cellular embryo?                         |           |
| 3.2 Cell division: how is it regulated?  |           |
| 3.3 Cell migration   |           |
| 3.3.1 Overview of the migration process  |           |
| 3.3.2 Migration of an individual cell: Dictyostelium as a model for chemotaxis           |           |
| 3.3.3 Migration of a group of cells: Border cell migration                               |           |
| 3.3.4 Migration as a signaling-mediated morphogenetic process: Tracheal cell migration   |           |
| <b>4. Some techniques relevant for the thesis.....</b>                                   | <b>39</b> |
| 4.1 Creation of genetic mosaics  |           |
| 4.1.1 Conventional techniques  |           |
| 4.1.2 MARCM  |           |
| 4.2 Genetic screens  |           |
| 4.2.1 Traditional genetic screens  |           |
| 4.2.2 Clonal screens   |           |
| <b>5. Aim of the thesis.....</b>   | <b>48</b> |
| <br>   |           |
| <b>II. Materials and Methods.....</b>  | <b>49</b> |
| <b>1. Drosophila strains</b>   |           |
| <b>2. Generation of MARCM clones</b>   |           |
| <b>3. Larvae sorting and dissection</b>  |           |
| <b>4. Mapping of lethal mutations</b>  |           |
| <b>5. (Flip-Out) clonal analysis</b>   |           |

- 6. BrdU feeding and antibody staining
- 7. Slide preparation & imaging
- 8. Statistical analysis

**III. Results.....55**

**1. A MARCM-based screen aiming to identify genes functioning in the process of tracheal cell migration during ASP morphogenesis.....57**

- 1.1 Screening procedures
- 1.2 Summary of the screening outcome
- 1.3 Mapping and complementation analysis

**2. A MARCM-based approach of direct candidate-testing to identify genes functioning in the process of tracheal cell migration during ASP morphogenesis.....67**

- 2.1 An overview
- 2.2 *arp2/3*, *wasp*, and *scar* mutant clones
- 2.3 *ena* mutant clones
- 2.4 *diap1* mutant clones
- 2.5 *hrs* mutant clones
- 2.6 *mmp* mutant clones

**3. Clonal analysis of larval tracheal growth.....76**

- 3.1 Different tracheal metameres are differentially sensitive to heat shock
- 3.2 Non-synchronous mitotic behaviors of Tr2 cells during L3
- 3.3 Some Tr2 cells do not intermix, others do
- 3.4 *in vivo* tracking of the repopulation process

**4. Clonal analysis of ASP morphogenesis.....86**

- 4.1 ASP consists of two layers that are different in morphology and in mitotic activity
- 4.2 ASP lower layer grows through “cell replenishment” provided by ASP upper layer and neighboring TC/LB
- 4.3 Other possible behaviors involved during ASP morphogenesis: only guesses?

**IV. Discussion.....97**

**1. The genetic screen: did we find anything new and unexpected?.....98**

- 1.1 Cell division and cell migration: two inseparable shaping forces for ASP morphogenesis?
- 1.2 From cell signaling to cell skeleton: always the same story for cell migration?
- 1.3 Oriented cell divisions (OCDs): an alternative explanation for ASP morphogenesis?
- 1.4 What are the possible roles of FGF signaling during ASP morphogenesis?

**2. The approach of direct candidate-testing: oh, did not I know that already?.....103**

- 2.1 Redundancy: the best way to provide robustness?
- 2.2 *hrs* and *stam*: two pieces of the same puzzle?

**3. Clonal analysis.....106**

- 3.1 Origin of L3 mitotic cells in Tr2: new hope for regenerative medicine?
- 3.2 When do different metameres become different from each other?

3.3 What regulates the mitotic behaviors of Tr2 cells during larval stage?

3.4 Is Tr2 regionalized?

3.5 What cell behaviors are involved during ASP morphogenesis?

3.6 Open questions.

**V. Short description of other projects.....112**

**1. Purification of Bnl core domain for antibody production**

**2. Generation of Bnl-GFP for *in vivo* imaging of FGF-FGFR interaction**

**VI. References.....125**

**Curriculum Vitae**

**Publications**

## Acknowledgements

First of all, I would like to thank Markus, who gives me inspiration and keeps alive my dream to become a scientist. Without his understanding, support and toleration, this thesis would not have been born.

I would like to thank Dr. Kornberg for showing me the reality of working as a scientist and teaching me things more than merely how to do research.

I would like to thank people from the Affolter and the Kornberg lab. Without their help, I would not have grown professionally. Special thanks go to Clemens for getting me started as a Ph.D student, to Helene and Alain for beautifully finishing the screen after my departure, to Magda and Alexandru for careful proofreading of my thesis and for their constructive advices, to David Iwaki for his guidance during protein purification, and to Songmei Liu for leading me through some difficult periods.

I would like to thank Prof. Rolf Zeller for being willing to join my thesis committee.

My thanks also go to the interactive fly community, which has provided me with necessary fly strains over the entire course of my Ph.D.

My appreciation goes to my friends all over the world, without whose company I would never have travelled this far.

Finally, my gratitude goes to my family, in China and in Germany. Without it, life would not be worth living.

## Summary

The discovery of the *de novo* formation of a tracheal structure, air sac primordium (ASP), in the second thoracic tracheal metamere (Tr2) during the 3<sup>rd</sup> instar larval stage (L3), challenged the assumption that the tracheal system established during embryogenesis would remain more or less unchanged until the onset of metamorphosis. ASP formation has since provided a novel system for studying cell behaviors such as cell migration.

For ASP to form properly, it was then discovered, a process called “repopulation”, during which the composition of Tr2 changes dramatically, from the initial 20 or so cells containing bigger nuclei at early L3 to about 500 cells containing smaller nuclei at late L3, had to take place. Two models were proposed to explain how repopulation could happen. In the “replacement” model, larval tracheal cells, presumed to be terminally differentiated, endo-replicated, and incapable of dividing, would get replaced by a distinct population of mitotically active cells, the so-called “tracheoblasts”. In the “de-differentiation” model, these presumably polyploid larval tracheal cells would somehow manage to re-enter mitosis, reduce their ploidy, and produce mitotically active offspring.

Using ASP morphogenesis as a model system, we performed a clonal screen to find genes important for FGF-mediated cell migration. This screen identified two major groups of genes. One group is important for cell migration, such as *myosin heavy chain* (*mhc*) and *signal transducing adaptor molecule* (*stam*); the other group is necessary for cell division.

To uncover the origin of mitotic cells repopulating Tr2 during L3, we designed an *in vivo* clonal analysis for cell-tracking. It turned out that the “de-differentiation” model contained more grains of truth. Tr2 larval cells, possibly arrested in cell cycle prior to L3, resume cell cycle progression during L3 and give rise to mitotically competent progenies.

To understand how mitotic behaviors of Tr2 cells are regulated during L3, a clonal analysis using flip-out clones was performed, which resulted in a descriptive report of the mitotic behaviors of Tr2 tracheal cells during L3. Although signals releasing Tr2 cells from cell cycle arrest and/or maintaining their proliferative state remain currently elusive, our analysis provides an assay for testing candidates likely involved. Some other interesting findings have also been revealed by this analysis, such as the existence of “regionalization” between different Tr2 branches and “cell replenishment” during ASP growth.

It has gradually become clear that *Drosophila* tracheal system, an old model for studying tubulogenesis, proves to be a new tool for generating insights into fundamental questions such as how *hox* genes function, how cell cycles are developmentally controlled, how signaling pathways can be functionally dissected, and how variegated behaviors cells employ for the purpose of constructing a functional organ.



# I. Introduction





Source: [http://image.poco.cn/photo/20060711/874515020060711223416\\_2\\_120.jpg](http://image.poco.cn/photo/20060711/874515020060711223416_2_120.jpg);

[http://www.geocities.com/kishan\\_nie/photos/butterfly1.jpg](http://www.geocities.com/kishan_nie/photos/butterfly1.jpg)

### ***Which came first, chicken or egg?***

Have you ever felt struck with awe at the sight of grass growing from below a thick paving slate? What strength of life, you may wonder, has enabled the feeble grass, during its strenuous struggle out into the sun, to crack the solid slate into pieces!

Have you ever sensed a serene amazement in yourself at seeing how elegantly a delicate butterfly perches in the wind? How much lifeblood, you may question, has Mother Nature put into designing the heavenly beauty of this little creature!

What is life?

How do patterns form?

These are only two of the many questions that have long fascinated developmental biologists. Developmental biology is a discipline studying the construction of organisms; it strives to understand how an entire, complex animal can develop from a single fertilized egg; it is a science of becoming, a science of process.

To discover Mother Nature's hidden secrets, to appreciate deeper the beauty of life, to achieve something meaningful and extraordinary—this is why I embarked on the following Ph.D journey...

### 1.1 Embryonic development of *Drosophila* tracheal system

As a counterpart of the human lung, *Drosophila* larval tracheal system, forming during embryogenesis, consists of an inter-connected epithelial tubular network extending from the anterior end of the organism to the posterior, providing the entire body with gases. Air enters this network through spiracles, specialized openings at both ends of the body, disperses into all branches, and reaches narrow capillary-like tubules with blind ends, where extensive gas exchange takes place with the surrounding target tissues.

After over a decade of continuous research effort made by labs all over the world, a coherent molecular picture of how this respiratory organ forms starts to emerge, although many questions still remain to be answered. In summary, the sequential processes of embryonic tracheal morphogenesis can be divided into the following steps:

Determination of tracheal cell fate.

Histologically, tracheal cell specification takes place during stage 10 (4:20-5:30 hr after egg lay, AEL). At this stage, tracheal primordia become recognizable, on each side of the embryo, as ten ectodermal placodes, which are slightly thickened regions of the epithelium with shallow central depressions, composed of slender, tightly packed columnar cells (Poulson 1950; Campos-Ortega and Hartenstein, 1985). During stage 10 and early stage 11 (5:20-7:20 AEL), tracheal precursor cells undergo their 15th (just prior to invagination) and 16th/final (while the cells are invaginating) cell divisions during embryogenesis. Afterwards, there are about 80 cells in each tracheal metamere 2, and 4 to 10 (Tr2, Tr4-Tr10), and roughly 150 cells in Tr1 and 50 cells in Tr3 (Manning and Krasnow, 1993; Samakovlis et al., 1996). At the molecular level, tracheal cell identity is determined by direct cooperative action of at least two transcription factors: Tracheless (Trh), a basic helix-loop-helix (bHLH)-PAS domain protein (Isaac and Andrew, 1996; Wilk et al., 2000); and Ventral veinless (Vvl, also called Drifter), a POU-domain containing DNA binding protein (Anderson et al., 1995; de Celis et al., 1995).

Invagination of tracheal placodes.

Tracheal primordia/placodes localized in the ectodermal epithelium invaginate to form tracheal sacs. During the process of invagination, tracheal cells internalize by an apical constriction mechanism, wherein the randomly positioned nuclei move to a basal position and the apical domains constrict to create wedge-shaped cells, a shape change likely contributing to the forces driving internalization. Apical constriction is observed in the dorsomedial region of the placode, where cells start to invaginate until all Trh-positive cells are internalized. Trh activates the expression of Rho,

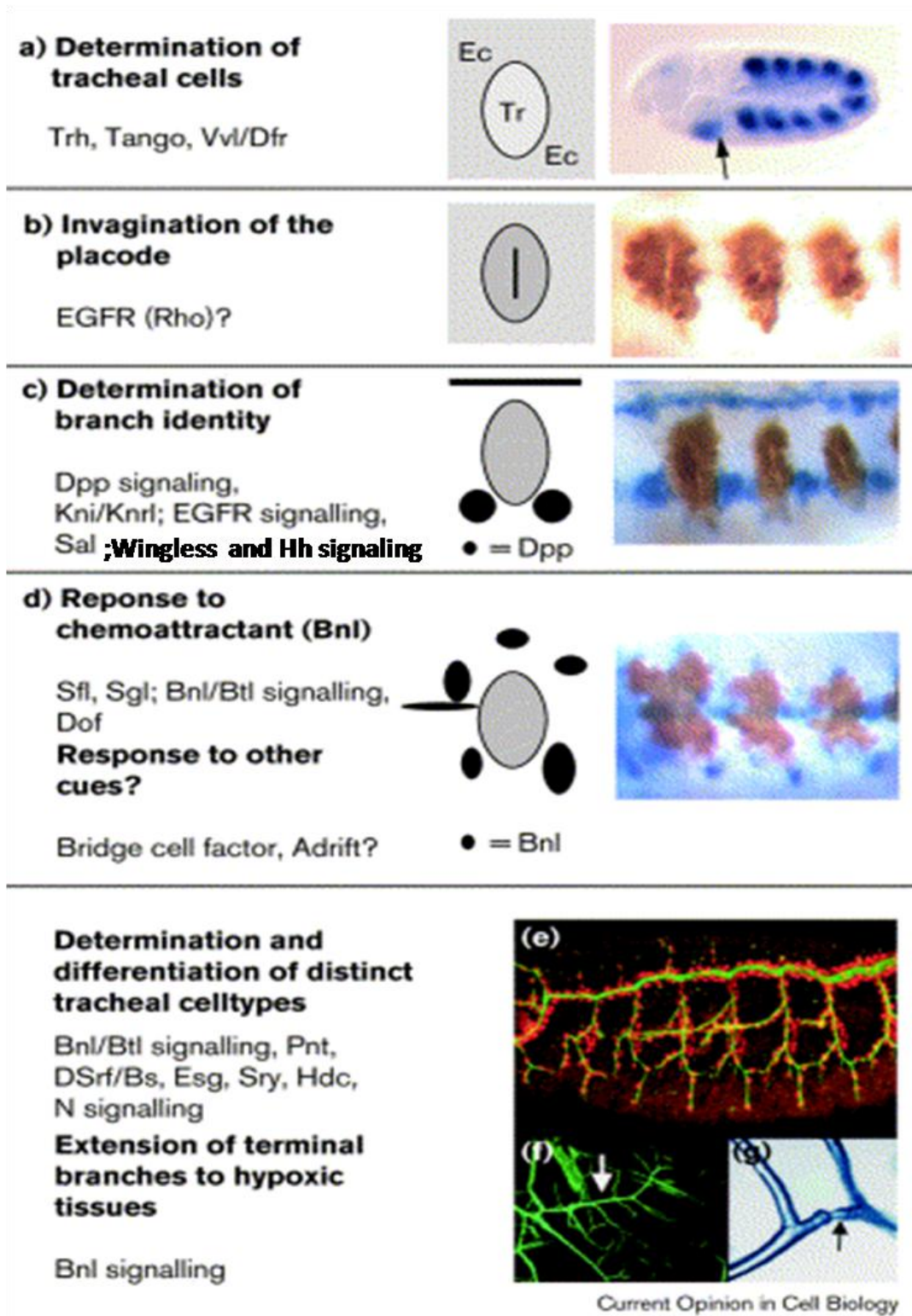


**Figure I1.** Sequential steps during embryonic tracheal morphogenesis. Modified from Affolter M, and Shilo BZ (2000).

which cleaves and activates the EGF ligand Spitz (Llimargas and Casanova, 1999). Spitz, in turn, activates EGFR signaling, which is required for invagination to take place. In *egfr* mutant embryos, the prospective tracheal cells fail to concentrate F-actin at the constriction site (Brodu and Casanova, 2006), and the invagination is partially defective (Llimargas and Casanova, 1999).

Allocation of branch identities.

Different signaling molecules such as Dpp (Vincent et al., 1997), Rho (Wrappner et al., 1997), Wingless (Wg), and Hedgehog (Hh, Glazer and Shilo, 1997) have been reported to be expressed in their own distinct and localized manner, leading to a local “regionalization” of the tracheal pit prior to the process of primary branch formation. Dpp is expressed in ectodermal stripes dorsal and ventral to the tracheal placode, setting up regional identities in the dorsal and ventral parts of the placode that will give rise to the formation of dorsal branch (DB), lateral trunk anterior (LTa), and lateral trunk posterior/ganglionic branch (LTP/GB). Rho and Wg, expressed in the central part of the placode, establish the domain which will become dorsal trunk (DT) and visceral branch (VB). Hh, secreted by cells just anterior to the placode, induces a change in gene expression along the anterior-posterior (A-P) axis. These different signaling pathways lead tracheal precursor cells down to different differentiation avenues, manifested by branch-specific expression of transcription factors. Dpp signaling is required in DB, LTa, and LTP/GB, and its activity leads to the activation of transcription factors Knirps (Kni) and Knirps related (Knrl) in the responding tracheal cells (Chen et al., 1998). Activation of EGF signaling by Rho expression enables tracheal cells to invaginate and ensures the proper development of DT and VB. The properties distinguishing DT from VB is conferred by Wg signaling, which specifies DT cell fates. The activation of a transcription factor Spalt major (Salm) is achieved through both EGF and Wg signaling, and is repressed by the presence of Kni and Knrl, which are activated by Dpp activity.

Formation of primary branches by FGF/Branchless (Bnl)-induced cell migration.

Following the local “regionalization” and branch identity specialization in the tracheal placode, tracheal cells initiate an extraordinary morphogenetic program, which lead to the formation of an intricate tracheal network. This morphogenetic program is characterized by Bnl/FGF-directed cell migration in the absence of any proliferation. A more detailed description will be provided later in this thesis.

Later events, such as secondary branching, branch fusion and terminal branching, finally creates the intricately connected structure of larval tracheal system.

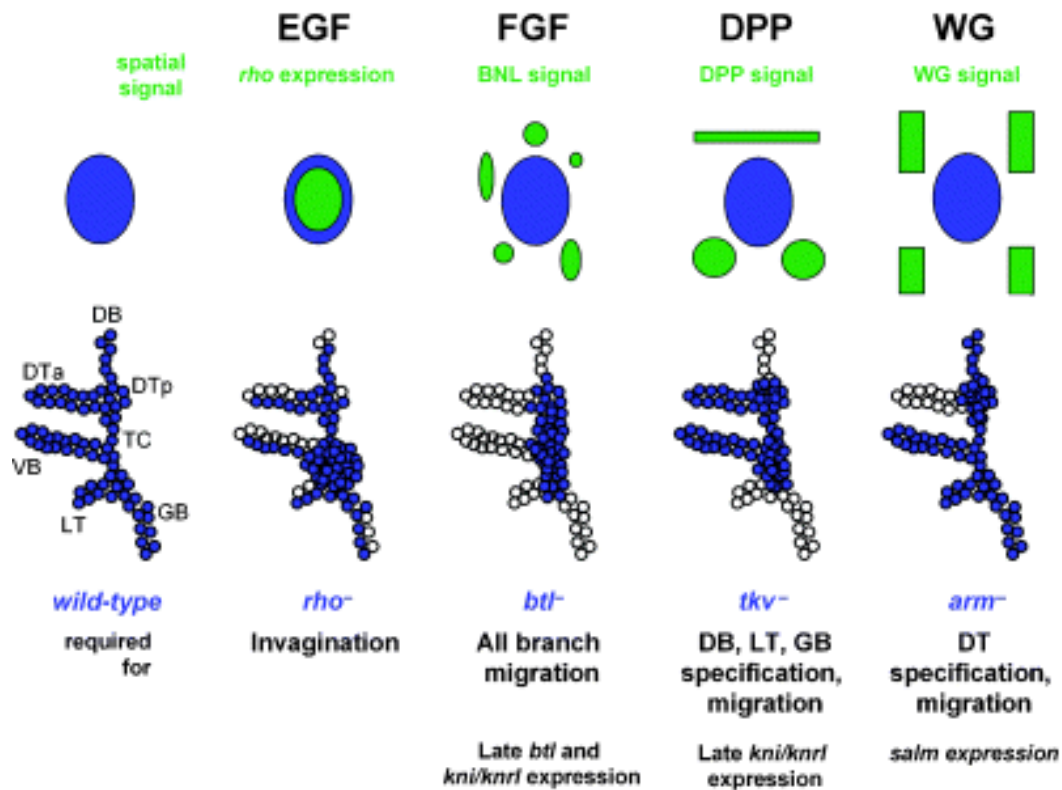


**Figure 12.** Local “regionalization” of the tracheal placode by different signaling pathways (see the main text) prior to the formation of primary branches, which endows different (future) branches with their distinct identities and ensures their proper, subsequent migration. (Adapted from Kerman B. et al., 2006).

## 1.2 Discovery of thoracic air sacs

The age of research on air sac primordium (ASP) started in 2002 with the publication of a paper in *Developmental Cell* titled „FGF is an essential mitogen and chemoattractant for the air sacs of the *Drosophila* tracheal system“ (Sato and Kornberg, 2002). In this paper, the *de novo* formation of *Drosophila* air sacs associated with wing imaginal discs was discovered and reported for the very first time, even if the structure itself, later on coined as ASP, was as ancient as other parts of the fly that had been observed earlier.

The discovery of thoracic air sacs illustrates an excellent example of „serendipity“ in science: something interesting gets found when it is not at all looked for. It started with an inquiry into the question of what role FGF could possibly play during the imaginal wing disc development. Sato began tackling this question by looking at the expression patterns of Bnl, the FGF ligand in *Drosophila*, and of Breathless (Btl) and Heartless (Htl), two FGF receptors that had thusfar been identified. To his surprise, he observed *btl*-expressing cells



in the adepthelial layer of the wing disc notum, which had not been identified previously. Sato didn't know he was „staring“ at tracheal cells, since these *btl*-expressing cells appeared not to be associated with tubules containing cuticle-lined lumen. Nevertheless, these cells did seem to maintain continuity with cells of the main tracheal branch attached to the wing disc notum.

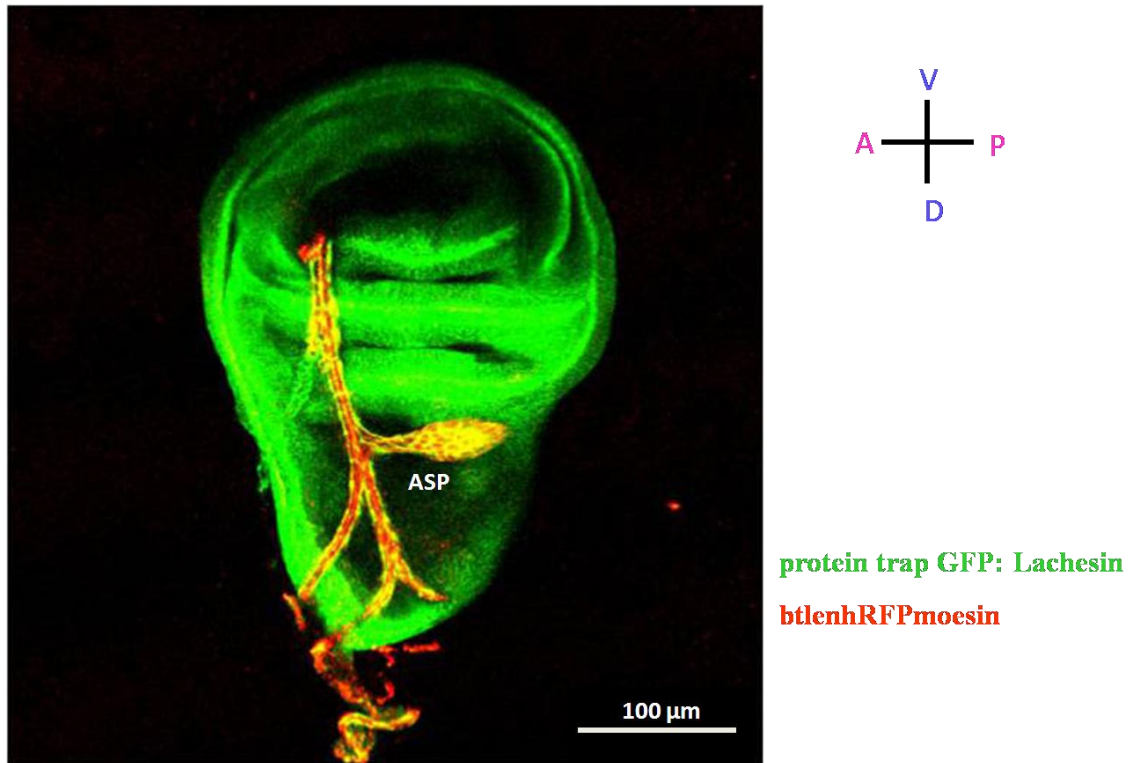


**Figure I3.** An example of ASP in late 3rd *instar* larval stage (L3). It remains associated with the wing imaginal disc throughout the L3 development.

To better understand the origin and fate of the *btl*-expressing adepthelial cells, Sato tracked them during larval and pupal development. In early 3rd *instar* wing discs, no *btl* expression was detected in adepthelial cells and only the major tracheal branch cells were *btl* positive. As 3rd *instar* discs matured, however, *btl*-positive cells were detected to bud from the major wing disc-associated tracheal branch, transcerse connective (TC). This bud structure continued to grow and expanded posteriorly toward the region of greatest *bnl* expression, with *btl*-expressing cells increasing in number due to cell proliferation. These *btl*-positive cells were followed into pupal stage and were seen to migrate dorsally between 12 and 23 hours after puparium formation (APF). After the dorsal migration, *btl*-positive cells then migrated anteriorly and posteriorly, forming three branches termed lateroscutal sac (l), medioscutal sac (m) and scutellar sac (s), respectively. At 32 hours APF, these cells ceased migration and began to elaborate into air sacs.



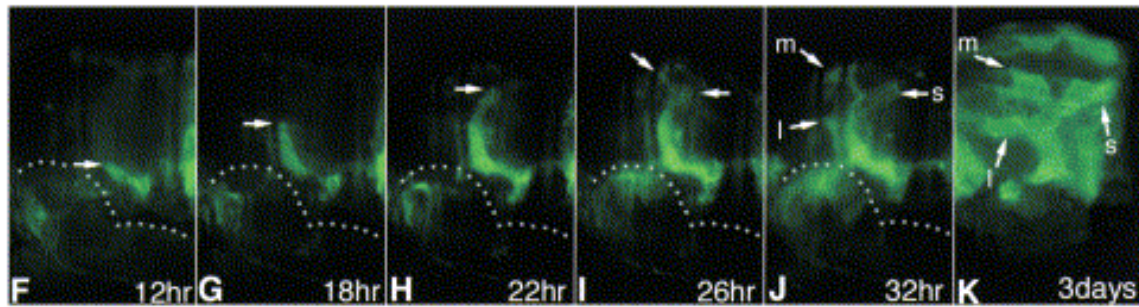


**Figure 14.** Air sac development during the pupal stage. The time labeled refers to after puparium formation (APF). “l” stands for lateroscutal sac, “m” for medioscutal sac, and “s” for scutellar sac. (Adapted from Sato and Kornberg, 2002)

In this paper, it was proposed that FGF signaling played multiple roles during the *de novo* formation of ASP, necessary for cell de-differentiation, cell migration and cell proliferation.

It was shown that ectopic Bnl/FGF expression was sufficient to induce *btl*-positive cells (tracheoblasts) to migrate and cells capable of responding to Bnl/FGF were not uniquely positioned at the site where ASP would normally bud out, suggesting a broad distribution of FGF-responsive cells. Based on these observations, FGF was proposed to function as an inducer of „de-differentiation“, since it could drive polyploid, terminally differentiated tracheal cells into proliferation and morphogenesis.

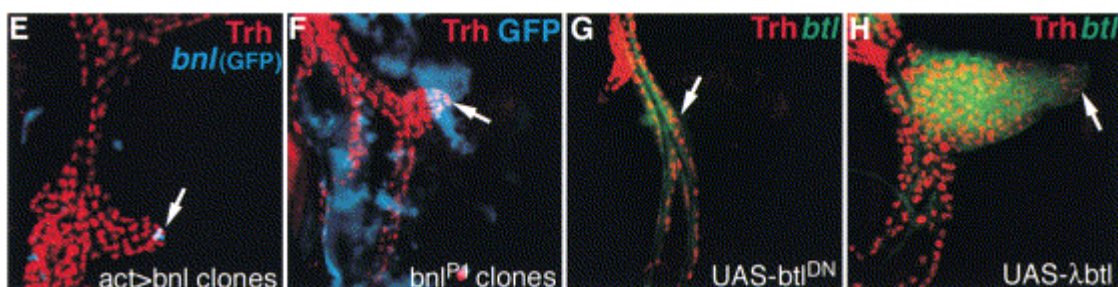


**Figure 15.** Data indicating possible functions of FGF in multiple processes during ASP formation: cell de-differentiation, cell migration and cell proliferation (see text). (Adapted from Sato and Kornberg, 2002)

It was observed that tracheoblast migration was significantly reduced in wing discs with large *bnl* clones. Over-expression of a dominant-negative form of Btl (Btl<sup>DN</sup>) under the control of *btl*-Gal4 reduced tracheoblast migration. Combined with the results of ectopic

Bnl/FGF expression experiment, FGF was proposed to be both necessary and sufficient for directed tracheoblast migration.

It was also observed that over-expression of a constitutively active form of Btl ( $\lambda$ Btl) under the control of *btl*-Gal4 caused a significant increase in the number of tracheoblasts. In the contrast, reduction of FGF signaling (by over-expressing Btl<sup>DN</sup> with *btl*-Gal4) decreased the number of tracheoblasts. So, FGF was proposed to function as a mitogen.

### 1.3 Discovery of “repopulation”

Repopulation, the next important finding in the field of ASP research following its initial discovery, was presented in 2005 in a paper titled “Tracheal branch repopulation precedes induction of the *Drosophila* dorsal air sac primordium”, published in *Developmental Biology* (Guha and Kornberg, 2005).

Simply put, “repopulation” describes the process during which the cell composition of the second tracheal metamere (Tr2) changes, from around a few dozens of cells bearing big nuclei at 0-2 hours after 3rd *instar* molt (0-2 L3) into hundreds of cells bearing smaller nuclei 48 hours later (48-50L3). During the same time window, cells in the neighboring Tr3 remain more or less unchanged.

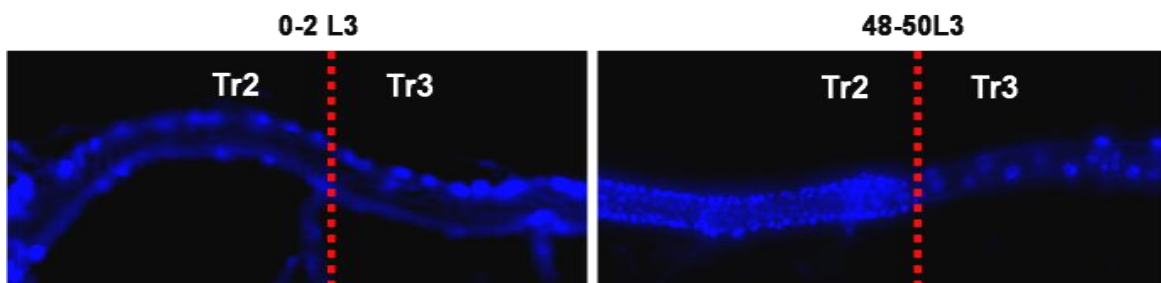


**Figure 16.** Pictures depicting the process of “repopulation” during L3, which takes place in Tr2 and not in Tr3.

Repopulation was also discovered by chance. In an effort aiming to identify the cells giving rise to ASP, Guha decided to determine the cell composition and dynamics of cell proliferation in the larval tracheae during L3. Unexpectedly, he found that Tr2 was unique in having only small nuclei (8-10  $\mu$ m in diameter) throughout the metamere (except for the VB), whereas most of tracheal branches in other metameres were populated by cells having large nuclei (15-20  $\mu$ m in diameter).

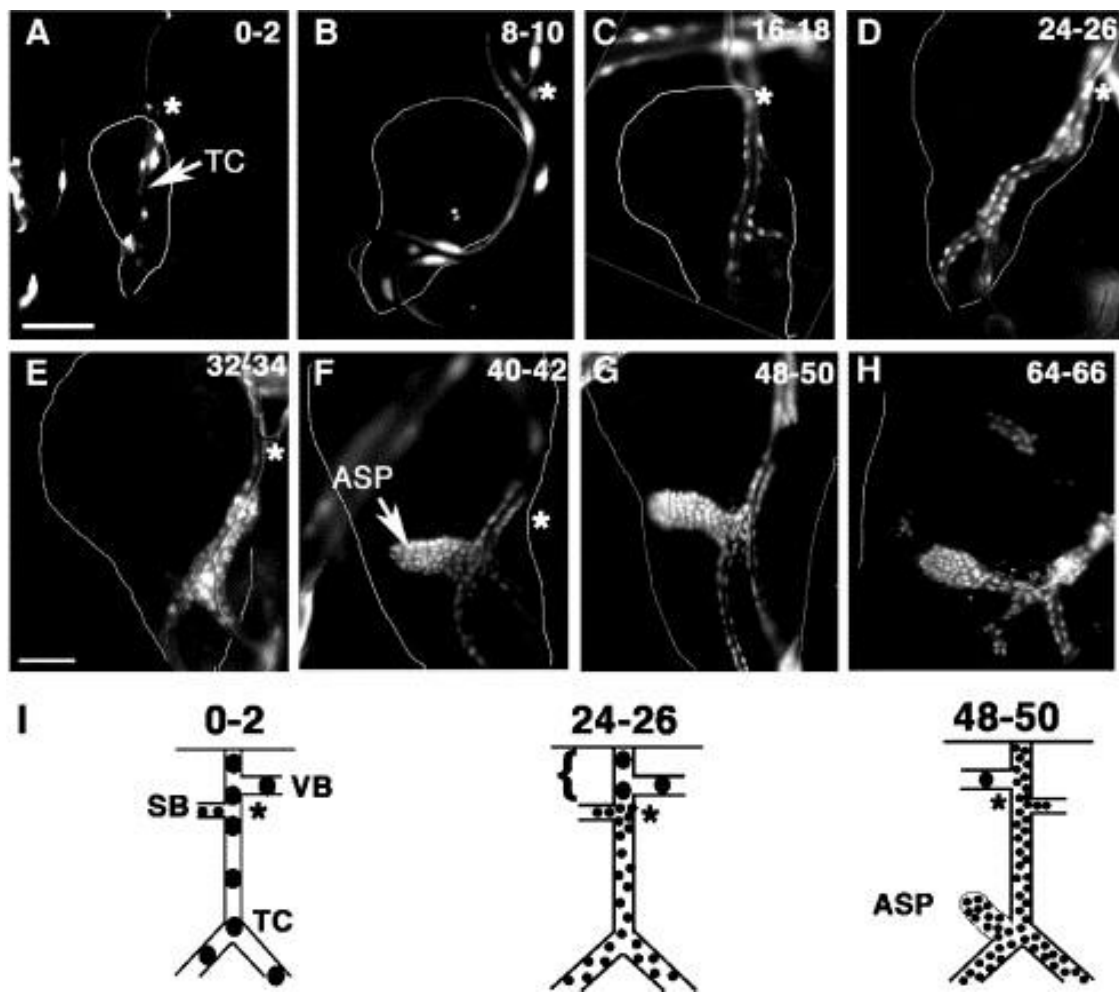


**Figure 17.** Repopulation of transverse connective (TC) in Tr2 during the 3rd *instar* period (L3). Cell composition starts to change at about 16-18 L3, as shown in C, which precedes the onset of ASP morphogenesis around 40-42 L3, as shown in F. See main text for detailed description. (Adapted from Guha and Kornberg, 2005)

To explore the origin of the unique Tr2 composition, the distribution of nuclei in larvae at selected developmental stages were examined. Nuclear GFP (nls-GFP) was expressed under the control of *bt/Gal4*. In 2nd *instar* (L2) larvae and 0-2 L3 larvae, a few dozens of cells could be observed throughout Tr2. At 24-26 L3, the transverse connective (TC) acquired a speckled appearance with many small nuclei distributed at regular intervals along its length. The density of small nuclei continued to increase over the next 16 hours. The dorsal-most region of the TC (close to its junction with the DT) became filled at a later time than the rest of the branch and was not completely filled until about 48-50 L3.

Other Tr2 branches underwent similar transformations during L3, although the timing varied. Whereas repopulation of the dorsal branch was at roughly the same stage as the

TC, small nuclei didn't colonize the DT until later in L3. The first signs of ASP growth became evident at 40-42 L3, and ASP continued to grow over the course of the ensuing 24 hours.

Two models were proposed for explaining the widespread distribution of proliferating cells in Tr2 trachea during L3. The first stated that the tracheal branches were repopulated by a set of mitotically active cells that were distinct from the larval cells comprising these branches. The second stated that the mitotic cells were descendents of the larval cells. The second model was considered to be unlikely, since terminally differentiated, endoreplicating larval cells had not been known in *Drosophila* to re-initiate a mitotic program.

Interestingly, Ubx, the product of a homeotic selector gene, was found to be dispensable in the Tr2 for the process of repopulation. Instead, Ubx function was required in the Tr3 to delay the replacement of its larval cells. In *ubx* mutants, repopulation would then take place in the Tr3 as well, as if it were the Tr2. These findings indicated that the contrasting behaviors of Tr2 and Tr3 cells in the wild type was a consequence of their intrinsic differences established by homeotic genes such as *ubx*.

#### **1.4 Development of thoracic air sacs during the 3rd *instar* larval (L3) stage**

Morphogenetically, development of thoracic air sacs during 3rd *instar* larval stage (L3) can be roughly divided into three steps: budding, directional growth, and stalk formation (See Figure 18).

Prior to the initiation of the budding process, the transverse connective (TC) has a bare appearance. At around 40 hours into the L3 molt, a regional proliferation of tracheal cells can be observed at, or very close to, the branching point of LTa and LTp, leading to the formation of a bud-like structure. This budding process is very likely FGF-dependent, for expressing the dominant-negative form of Btl (Btl<sup>DN</sup>) under *btl*-Gal4 control could completely abolish the bud formation (Sato and Kornberg, 2002). In addition, the budding site is often found at the site closest to the FGF/Bnl source. The budding stage appears to be purely a proliferative phase during which tracheal cells undergo non-directional mitoses, resulting a bulge-like structure showing no clearly visible "leading front".

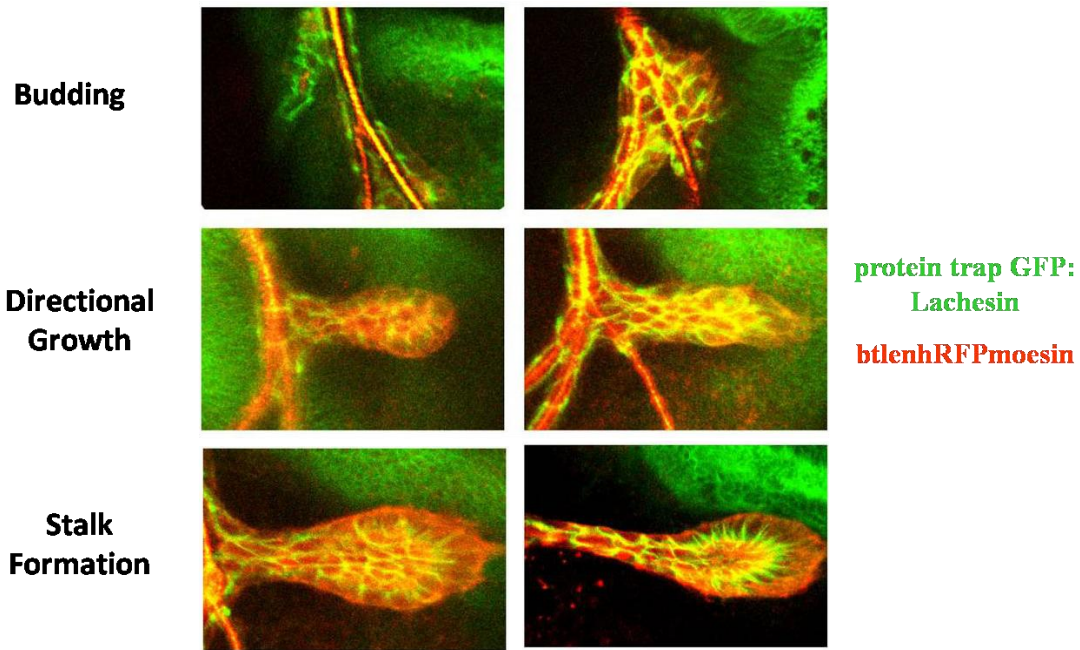


**Figure 18.** Three stages of ASP formation during 3rd *instar* larval stage: budding, directional growth and stalk formation.

Under the guidance of FGF/Bnl, the bulge-like non-polarized bud develops into a rod-like structure with an easily recognizable tip, showing directional growth reaching towards the source of FGF/Bnl (See Figure 19 for *FGF/bnl* expression pattern). It has been proposed that cell migration under the guidance of FGF operates during this stage of growth, and clonal cells mutant for *FGFR/btl* or its downstream effector *dof* (*d*ownstream *o*f *E*GF) were found to be always localized at the back of the ASP, losing out in competition for “leadship” to their wild-type counterparts (Cabernard and Affolter, 2005).

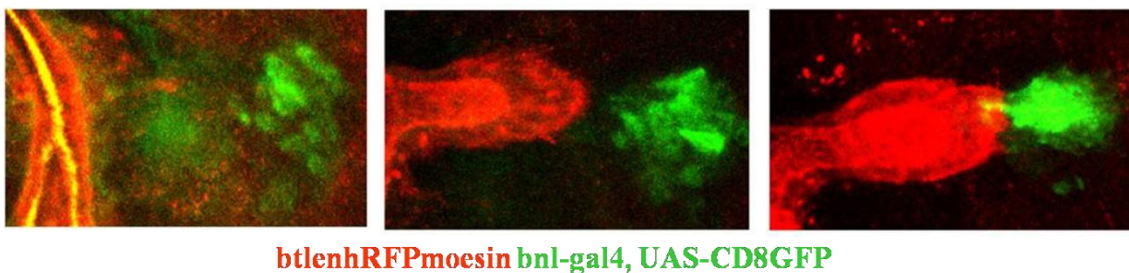


**Figure 19.** Expression pattern of *Drosophila fgf/bnl* (in green) and the relative position of *btl*-expressing tracheal cells (in red) to the FGF/Bnl source during ASP morphogenesis.



As ASP continues to grow in size and more posteriorly (relative to the associated wing disc), cells located most proximal to the budding site appears to stop proliferation and undergo a dramatic morphogenetic change, leading to the formation of a stalk-like

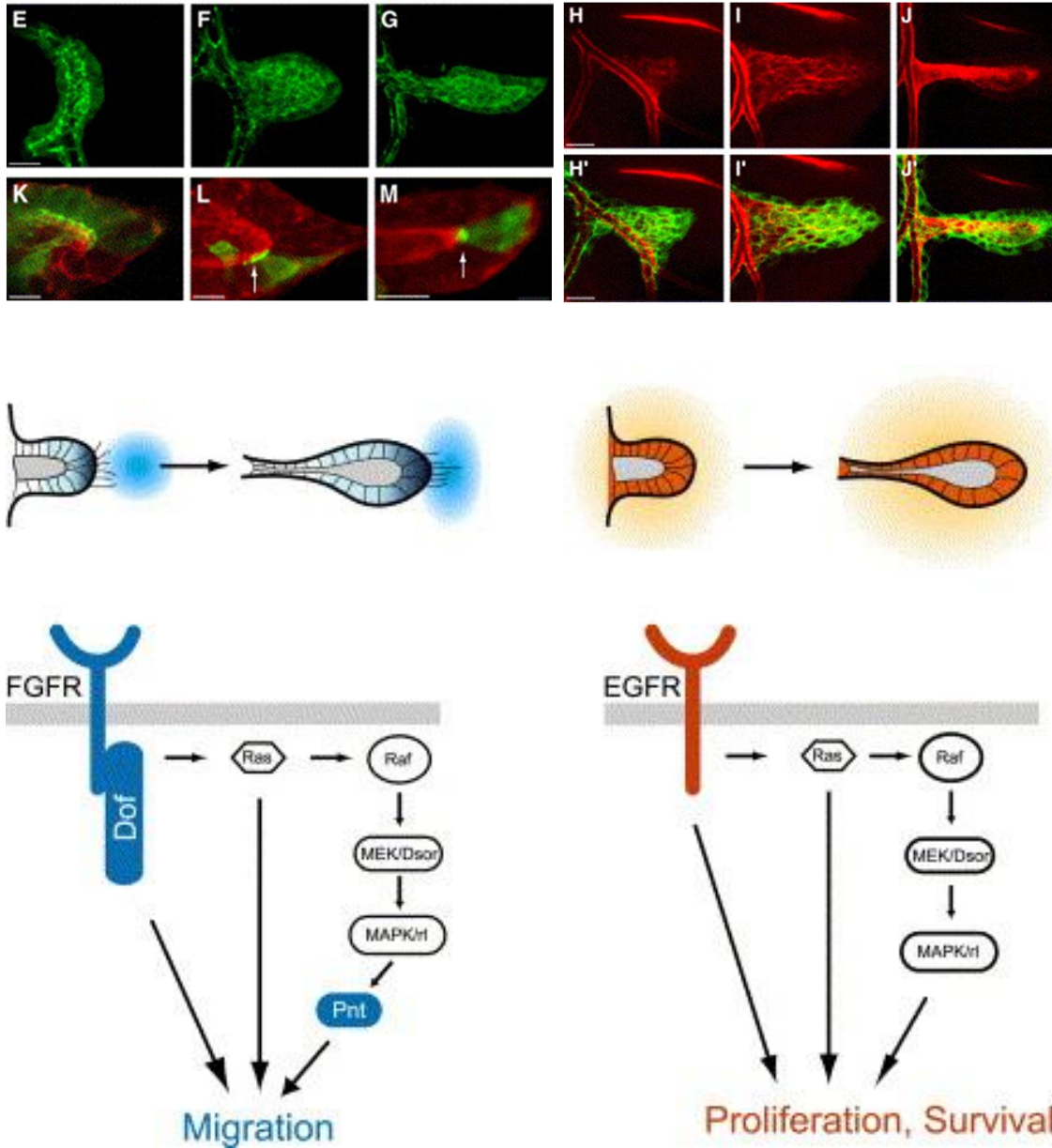


**Figure I10.** The epithelial nature of ASP and the model of distinct roles played by FGF and EGF signaling pathways. On the top panel, the epithelial nature of ASP was demonstrated by labeling adherens junctions (AJs) in green (E, F, G) and by flip-out clones (K, L, M.). ASP lumen was shown by antibody staining of a luminal protein Piopio (Pio) in red (H, I, J). In the bottom panel, a model was presented to propose that FGF signaling directed cell migration at the tip of the structure, whereas EGF signaling was essential for cell division and cell survival in the growing epithelial structure. (Adapted from Cabernard and Affolter, 2005).

structure narrower than the more distal part of the ASP. This stalk formation could possibly be a planar cell polarity (PCP) phenomenon, although definitive evidence is still lacking.

As has been beautifully shown, ASP consists of a tube containing a well-defined lumen surrounded by a single-cell-layered epithelium (Cabernard and Affolter, 2005). As presented in Figure 10, the epithelial nature of ASP could be demonstrated to be present very early on, during the budding step of ASP morphogenesis, as revealed by *bt*/Gal4-driven UAS-D $\alpha$ -cat-GFP, a fusion protein that specifically labels adherens junctions (AJs). Single-celled flip-out clones were generated to show that the epithelium enclosing the lumen was only one cell thick and the fusion protein D $\alpha$ -cat-GFP concentrated at the apical side of the epithelial layer. And the presence of the lumen was clearly revealed by the antibody staining of a luminal protein Piopio (Pio). It has been concluded that the formation of ASP does not require a mesenchymal-to-epithelial transition. Instead, it is modeled out of the existing tracheal epithelium, and the luminal space is generated by the migration of a few cells away from the cuticle of the existing tracheal branch. The expansion of the luminal space is achieved by increasing the cell number in the sac-like structure via cell division (Cabernard and Affolter, 2005).

To figure out what cell signaling events may be operating during the morphogenetic process of ASP, Cabernard tested components of multiple signaling pathways such as Dpp, Hh, Wg, and so on. Two receptor tyrosine kinase (RTK) signaling pathways, FGF and EGF, were identified to play important but distinct roles. It was proposed that FGF signaling directed cell migration at the tip of the structure, whereas EGF signaling was essential for cell division and cell survival in the growing epithelial structure. Ras and MAPK pathway were found to be required in both FGF and EGF signaling pathways during ASP formation, with different downstream nuclear responding factors. One example was that Pointed, a erythroblast transformation specific (ETS) family transcription factor, was indispensable in the FGF signaling pathway but unnecessary in the EGF.

## 2. FGF SIGNALING

---

In developmental biology, the term “induction” describes the process in which one tissue instructs the development of another neighboring tissue. Induction was discovered in 1924, when Spemann and Mangold observed that two-headed salamanders could be generated by transplanting a specific piece of embryonic tissue from one embryo into another. This demonstrated that the transplanted tissue could “talk” to the neighboring host cells and determine their fates, revealing the possibility that cell-cell communication may exist. Today, it is textbook knowledge that cells interact with each other through signaling transduction pathways. Typically, signaling transduction pathways are activated by the binding of ligands to their corresponding transmembrane receptors, which in turn relay extracellular signals by modifying cytoplasmic transducers. Subsequently, these transducer molecules will activate downstream effectors, leading ultimately to the nuclear localization of certain transcription factors and changes in gene expression profiles.

Surprisingly, only a few signaling transduction pathways have been discovered so far and they are responsible for most of animal development. These signaling pathways include Hedgehog (Hh), wingless related (Wnt), receptor tyrosine kinase (RTK), transforming growth factor- $\beta$  (TGF- $\beta$ ), Notch, Janus kinase/Signal transducer and activator of transcription (Jak/STAT), and nuclear hormone pathways (Gerhart J., 1999).

Fibroblast growth factors (FGF) signaling pathway belongs to the category of RTK signaling transduction pathway.

### 2.1 Overview of FGF signaling pathways

FGFs constitute a large family of secreted polypeptide molecules. Upon binding to their cognate receptors, FGFs activate signal transduction pathways indispensable for multiple developmental processes, both in invertebrates and vertebrates. This signaling system is conserved throughout metazoan evolution.

All FGFs share an internal core domain of around 120 amino acids and a high affinity for heparin (See Figure 11 for FGF domain structures). In invertebrates, three fruit fly (*Drosophila melanogaster*) *fgf* genes (*branchless*, *pyramus* and *thisbe*) have been found and two (*egl-17* and *let-756*) in the round worm (*Caenorhabditis elegans*). In contrast, in vertebrates, a larger number of *FGF* genes have been identified: 10 *FGFs* in the zebrafish (*Danio rerio*), 6 in the African clawed toad (*Xenopus laevis*), 13 in the chicken (*Gallus gallus*), and 22 genes in the mouse (*Mus musculus*) and human (*Homo sapiens*). FGFs can be classified into subgroups according to structures, biochemical properties and expression patterns (Ornitz DM, Itoh N, 2001).



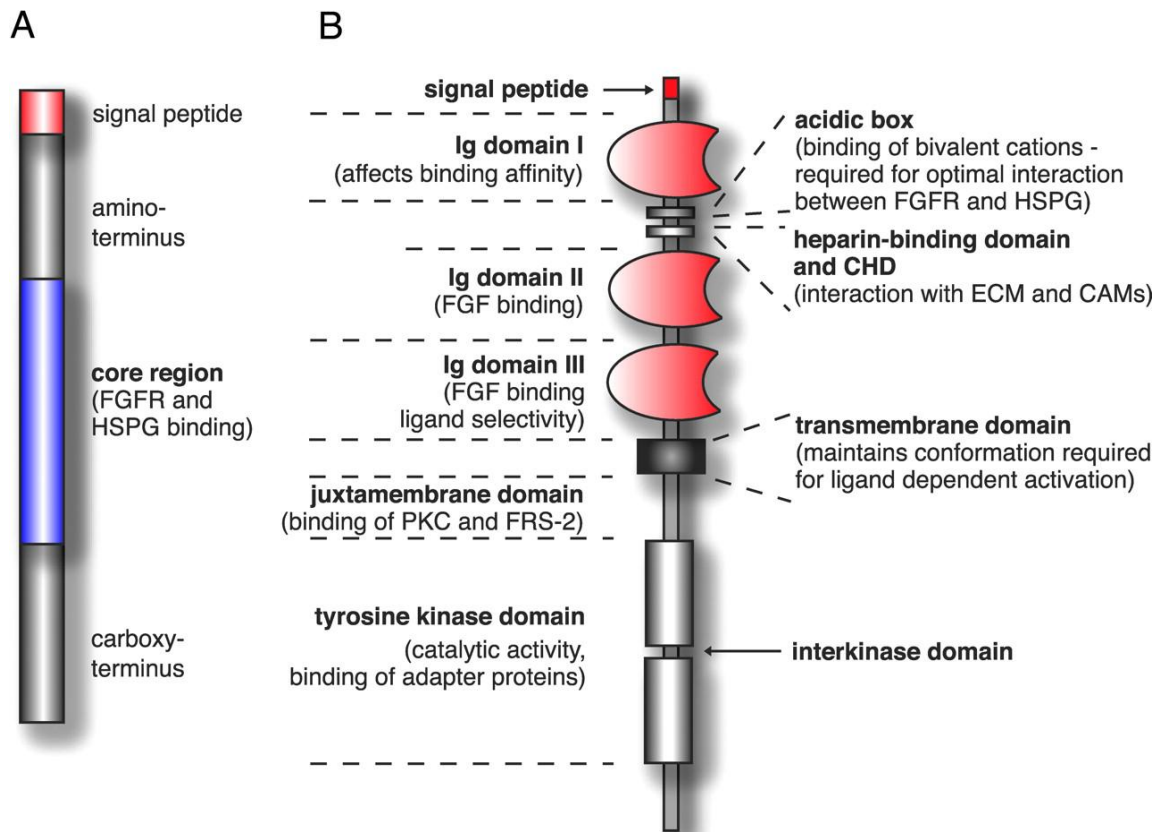


**Figure I11.** Domain structures of generic FGF and FGFR proteins. (Adapted from Boettcher and Niehrs, 2005).

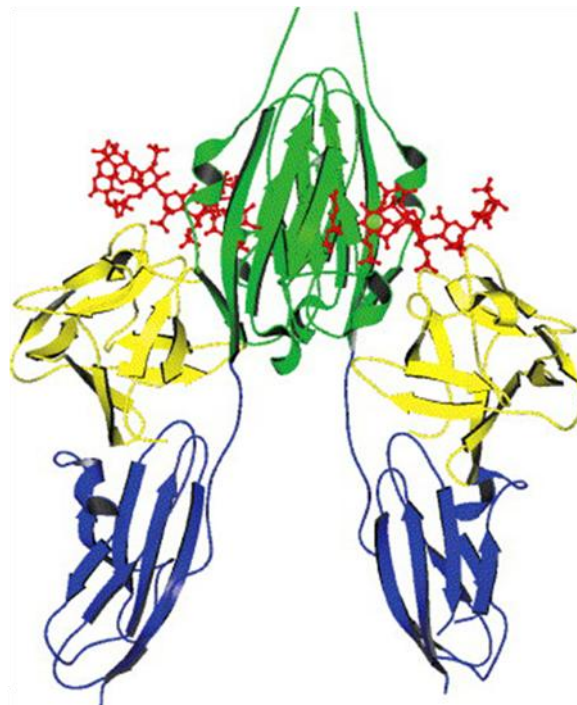


**Figure I12.** The crystal structure of a ternary FGF2/heparin/FGFR1 complex—a ribbon diagram showing FGF2 in yellow, Ig-domain II and III in green and blue, and heparin in red (Adapted from Eswarakumar et al. 2005).

FGFs illicit their biological responses through binding and activating FGFRs, which belong to the family of single-spanning transmembrane proteins containing an extracellular ligand-binding domain and an intracellular signal transduction domain carrying tyrosine kinase activity. The extracellular region consists of immunoglobulin-like (Ig-like) domains required for FGF binding and for regulating ligand binding specificity and affinity. Located between Ig-like domains I and II is a stretch of acidic amino acids (acidic box domain), followed by a heparin-binding region and a cell adhesion homology domain (CHD)—all these domains are required for the interaction between the receptor and components of the extracellular matrix (ECM), in particular heparin sulfate proteoglycans (HSPG) and cell adhesion molecules (CAMs). The intracellular part of the receptor includes the juxta-membrane domain, the split tyrosine kinase domain, and a short carboxy-terminal tail. In addition to its enzymatic activity, the intracellular domain also contains protein binding and phosphorylation sites as well as several autophosphorylation sites that interact with intracellular substrates. Different FGFR forms are produced by the expression of splice variants of a given *FGFR* gene or by the expression of different *FGFR* genes.

FGF signaling pathway is initiated by the effective binding of FGF to FGFR, facilitated by ECM components such as HSPGs (See Figure I12 for the crystal structure of a ternary FGF2/heparin/FGFR1 complex). Effective FGF binding causes monomer FGFR to dimerize, which in turn triggers tyrosine kinase activation, leading to the autophosphorylation of the intracellular domain at specific tyrosine sites. Subsequently, these phosphorylated tyrosines function as binding sites for proteins containing phosphotyrosine-binding (PTB-binding) domain such as Src homology 2 (SH2), resulting the activation of more downstream components. Three major signaling cascades have been demonstrated by experimental data to operate downstream of FGF-FGFR activation: Ras/MAPK pathway, PI3 kinase/Akt pathway, and the PLC $\gamma$ /Ca<sup>2+</sup> pathway (Boettcher and Niehrs, 2005) (See Figure I13 for details).

Among the three pathways listed above, Ras/MAPK pathway is the most commonly employed downstream mediator by different FGFs and it leads to the phosphorylation of target transcription factors such as c-Myc and ETS family of transcription factors. Activities of these transcription factors lead to the succeeding production of effector molecules, which will ultimate change cell behaviors, and the production of negative regulators such as Sprouty (Spry) and Sef (Similar expression to *fgf* gene), completing a negative feedback loop and leading to the attenuation of the initial signaling.

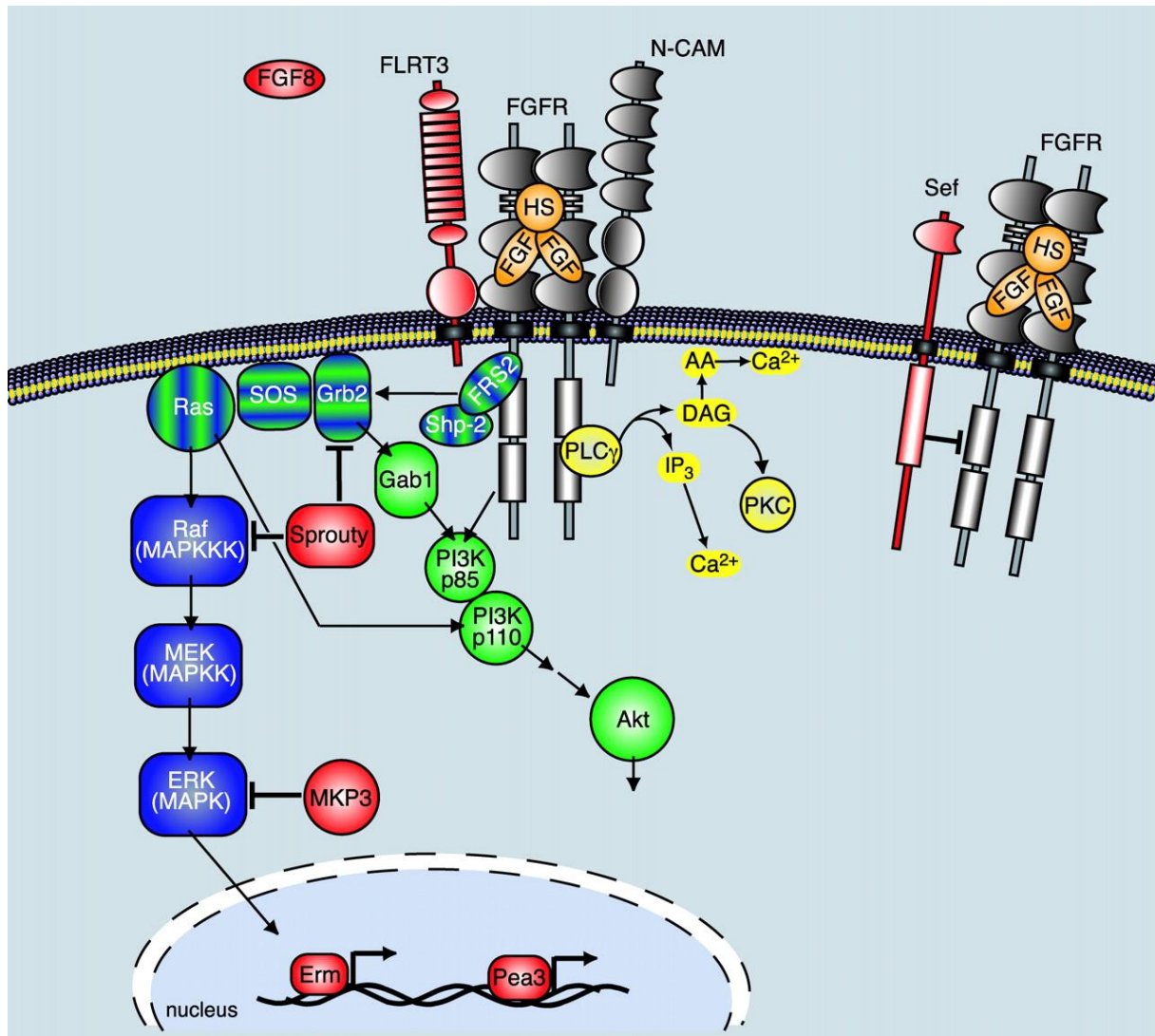


**Figure I13.** Intercellular signaling pathways activated through FGFRs. Formation of a ternary FGF-heparin-FGFR complex leads to receptor autophosphorylation and activation of intracellular signaling cascades, including the Ras/MAPK pathway (in blue), PI3 kinase/Akt pathway (in green), and the PLC $\gamma$ /Ca $^{2+}$  pathway (in yellow). Proteins involved in two pathways are striped. Sprouty (Spry) and Sef (Similar expression to *fgf* gene) are two negative regulators of FGF signaling, with Spry being an intracellular regulator and Sef being a trans-membrane regulator. (Adapted from Boettcher and Niehrs, 2005).

## 2.2 FGF signaling in animal development

During invertebrate development, as well summarized in the review paper of Hung and Stern (Huang and Stern, 2005), FGF signaling pathway is a major mediator. In *Drosophila*, it has been demonstrated that FGF signaling plays an important role in axon outgrowth,

differentiation of mesodermal derivatives, glial development, migration of mesoderm and tracheal cells and sexual differentiation of male genital discs. Similarly, in the nematode *Caenorhabditis elegans* (*C. elegans*), another invertebrate system, FGF signaling has been reported to be required during the process of axon outgrowth and maintenance, differentiation of sex muscle cells, fluid homeostasis, mesoderm migration and muscle protein degradation (Huang and Stern, 2005).

During vertebrate development, FGF also functions as an indispensable participant, and its role appears to be even more complex and diverse. Using model systems such as toad, zebrafish, chick or mouse, FGF signaling pathways have been demonstrated to function during early patterning, dorsal-ventral axis formation, cell movements, neural induction, limb induction and morphogenesis, and bone formation (Böttcher RT, Niehrs C, 2005).

### 3. CELL BEHAVIORS DURING DEVELOPMENT

---

A cell's identity is determined by its gene expression profile, which in turn dictates the assembly of the major “workforce” of the cell: functional protein molecules. These proteins, often capable of performing multi-tasks, will ultimately determine the possible behaviors of a living cell: to divide, to change shape, to differentiate, to remain quiescent, or to die.

#### 3.1 Overview: what does it take to make a multicellular embryo?

The embryonic development of a multi-cellular organism starts with a single fertilized cell. At the end of the embryogenesis, a well-structured embryo containing functionally distinct organs and up to hundreds of different cell types will emerge.

How does this all happen?

Simply put, embryogenesis can be divided into six major developmental processes, even though in reality they overlap and influence one another considerably. And each process consists of one or more particular cell behaviors. These developmental processes include: increase in cell number—cleavage divisions, pattern formation, gastrulation—cells in motion, differentiation, growth, and programmed cell death/apoptosis.

#### 3.2 Cell division: how is it regulated?

An archetypal cell cycle consists of four phases, **G**ap1-**S**ynthesis-**G**ap2-**M**itosis (G1-S-G2-M), which are responsive to extrinsic cues promoting cell cycle progression or cell cycle exit. Most organisms employ, in addition to the stereotyped cell cycle, modified cell cycles for specific developmental strategies. During meiosis, for example, two rounds of chromosome segregation take place after a single round of DNA replication to produce haploid gametes. Organisms engaging rapid embryogenesis, such as insects, amphibians, and marine invertebrates, utilize embryonic cycles consisting solely of S and M phases without gaps. These early cycles, during which growth and gene expression become absent, depend on maternal materials deposited during oogenesis by the mother. Most organisms contain some tissues with polyploid or polytene cells, which are often large in size and exhibit high metabolic activity. Such cells result from multiple rounds of S-G cycling without mitosis. These “endo-cycles” produce either polytene chromosomes in which sister chromatids are held in tight register or more dispersed polyploid chromosomes.

In *Drosophila* embryos, the first 13 cell cycles are alternating S-M cycles driven only by maternal components, in the absence of zygotic transcription. Nuclei divide in a shared

cytoplasm (syncytium) in which cell cycle regulators are restricted to the vicinity of each nucleus. During late syncytial cycles, interphase gradually lengthens and a G2 phase is added after S phase 14, following cellularization of the embryo. During post-blastoderm divisions (cycles 14–16), G2 length is under developmental control and groups of cells undergo mitosis in domains responsive to patterning events. After mitosis 16, epidermal cells exit the cell cycle and cells in the nervous system continue to divide using S-G2-M cycles. Cells that differentiate into larval tissues enter S-G cycles during late embryogenesis, which continue during larval stages. Increasing ploidy and coincident increases in cell size result in dramatic larval growth. Groups of cells that differentiate into adult tissues during pupation, such as imaginal discs and abdominal histoblasts, become determined in the embryo. Imaginal discs use archetypal cycles during larval stages, whereas histoblasts arrest in G2—these tissues undergo further divisions while differentiating into adult structures and larval tissues are histolyzed (Lee and Orr-Weaver, 2003).

As in yeast and mammalian cells, G1-S and G2-M transitions in *Drosophila* are driven by Cyclin/Cdk (cyclin-dependent kinase) complexes, which are inactivated by proteolytic degradation triggered by the SCF (Skp1/Cullin/E-box protein) complex in S phase and by the Anaphase Promoting Complex/Cyclosome (APC/C) in mitosis.

To summarize briefly, the control of cell cycle progression can be achieved in the following ways: regulation of the G1-S transition, regulation of DNA replication during S phase, regulation of the G2-M transition, regulation of progression through mitosis, regulation through checkpoints, regulation of exit from the cell cycle, and regulation of the coordination of cell growth with the cell cycle (Lee and Orr-Weaver, 2003).

### 3.3 Cell migration

#### 3.3.1 Overview of the migration process

Cell migration describes the cell behavior that enables a cell or a population of cells to move physically from one place to another. Cell migration is often initiated by guidance molecules such as chemotactic agents, whose binding to the cell surface triggers various signaling events and leads to changes in cytoskeleton dynamics and cellular architecture. Effective migration consists of repeated cycles of four integrated and artificially divided processes: polarization, protrusion, traction and retraction (Cell Migration Consortium, <http://www.cellmigration.org/science/index.shtml>).

Polarization.

For a cell to migrate efficiently, it needs to know where to go. The source of a guidance cue often defines the final destination of cell migration. The binding of guiding molecules and subsequent signaling events induce a spatial asymmetry within the cell, namely, a “front” and a “rear”, which can transform intracellularly generated forces into net cell body

translocation. The process of this asymmetry formation is called “polarization” and is mediated by molecules such as Cdc42, PAR proteins (PAR6 and PAR3) and atypical protein kinase (aPKC). A bunch of positive feedback loops involving PI3K, microtubules, Rho family GTPases, integrins and vesicular transport operate in an interconnected manner to maintain the effect of polarization once it is initiated.

#### Protrusion.

Protrusion, the formation of membrane extensions, marks the easily observable behavioral response of a migrating cell to its guidance cues, which depends heavily on the use of the actin cytoskeleton as its basic machinery. Actin filaments themselves are intrinsically polarized into fast-growing “barbed” ends and slow-growing “pointed” ends, providing an inherent drive for membrane protrusion. There are two major forms of membrane extensions, which appear to be functionally distinct: filopodia and lamellipodia. Filopodia are spike-like structures, in which actin filaments form long parallel bundles, making them well suited to act as sensors of and to explore the local environment. Lamellipodia are large broad membrane structures, where actin filaments form a branching “dendritic” network in the direction of migration, providing an important mediator with which the cell can move forward. Molecules such as Ena/VASP family proteins, Arp2/3 complex proteins, Wasp/Wave family members, ADF/cofilin family proteins and others, such as cortactin, filamin A and  $\alpha$ -actinin, are important actin regulators in the process of protrusion.

#### Traction.

After forming membrane protrusions, a cell must attach them to the surroundings and stabilize them, providing itself a means of traction to pull the cell body forward. Integrins, mediators of cell adhesion, prove to be the major physical component of traction. Tractional force gets created at sites of adhesion by the contractile properties of myosin II molecules, which interact with actin filaments attached indirectly to integrins through the action of adaptor molecules.

#### Retraction.

To complete the cycle of migration and to enable cell translocation, the disassembly of adhesions at the rear of the cell and the retraction of the cell’s tail have to be achieved. Myosin II is the indispensable player for retraction, mediating the development of tension between adhesions at the rear and the retraction machinery. This tension leads to the opening of stretch-activated calcium channels and the activation of calpain, a protease contributing to adhesion disassembly by cleaving focal adhesion proteins, such as integrins, talin, vinculin and FAK. Disrupting the regulation of myosin II by interfering with PAKa and Rho/Rho kinase signaling pathways severely impairs retraction in migrating cells. The release of adhesions at the rear of the cell coordinates with the protrusive activity at the front of the cell, contributing to the overall polarization and providing positive feedback for the continued cycle of migration.

### 3.3.2 Migration of an individual cell: Dictyostelium as a model for chemotaxis

Eukaryotic cell chemotaxis, during which cells migrate along concentration gradients of diffusible signals, was first described for the soil amoeba *Dictyostelium discoideum*. And *Dictyostelium* has since proved to be an excellent system for studying chemotactic behaviors of single isolated cells placed in a chemoattractant gradient, facilitated by the development of *in vivo* labeling and microscopic techniques. Three characteristics have been observed in chemotaxing cells: cell polarity, cell motility and the ability to detect and respond to gradients of chemoattractants.

When cells are placed into a uniformly distributed chemoattractant, they become elongated and polarized, with clear leading and trailing ends. A behavior termed „chemokinesis“ can be observed, in which cells increase their random motility. When placed into a chemoattractant gradient, cells demonstrate chemotactic response, migrating toward higher concentrations of chemoattractants. „Adaptation“ and „amplification“ are two key features of chemoattractant-induced responses. Adaptation describes the process in which cells rapidly terminate their responses to sustained, uniformly applied chemoattractants. Amplification describes cells' ability to detect and

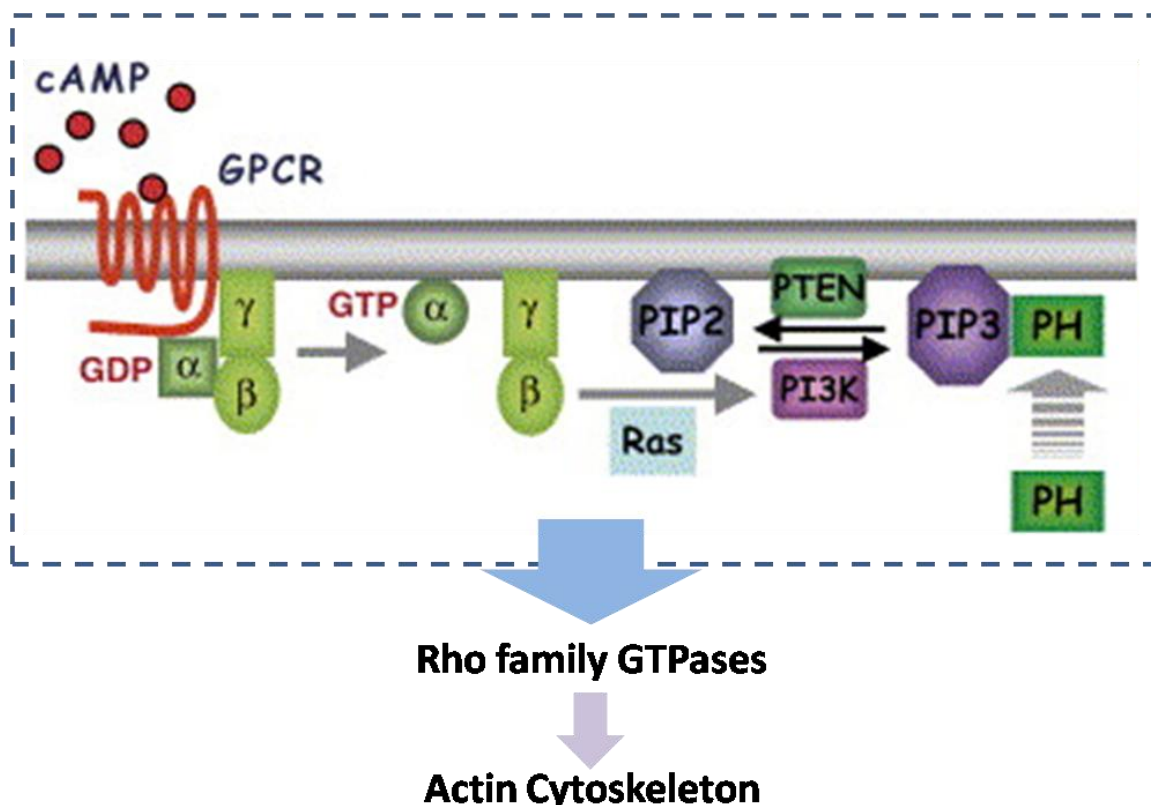


**Figure I14.** A model for major molecular players of the cAMP-induced intercellular response (Adapted from Jin et al. 2008).



translate shallow, extracellular chemoattractant gradients into highly polarized intracellular responses. These features allow the cells to detect and respond to a wide range of concentrations of chemoattractants and concentration differences as small as 2% across the cell's length. Chemoattractants induce dynamic assembly of actin at the leading edge, driving the cell forward. cAMP has been identified as such an chemoattractant.

cAMP receptors in *Dictyostelium* belong to the family of seven-transmembrane G-protein-coupled receptors (GPCRs)/serpentine receptors. Upon cAMP binding, heterotrimeric G-proteins dissociate into  $G\alpha$  and  $G\beta\gamma$  subunits. Freed  $G\beta\gamma$  subunits activates Ras, which subsequently stimulates PI3K, converting PI(4,5)P<sub>2</sub> (PIP<sub>2</sub>) to PI(3,4,5)P<sub>3</sub> (PIP<sub>3</sub>) on the inner plasma membrane. Increased PIP<sub>3</sub> level results in the recruitment of cytosolic proteins containing a PIP<sub>3</sub>-binding pleckstrin homology (PH) domain to the plasma membrane, leading to the localized activation of kinases such as Akt/PKB and GTP exchange factors (GEF) for the Rho family of small GTPases, which govern the spatiotemporally dynamics of actin polymerization—the ultimate force that drives cell migration. Rho family of small GTPases function through at least three different avenues: the activation of WASP/SCAR proteins, the activation of Rac proteins, and the inhibition of ADF/cofilin (Jin et al. 2008 ).

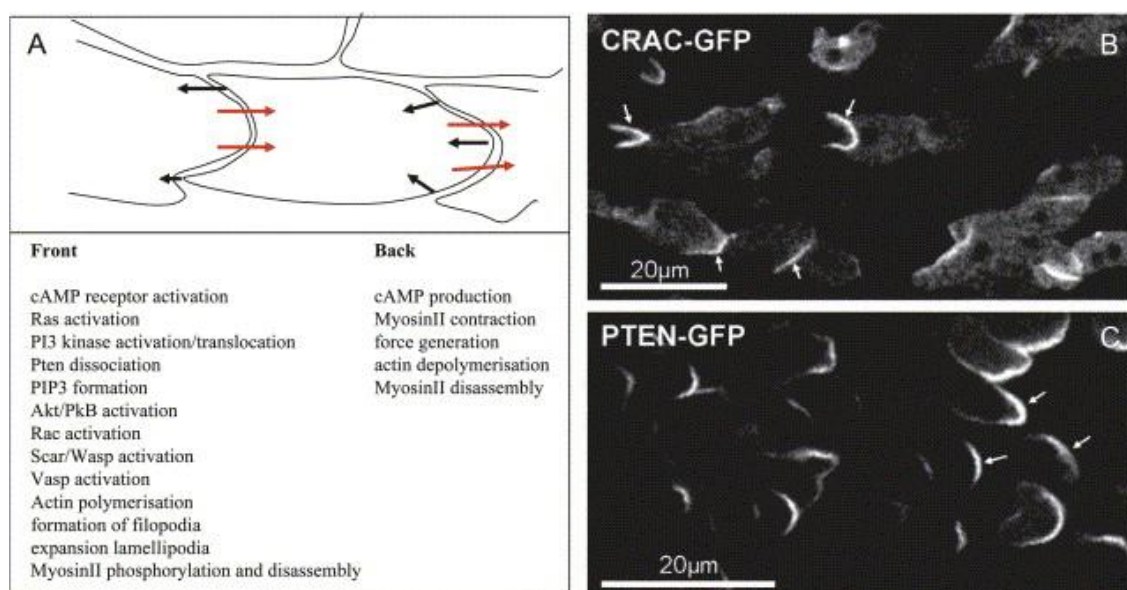


**Figure I15.** Polarization in chemotaxing *Dictyostelium* cells. A. Schematic representation of polarization, with red arrows indicating the direction of cAMP propagation and the black arrows indicating the direction of force generation. B. Localized distribution of PIP<sub>3</sub> at the leading edge, as visualized by the GFP-tagged PH domain-containing protein of cytosolic regulator of adenylcyclase (CRAC). C. GFP-tagged PTEN is mainly localized in the back of cells, contributing to the sharpening of the PIP<sub>3</sub> localization to the leading edge. (Adapted from Affolter and Weijer, 2005)

PTEN, a membrane-associated phosphatase, antagonizes PI3K, dephosphorylating PIP<sub>3</sub> back into PIP<sub>2</sub>. During chemotaxis, PTEN is prevented from binding to the leading edge and can be found only in the lateral and rear parts of the cell membrane, making the leading edge the only place where high PIP<sub>3</sub> can be produced. This uneven localization of PIP<sub>3</sub> is believed to be essential for maintaining a directed movement up the chemical gradient.

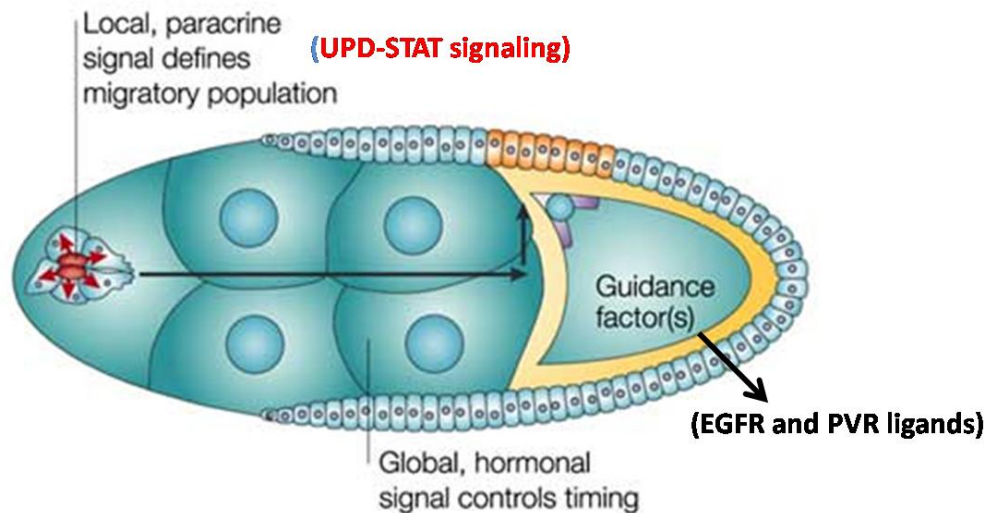
For a cell to constantly migrate up a gradient, it needs to maintain dynamic GPCR signaling. Negative feedback loops mediated by several signaling components have been proposed to dampen GPCR signaling. In bovine cells, free Gβγ dimers have been shown, following GPCR activation, to interact with the receptor-associated kinase GRK2, blocking the signaling. And one *Dictyostelium* Gα subunit has been shown to function as negative regulators in the GPCR-mediated signaling network (Affolter and Weijer, 2005).

### 3.3.3 Migration of a group of cells: Border cell migration

Studies on migrating single cells, such as chemotaxing *Dictyostelium*, have provided much understanding for the basic mechanisms and mechanics operating during cell migration. During morphogenesis, however, cells often take up a migrating journey together, instead of alone. *Drosophila* border cells (BCs) have provided a simple and powerful *in vivo* system to study how a group of cells migrate during development.

Border cells consist of a small group of follicle cells that delaminate from the follicle epithelium of a developing egg and migrate, between nurse cells, down the center of the developing egg chamber during oogenesis. They migrate as an organized rosette-shaped cluster of four to six outer migratory cells surrounding a central pair of non-migratory cells, called polar cells, which come from the anterior pole of the egg chamber. The polar cells express a secreted ligand called Unpaired (UPD), activating the receptor Domeless and a kinase called Hopscotch in surrounding cells and the downstream STAT (signal transducer and activator of transcription) signaling cascade. STAT-mediated UPD signaling not only specifies the migratory border cell population prior to migration; it is also indispensable for border cells to migrate. This signaling event needs to take place continuously throughout the migration process to maintain the fate of border cells and ensure their proper migration (Montell, 2003).

Even if the migratory path of border cells, from the posterior end of the egg chamber to the oocyte, is a relatively simple straight line, two guidance receptors, PVR (PDGF/VEGF receptor) and EGFR, along their respective ligands, are required for them to migrate properly. Ras/MAP-kinase pathway has been shown to be a key downstream effector of EGFR signaling, but not PIK3, which is essential for *Dictyostelium* chemotaxis. Myoblast city (Mbc), a Rac activator and Rac have been demonstrated to act downstream of PVR.



Nature Reviews | Molecular Cell Biology

**Figure I16.** An overview of border cell migration between nurse cells during oogenesis. UPD-STAT signaling is required for border cell fate determination, identity maintenance and its proper migration; both EGFR- and PVR-signaling are essential for border cell migration. (Adapted from Montell, 2003).

Interestingly, a single long cellular extension (LCE), several cell diameters long, has been reported to extend from the border-cell cluster toward the oocyte during migration, whose formation requires directional guidance cues and specific adhesion to the substratum. The LCE has been proposed to function as a “pathfinder” in response to PVR and EGFR ligands, consistent with the fascinating observations that the LCE breaks off from clusters failing to migrate efficiently and the cytoplasmic fragments generated in this process (presumably include the LCE) continue to migrate and eventually reach the oocyte, whereas the cell cluster lags behind (Fulga and Rørth, 2002).

Myosins have been shown to play important roles during border cell migration. Genetic analysis has revealed the dispensability of Myosin II for LCE extension, but it is essential for the subsequent translocation of the cell body. Myosin VI, an unconventional myosin functioning as a pointed-end-directed motor protein, appears required for border-cell migration—it is highly expressed in border cells and associates with E-cadherin and  $\beta$ -catenin. Myosin VI is attached to junctional complexes and its movement along actin filaments could result in protrusive forces, consistent with the observation that protrusions are not detected in border cells depleted in myosin VI.

Mechanical regulation seems to operate during border cell migration. MAL-D, a cofactor of the transcriptional regulator serum response factor (SRF), has been proposed to accumulate in the nuclei of border cells under tension or deformation, leading to the upregulation of

genes, such as *actin*, that are important for cytoskeleton dynamics. This is consistent with the observation that border cell clusters fail to migrate efficiently in the absence of the transcription factor complex SRF/MAL (Somogyi and Rørth, 2004).

Intriguingly, delaminated migrating border cells have been shown to maintain their epithelial properties, such as the apical/basal polarity, since the apical epithelial proteins Par-6, Par-3/Bazooka, and aPKC remain asymmetrically distributed throughout and are even required for efficient migration. This suggests that cells do not have to undergo epithelial-mesenchymal transition (EMT) in order to invade neighboring tissues and to undergo chemotaxis (Montell, 2006).

Surprisingly, DIAP1, the *Drosophila* inhibitor of apoptosis 1, identified in a genetic screen looking for genes suppressing the border cell migration defect induced by overexpression of dominant-negative Rac. Border cells mutant for *diap1* do not die; instead, they fail to migrate properly (Geisbrecht et al., 2004). It remains interesting to demonstrate how DIAP1 mediates an apoptosis-independent role in Rac-mediated cell motility.

Not all questions concerning border cell migration have been answered. An important question that still remains to be elucidated is how cell-ECM adhesion and cell-cell adhesion among a migrating group get regulated.

#### 3.3.4 Migration as a signaling-mediated morphogenetic process: Tracheal cell migration

At stage 10, all tracheal cells within the tracheal metameres switch on their expression of Btl, a tyrosine kinase receptor homologous to the mammalian FGF receptors, right before the initiation of the primary branching event (Glazer and Shilo, 1991; Klambt et al., 1992). Branchless (Bnl), the ligand for FGFR/Btl, is activated in six clusters of cells surrounding the Btl-expressing tracheal cells, providing the source of a chemottractant and the instruction of “where to go”. Btl-expressing cells respond to Bnl by orienting and moving themselves, out of the placode, towards the Bnl source, leading to the formation of six primary branches: dorsal trunk anterior (DTa), dorsal trunk posterior (DTp), DB, VB, LTa, and LTp/GB. In the absence of *bnl* or *btl*, mutant embryonic trachea consists of 20 unconnected elongate sacks of tracheal cells. Localized ectopic expression of Bnl in epidermal cells, on the other hand, can redirect primary branches to the new site of Bnl expression (Sutherland et al., 1996).

During tracheal cell migration, each branch appears as a finger-like extension and grows away from the site of invagination in a stereotyped manner similar in all metameres. All primary branches form multicellular tubes and maintain their tubular structure and integrity as they continue to grow. The outgrowth is begun with the extension of broad cellular protrusions from the tip cells in each bud. Afterward, the cell nucleus moves into the same direction and the apical surface enlarges to promote lumen extension. As described above, three branches grow out of the dorsal region of each placode to form DTa, a short DTp, and DB, one from the central region of the metamere forming the VB, and two from the ventral region forming LTa and LTp/GB. Cells located within the central

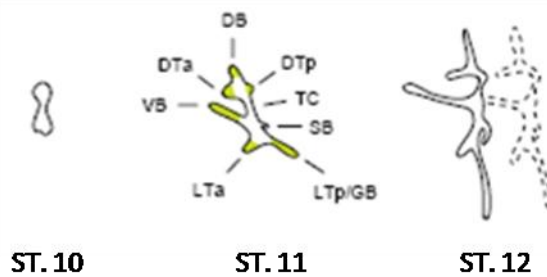


**Figure 117.** Primary branching of *Drosophila* tracheal system is mediated by FGF/Bnl-mediated cell migration. A developing tracheal placode at stage 10 (ST.10), ST. 11 and ST. 12 are shown. (Adapted from Samakovlis et al., 1996)

region of the placode form the transverse collective (TC), connecting the dorsal and ventral parts of the tracheal metamere. The spiracular branch (SB) is constituted by cells remaining near the site of invagination. SB closes during stage 12 (Campos-Ortega and Hartenstein, 1985) and it collapses. Thus, the SB has no respiratory function in the *Drosophila* larvae, but it opens at each molt to expel the tracheal cuticle.

Bnl expression is dynamically regulated and appears to be switched off once the Btl-expressing tracheal cells reach the Bnl-expressing cluster. For some branches, Bnl-expressing cells reappear at a new site further along the stereotypical migratory track, facilitating the ensuing extension of the branch. It still remains elusive how the expression pattern of Bnl is exactly regulated. It is highly likely to be complex. What is known, however, is that the dorsal cluster of Bnl-expressing cells, which is responsible for the proper formation of DB, becomes absent in *dpp* mutant embryos, revealing one possible mechanism for Bnl expression regulation.

Btl expression is also under regulation in the primary branches. Its expression is first observed in all tracheal cells at stage 10, which declines in DT and TC during stage 12, and becomes restricted almost entirely to growing branches like DB, VB, LTA, and LTP, during late stage 13 (Ohshiro et al., 2002). A positive feedback loop seems to be operating during stage 12 and stage 13. Bnl-Btl signaling leads to the downstream activation of Rolled (RI), the *Drosophila* mitogen activated protein kinase (MAPK), which in turn destabilizes Anterior-open (Aop), a repressor of *btl* transcription. In this way, a continuous supply of Btl receptors is provided to cells/membrane regions where FGF signaling is mostly engaged.

For Bnl/FGF-Btl/FGFR signaling to take place normally, heparan sulfate proteoglycans (HSPGs) need to be deposited properly. If either of the two genes *sugarless* (*sgl*) and *sulfateless* (*sfl*), which encode HSPGs synthesizing enzymes, is mutant, the event of primary branching will be blocked (Lin et al., 1999). It has been proposed that HSPGs may function as coreceptors mediating and facilitating the formation of active Bnl-Btl signaling

complexes (Pellegrini, 2001), and MAPK activation, in *sgl* and *sfl* mutants, is blocked, which can be restored by Bnl over-expression.

In addition to the chemoattractant activity of Bnl, for the proper outgrowth of all primary branches, supplementary branch-specific environmental cues also seem necessary. Slit (Sli), a phylogenetically conserved cell migration signal (especially for neural cells), may provide such an additional guidance cue. Expression of Sli is dynamic in many tissues surrounding the developing trachea. Mutations in *slit* and one of its three *Drosophila* receptors, *roundabout 2 (robo2)*, hamper the outgrowth of DB, GB, and VB (Englund et al., 2002). Ectopic Slit is sufficient to redirect and attract new primary branches towards its ectopic expression site, and the phenotype requires the right combination of Robo and Robo 2 receptors in the receiving tracheal branches. However, in the absence of functional Bnl signaling, the long-range attractant function of Slit is not sufficient to induce primary branching. This suggests a sequential requirement in the activation of different pathways in the process of primary branch formation.

A single cell of mesodermal origin, the bridge cell, is indispensable for the correct migration and succeeding branch fusion of DT branches, despite the fact that the distance DTa and DTp have to travel is relatively short and straight. Bridge cells are distinguished by their selective expression of the transcription factor *Hunchback (Hb)* and are localized at the position where DTa and DTp branches meet. In the absence of Hb, bridge cells undergo apoptosis, resulting DT fusion defects. Ectopic expression of Hb in additional cells, close to the bridge cell, interferes with DT formation. Hb activity appears to not only ensure bridge cell viability, but also provide an adhesion-dependent guiding post for branch formation.

As described above, FGF/Bnl-mediated cell migration plays a major role in the morphogenetic process of primary branching during *Drosophila* tracheal development.

#### 4. SOME TECHNIQUES RELEVANT FOR THE THESIS

---

*Drosophila*, commonly known as fruit flies, has a life cycle of about 2 weeks, which consists of an embryonic stage, three larval stages, a pupal stage and an adult stage. This short life cycle facilitates genetic crosses and large-scale genetic screens. Moreover, their small size, the ease to handle them, their fully sequenced genome, an enormous amount of knowledge of their genetics and development, and a wide array of available techniques have made *Drosophila* one of the favourite model organisms of developmental biologists.

In ancient times, scientists like Greek philosophers did scarcely more than observe and speculate. Millennia later, scientists were still doing more or less the same. T. H. Morgan, one of the first *Drosophila* geneticists, made his important, serendipitous discovery of sex-linked traits by luck—he „waited“ for spontaneous mutations and stumbled across one.

Things are different these days. Scientists no longer passively wait, neither do they merely observe and speculate. Instead, they can actively manipulate Nature by inducing random mutations in the genome and see what happens. Constant emergence of new technologies and improvement of old ones have been enabling scientists to ask questions in a ever-finer manner. For *Drosophilists*, the creation of genetic mosaics and the possibility of performing genetic screens in various ways are just two such examples.

##### 4.1 Creation of genetic mosaics

Do cells observable in an early embryo contribute to adult structures? If yes, to what structures?

Is a particular adult structure derived from a single cell lineage or from multiple cell lineages?

Is a given gene required for different developmental stages?

Questions like these are fascinating to developmental biologists. Historically, *Drosophila* mosaics, composed of cells of different genotypes, have been invaluable in providing insights into the above-mentioned inquiries. Traditionally, methods employed for generating mosaics include: chromosome loss induced by unstable chromosomes or mutations, cell or nuclear transplantation, local gene inactivation/activation, and mitotic recombination induced by ionizing radiation.

## The life cycle of *Drosophila melanogaster*

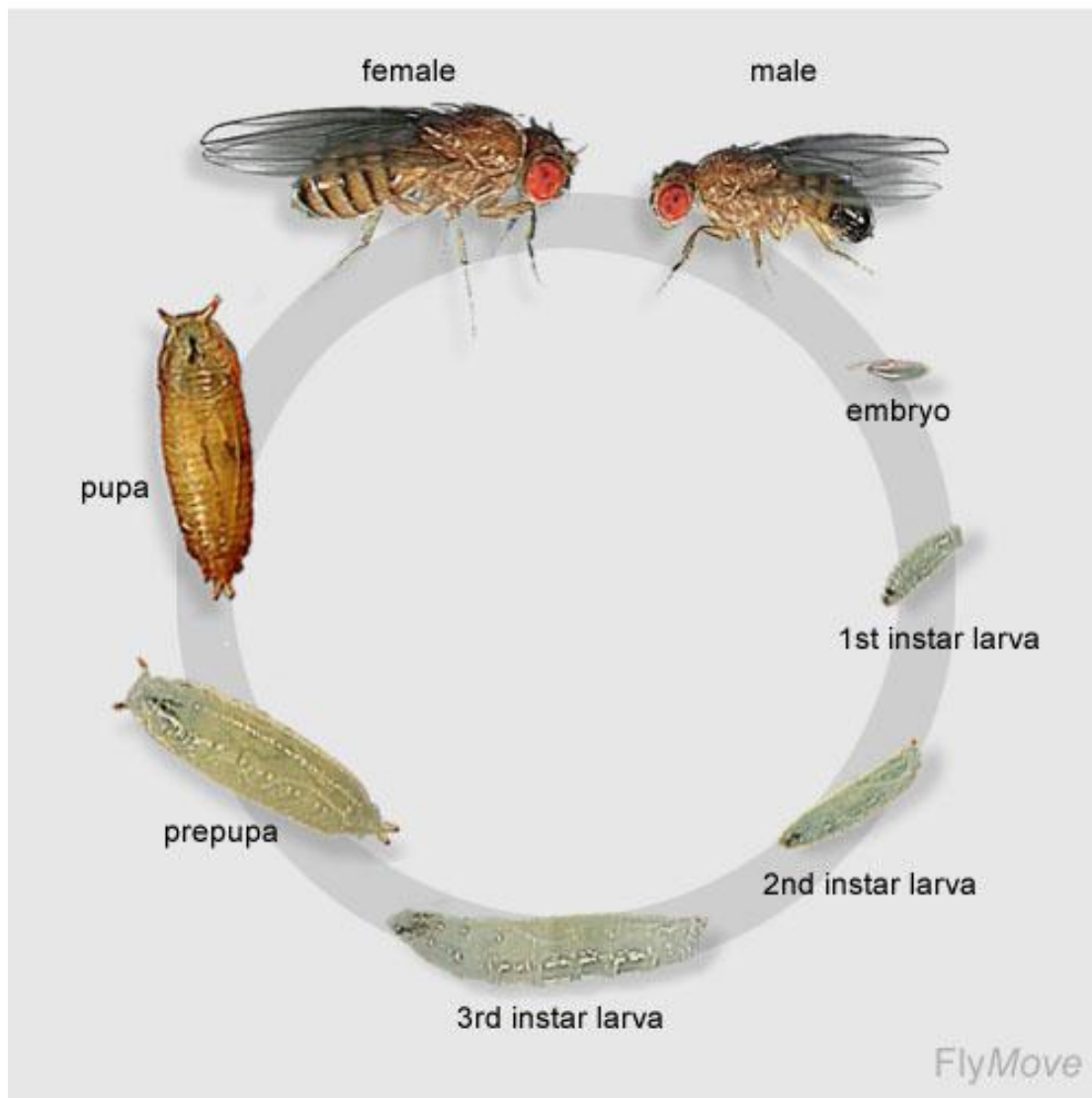


**Figure I18.** The life cycle of *Drosophila melanogaster*.

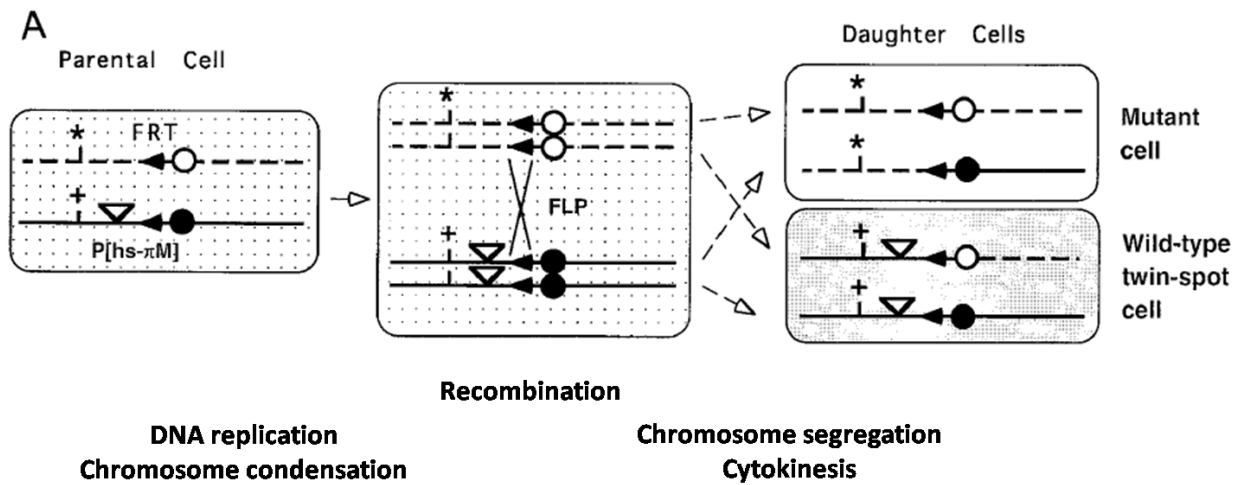
Source: [http://www.anatomy.unimelb.edu.au/researchlabs/whittington/img/life\\_cycle.jpg](http://www.anatomy.unimelb.edu.au/researchlabs/whittington/img/life_cycle.jpg)

However, drawbacks such as low frequencies of mosaicism and absence of useful cell markers, render these methods impractical for wide-spread use.

For high frequency clone inductions, flipase (FLP), a yeast site-specific recombinase, and the sequence it recognizes, FLP recombination target (FRT), have been introduced into *Drosophila*, together with different cell markers.



## Induction of mitotic clones



## Induction of flip-out clones

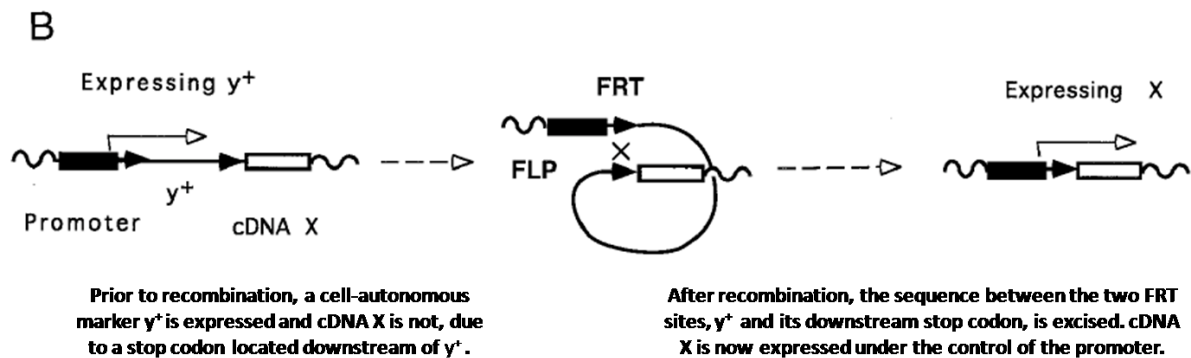


**Figure I19.** Generating and labeling mutant clones using FLP/FRT and cell markers.

A. Induction of mitotic clones. In a heterozygous parental cell, FLP induces mitotic recombination between FRT sites (solid arrows) on homologous chromosome arms. Segregation of recombinant chromosomes and cytokinesis produce two daughter cells: a mutant cell bearing two copies of the mutant allele (\*) and a wild type twin-spot cell homozygous for the wild type locus of the gene (+). The cell marker P[hs- $\pi$ M] ( $\nabla$ ) co-segregates with the wild type gene, labeling the mutant cell by its absence. Subsequent cell divisions result in clones from each of these original daughter cells. B. Induction of flip-out clones. In the parental cell, a constitutive promoter drives the expression of an autonomous cell marker  $y^+$  (containing a downstream stop codon). The  $y^+$  gene is flanked by two FRT sites with the same orientation. Upon the induction of FLP (usually by heat shock), a recombination event is induced between the FRT sites and the intervening  $y^+$  and its downstream stop codon will be excised. Consequently, the constitutive promoter drives the expression of a downstream gene, X. (Adapted from Theodosiou and Xu, 1998)

#### 4.1.1. Conventional techniques

Conventional mosaic techniques are used to induce clones in both proliferating and non-proliferating tissues. „Mitotic clones“, whose induction requires the entry into mitosis, can be induced only in proliferating cells. „Flip-out clones“, whose induction is independent of mitosis, can be induced in each and every cell, limited only by the promoter used.

Mitotic clones are often used to create homozygous mutant cells for a gene of interest in heterozygous tissues and then to examine their phenotypes in an otherwise phenotypically wild-type organism. After cytokinesis, cells in which a recombination event has taken place give rise to two populations of progenies: one homozygous for the mutation and one homozygous for the wild type allele. Practically, mutant cells are often „negatively“ labeled, meaning labeled by the absence of a cell marker, while wild type cells (also called twin spots) are positively labeled by the presence of the cell marker, which is often located in the same chromosome where the wild-type locus resides.

Flip-out technique is used to create a group of cells (a clone) that are genetically identical and distinct from all surrounding cells in an organism, and to subsequently trace these labeled cells during development. To induce such clones, two FRT sites bearing the same orientation and flanking the sequence of an autonomous cell marker and a downstream stop codon, are placed in the same chromosome. Cells in which a recombination event has taken place end up having the sequence located between these two FRT sites (also called the „flip-out cassette“) permanently removed. This removal enables the expression of a transgene which is localized outside of the flip-out cassette and downstream of the stop codon. These cells therefore acquire a distinct genotype and phenotype different from surrounding neighbors in which no recombination has occurred. Flip-out clones are labeled by the absence of the original cell marker and possibly the presence of a new cell marker, depending on the exact experimental design.

The induction of both mitotic and flip-out clones is mediated by flipase (FLP). Generally, FLP expression is placed under the control of a heat shock (HS) promoter. In this way, temporal control of clone induction is made possible and recombination can be induced at whatever developmental stage of interest, simply by placing the embryos/larvae/pupae/adults (usually in a tube) into a water bath. Spatial control of clone induction is determined by the tissue-specific promoter employed. For the purpose of ubiquitous clone induction, the promoter of the gene actin 5C is often used.

#### 4.1.2. MARCM

MARCM stands for Mosaic Analysis with a Repressible Cell Marker. It provides an alternative to the conventional technique for making mitotic clones.

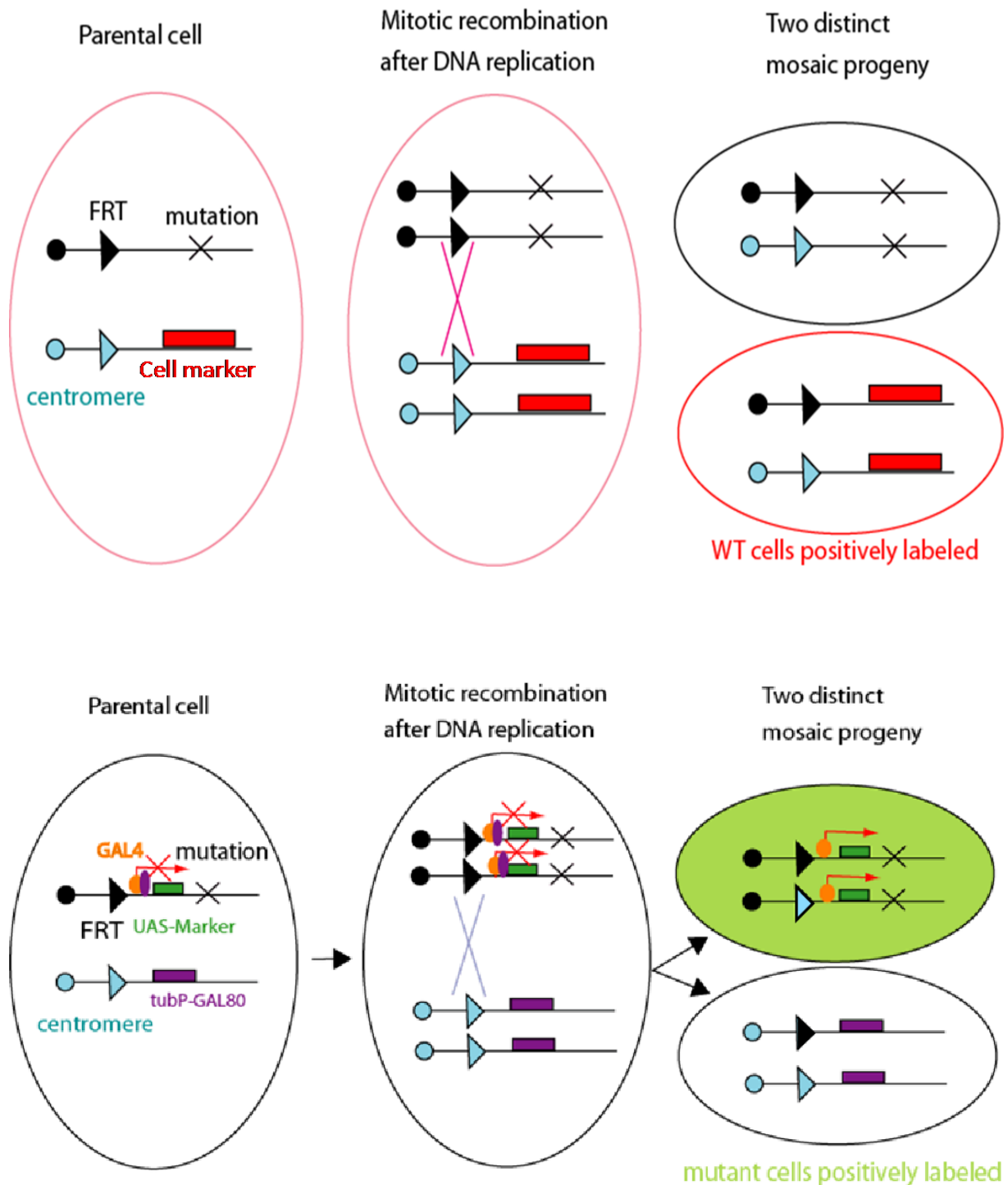


**Figure 120.** Comparison between the conventional technique for inducing mitotic clones and MARCM. In the former case, cells homozygous for the wild-type allele of a certain gene are positively labeled by the marker (2 copies); cells homozygous for the mutation express no marker; and cells in which no recombination has taken place are labeled by 1 copy of the cell marker. In MARCM clones, only mutant cells are positively labeled by a UAS-Marker (such as GFP), and all other cells remain unlabeled, facilitating the imaging and tracing of mutant clones.

As described earlier, in mitotic clones induced by the conventional technique, cells homozygous for a mutation in the gene of interest are often negatively labeled, carrying no cell marker. This makes it difficult to clearly identify and image the morphology of the clones, and almost impossible to trace the fate(s) and distribution of them.

In order to positively label the clonal mutant cells, MARCM technique has been devised (Lee and Luo, 2001), in which a Gal4 repressor, the yeast Gal80 protein is introduced into the Gal4-UAS binary expression system in *Drosophila*. Before MARCM clones are induced, all cells in the fly body are heterozygous for a transgene encoding the Gal80 protein, which prevents the transcription factor Gal4 from activating its target genes. Following FLP/FRT-mediated mitotic recombination, chromosome segregation and cytokinesis, the Gal80 transgene is removed from one of the daughter cells, thus allowing the expression of a Gal4-driven reporter gene/cell marker specifically in this daughter cell and its progeny (Fig. 13). If a mutation of a gene of interest is located on the chromosome arm *in trans* to the chromosome arm containing the Gal80 transgene, cells homozygous for this mutation will be uniquely labeled, making it possible to easily identify, trace, and image the mutant clones.

The MARCM system has been demonstrated to be a useful tool for the following studies: cell lineage analysis, functional analysis of candidate pleiotropic genes, and genetic screen to identify new genes of interest.

## 4.2 Genetic screens

A genetic screen is a procedure by which selected phenotypes of interest are identified or tested among a mutated population. Genetic screens can be divided into two categories: forward genetic screens and reverse genetic screens. The former starts with certain phenotypes and aims to find (new) genes responsible for these phenotypes, and the latter starts with a known gene and focuses on uncovering the possible functions of this particular gene.

The success of *Drosophila melanogaster* as a model organism can be ascribed largely to its power of forward genetic screens, which have identified numerous genes as potentially indispensable for various biological processes operating early in embryogenesis. The Nobel-prize-winning screen for embryonic-patterning genes, performed by Christiane Nüsslein-Volhard and Eric Wieschaus, demonstrated for the first time the power of traditional genetic screens. These screens, however, can reveal only the earliest phenotype caused by a mutation in an essential gene. In the past decades, many ingenious approaches have been devised for performing a genetic screen, making it possible to seek for genes causing almost any phenotype in any cell at any stage of development (D.S. Johnston, 2002).

In the following part, traditional genetic screens and clonal screens will be described in details. Other screen methods also exist, such as mis-expression screens and enhancer and suppressor screens.

#### 4.2.1 Traditional genetic screens

Ethyl methane sulphonate (EMS) is the most commonly used mutagen in *Drosophila* because it's easy to administer and causes the highest frequency of mutations. EMS predominantly induces point mutations, and other forms of mutations have also been reported.

A typical crossing scheme for traditional forward genetic screens is described as the following (see Figure I21. for illustration). Male flies are starved and then fed EMS of appropriate concentration to induce mutations before being crossed *en masse* to virgin females carrying a balancer for the chromosome to be screened. Since mutations are induced randomly in mature spermatids, different F1 males should inherit mutagenized chromosomes carrying mutations in different genes. Single F1 males are then backcrossed to balancer females to generate F2 males and females that carry the same mutagenized chromosome. When these F2 males and females are crossed with each other, 25% of the F3 progeny will be homozygous for the mutagenized chromosome. If such adult flies are not to be found among viable progenies (judge by the absence of the balancer chromosome), a zygotic lethal mutation is often identified. Subsequently, embryos will be screened for phenotypes. These traditional screens are F3 screens.

This kind of embryonic lethal screens identified mutants in most of the signaling molecules involved in patterning the embryo, such as Wg, Dpp, Hh, Spitz (Spi, an EGF ligand), and Delta (DI, a Notch ligand). However, other components of the signaling transduction pathways through which these ligands act were not identified in the screen, probably because their maternal contribution was sufficient for signaling.

The description above illustrates a general limitation of traditional screens using homozygous lethality as screening criterium, namely, mutations not homozygous lethal will not be identified. In addition, only the first essential function of a gene can be analyzed.

#### 4.2.2 Clonal screens

As described previously, induction of mitotic clones makes it possible to produce cells homozygous for a certain mutation in an otherwise heterozygous organism. This kind of "spatial control", in addition to temporal control exerted through a planned heat shock, enables the studies of genes having pleiotropic functions and of genes which also function at a later developmental stage beyond embryogenesis, by avoiding un-interpretable over-mixed phenotypes or circumventing the lethality caused by a complete removal of the same genes. Additional spatial control can be employed by driving the expression of FLP with a tissue-specific promoter/enhancer.

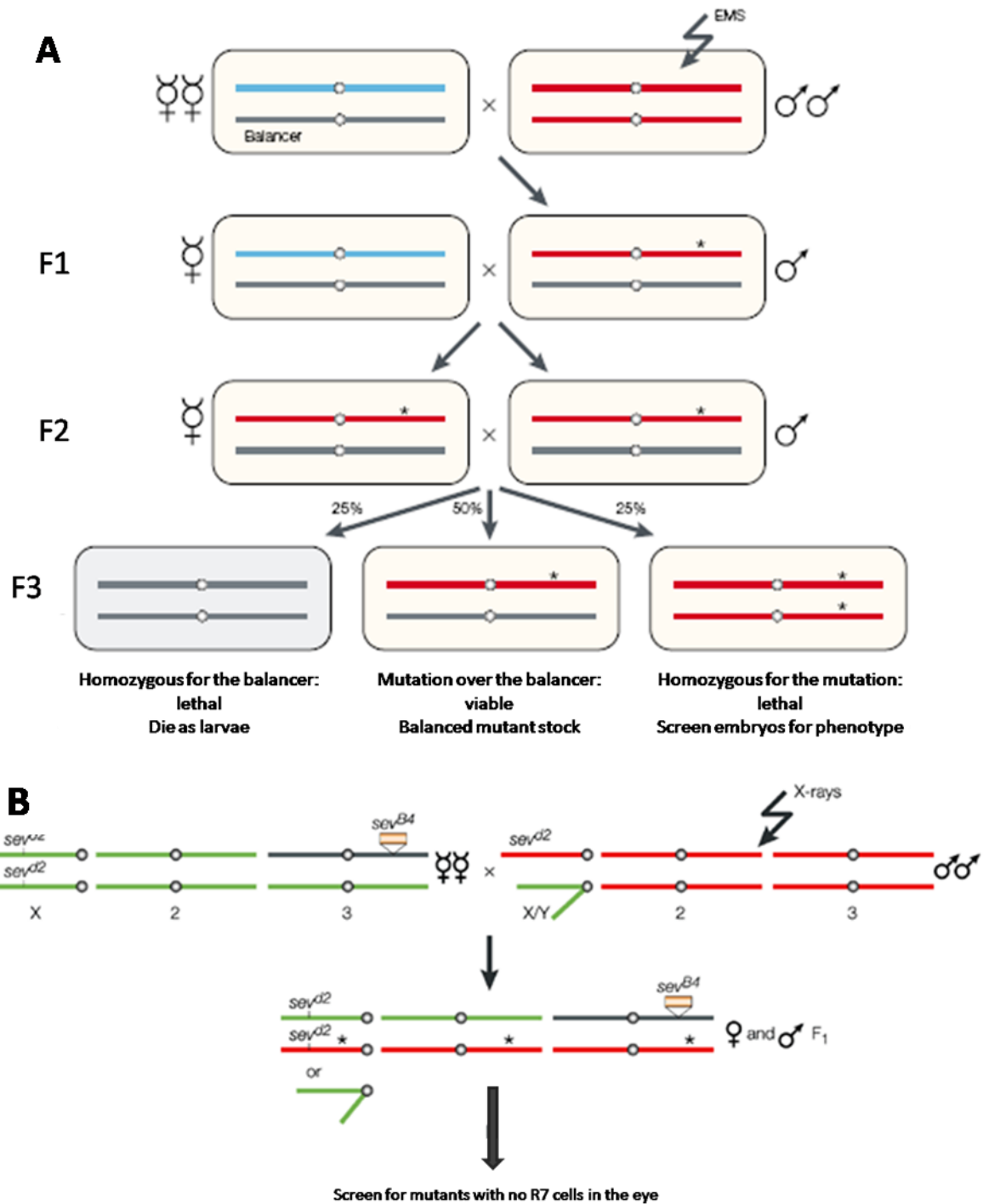


**Figure I21.** A. Outline of the crossing scheme for a traditional forward genetic screen, using homozygous lethality as the criterium for identifying mutations. B. The crossing scheme for the original screen for enhancers of *sev*. Males hemizygous for a null allele of *sev* ( $sev^{d2}$ ) were mutagenized with X-rays and crossed to  $sev^{d2}$  homozygous females that carry a temperature-sensitive allele of *sev* ( $sev^{B4}$ ) as a transgene inserted on the third chromosome balancer, TM3. The F<sub>1</sub> TM3 flies were then screened for a reduction in the number of R7 photoreceptor cells in the eye. (Adapted from D.S. Johnston, 2002)

Dominant female sterile (DFS) technique, an ingenious refinement to the FLP/FRT system, has been developed to screen for the maternal-effect phenotypes of lethal genes. The DFS method uses the dominant *ovoD* mutation to kill the non-recombinant germ cells, so that females only lay eggs that derive from homozygous mutant germline clones. This approach has allowed the identification of many essential genes which are missed in previous screens due to “maternal effect”.

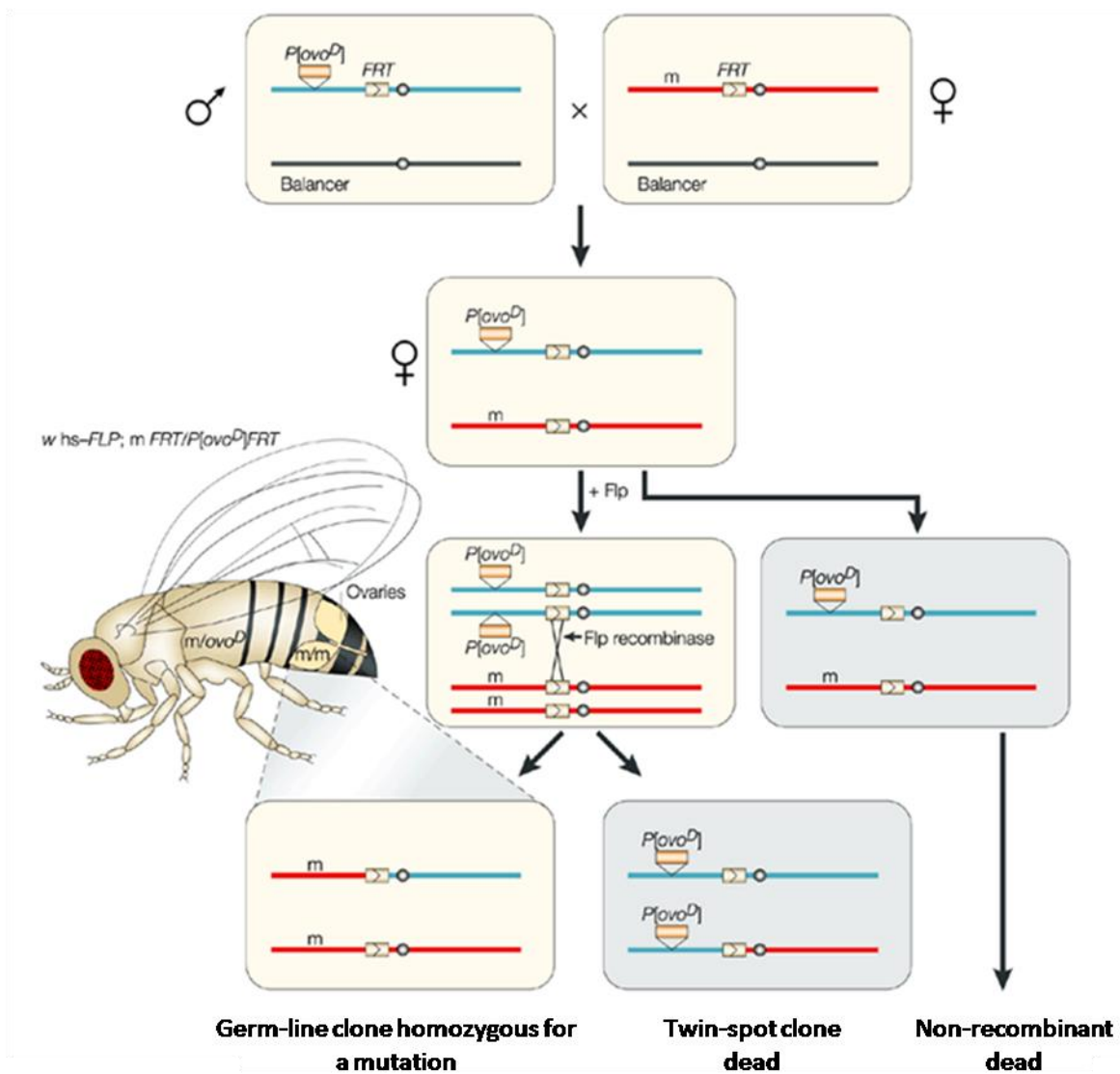


**Figure I22.** The DFS technique for selecting homozygous germ-line clones. (Adapted from D.S. Johnston, 2002)

## 5. AIM OF THE THESIS

---

Prior to the onset of my Ph.D, the following facts were known.

The *de novo* formation of air sac primordium (ASP) during the 3<sup>rd</sup> instar larval stage (L3) in the second thoracic tracheal metamere (Tr2) was dependent on FGF, which had been shown to mediate morphogenetic processes such as tracheal cell migration.

Repopulation, a prerequisite for ASP to develop properly, was proposed to take place through “cell replacement” or “cell de-differentiation”. Exactly how repopulation happened remained elusive.

The aim of the thesis, first and foremost, is to present a detailed report of findings from our research effort:

- 1) to identify, in *Drosophila* trachea, novel genes functioning in the FGF-mediated cell migration during air sac primordium (ASP) formation;
- 2) to elucidate the origin of mitotic cells during “repopulation” of the second tracheal metamere (Tr2);
- 3) to understand how mitotic behaviors of Tr2 tracheal cells are regulated during the third instar larval stage (L3);
- 4) to understand how ASP lower layer grows in the absence of cell proliferation.

In addition, the thesis also tries to summarize what still remains unanswered and awaits further investigation.



# **IV. Materials & Methods**



## 1. *Drosophila* strains

For the screen:

Stocks generated from EMS-mutagenized FRT40A males (which carried randomly induced mutations throughout the genome, of which only those on the 2<sup>nd</sup> chromosome would get maintained).

MARCM strain: 70hsFLP/70hsFLP; tubGal80, FRT40A/CyO; btlenhancer-mRFP1moe, btIGal4-UAS-CD8-GFP/TM6C.

Deficiency lines generated by Exelixis ([Parks et al. 2004](#)) were used for complementation tests.

For the candidate-testing:

*wasp3*, *scar-delta37*, *scar-K13811*, *sop-Q25st*, *sop-W108R*, *sop-Q25sd*, *ena*, *diap1*, *hrs*, *mmp2 (K07511)*, *mmp1 (Q112)*, *mmp2 (W307)*

For the clonal analysis:

*ywhsflp;;act>CD2>Gal4*  
*yw;; btlenhancer-mRFP1moe-UASGFPnls*

## 2. Generation of MARCM clones

MARCM virgin females were crossed *en masse* to the mutant *FRT40A* lines of interest. Embryos of the progeny were submitted to a heat shock 4–6 hr after egg laying for 1 hr at 38° in a circulating water bath and kept at 25° until larvae reached the wandering third instar larval stage.

Clones were induced in a similar way for direct candidate-testing experiments.

## 3. Larvae sorting and dissection

For the screen and the candidate-testing:

Third instar larvae bearing GFP-positive clones were collected using a Leica MZFLIII GFP stereomicroscope. Larval wing discs were dissected in PBS and mounted in Schneider Cell Medium (GIBCO, Grand Island, NY).

## 4. Mapping of lethal mutations

Lethal mutations induced on the left arm of the second chromosome were genetically mapped by screening for non-complementation of lethality, using deficiencies generated by Exelixis, which uncover 80% of the left arm of the second chromosome ([THIBAUT et al. 2004](#)). In a further candidate gene approach, known lethal mutations affecting genes located in the genomic regions determined by deficiency mapping were tested for lethality in *trans* to mutant candidate lines. Other mutant lines were obtained from the Bloomington Stock Center.

## 5. (Flip-out) clonal analysis

For the in vivo tracking of repopulation:

Embryos [*y w Hs-FLP/w*; ; *Act>CD2>GAL4/UAS-GFP(nls)*] were subjected to heat shock (15 min, 37°C) and a 54- to 56-h incubation at 23°C; larvae were examined 0–2 h after the L3 molt for GFP-positive nuclei in the Tr2 dorsal trunk, and animals with fluorescent nuclei were examined 24 and 48 h later.

For comparing the clone induction efficiencies of Tr2, Tr3 and Tr5, 12-minute heat shock was used.

For analyzing the mitotic behaviors of Tr2 cells, 15-minute heat shock was applied at 37°C, 55 hours prior to 0-2 L3, and animals were sacrificed at different time points into L3, as summarized in the Results section.

For excluding the presence of spontaneous clone induction, 102 un-heat-shocked DT were examined and none of them were found to bear GFP-positive cells.

For the purpose of calculating clone induction efficiencies, the average number of nuclei per metamere at 0-2 L3 was counted (after DAPI staining) calculated as listed in the table M1.

To calculate the clone induction efficiency, the total number of labeled cells was divided by the total number of cells recorded, which was, the average cell number in the metamere multiplied with the number of DT examined. The concrete calculation will be listed in Table M2.

## **6. BrdU feeding and antibody staining**

3rd instar larvae were fed on cornmeal agar medium containing BrdU (0.2 mg/ml) for a period of 48 h according to a modified version of the method of [Truman and Bate \(1988\)](#). Fixation and immune-staining were performed according to *Drosophila protocols* ([Sullivan et al., 2000](#)) using primary mouse anti-BrdU antibody (1:50, Becton Dickinson) and Cy3-conjugated donkey anti-mouse secondary (1:750, Jackson Labs).

**Table M1. Counting of nuclei after DAPI staining and calculation of average number of nuclei per metamere at 0-2 L3**

|                 | <b>Tr2</b> | <b>Tr3</b> | <b>Tr5</b> |
|-----------------|------------|------------|------------|
| <b>Sample 1</b> | 20         | 14         | 18         |
| <b>Sample 2</b> | 20         | 15         | 18         |
| <b>Sample 3</b> | 21         | 15         | 14         |
| <b>Sample 4</b> | 20         | 16         | 18         |
| <b>Sample 5</b> | 20         | 15         | 22         |
| <b>Sample 6</b> | 20         | 15         | 18         |
| <b>Sample 7</b> | 19         | 14         | 19         |
| <b>Average</b>  | 20         | 15         | 18         |

**Table M2. Calculation of clone induction efficiencies for metameres Tr2, Tr3 and Tr5.**

| <b>Larvae dissected at 0-2 L3</b>  |                                    |                                    | <b>Larvae dissected at 48-50 L3</b> |                                    |                                    |
|------------------------------------|------------------------------------|------------------------------------|-------------------------------------|------------------------------------|------------------------------------|
| <b>Tr2</b>                         | <b>Tr3</b>                         | <b>Tr5</b>                         | <b>Tr2</b>                          | <b>Tr3</b>                         | <b>Tr5</b>                         |
| $\frac{21}{20 \times 349} = 0.3\%$ | $\frac{27}{15 \times 349} = 0.5\%$ | $\frac{82}{18 \times 349} = 1.3\%$ | <b>N.A</b>                          | $\frac{43}{15 \times 366} = 0.8\%$ | $\frac{68}{18 \times 366} = 1.0\%$ |

## 7. Slide preparation & imaging

For the screen and the candidate-testing:

Freshly dissected discs were placed on a slide containing a drop of S2 Schneider cell media (Schneider's insect medium [Invitrogen] supplemented with 10% fetal calf serum, 2 mM L-glutamine, 50 U/ml penicillin, and 50 µg/ml streptomycin), which was surrounded by a ring of Voltalef immersion oil. In order to avoid tissue damage upon placing the cover slip, two small cover slips were placed on each side of the Voltalef-S2 media ring acting as a support.

Pictures of air sac primordia were taken using a Leica TCS SP2 confocal system with the Leica Confocal Software and deconvoluted with Huygens Essential (Version 2.3.0) and subsequently processed with the Imaris 4.0.4 software (Bitplane).

For the flip-out clonal analysis:

Dorsal trunks, together with associated wing discs were dissected and mounted in 1XPBS using the "hanging drop" preparation method (as described in Sato and Kornberg, 2002).

Samples were imaged with a deconvolution imaging system (Intelligent Imaging Innovations).

## 8. Statistic analysis

To analyze the statistical significance of values presented in table R4, Chi-Square Test was employed to calculate the possibility that Tr2 and Tr3 could be similar in properties. The resulted P equaled 0.0832, which is larger than 0.05. This means that Tr2 and Tr3 could be essentially the same. This statistical analysis was also applied to calculate the possibility that Tr2 and Tr5 could be similar in properties and the resulted P equaled 0.0001, which is smaller than 0.05. This means that Tr2 and Tr5 could, as a matter of fact, be essentially distinct.

For the purpose of interpreting our data in clonal analysis aiming to understand the mitotic behavior of Tr2 cells, we calculated the probability of acquiring single-cell labeling using our heat shock scheme. Based on the assumption that no Tr2 cells have started to divide yet, the average clone induction efficiency is calculated as  $p^* = (1 \times 22 + 2 \times 2) / (20 \times 225) = 0.006$ . So the possibility of labeling one Tr2 cell at clone induction is  $P1 = 0.006 \times 20 = 0.12$ ; the possibility of labeling two cells at the same time during clone induction is:  $P2 = p^* \times p^* \times C_{20}^2 = 0.007$ . Similarly, the possibility of labeling three cells at the same time during clone induction is:  $P3 = p^* \times p^* \times p^* \times C_{20}^3 = 0.0002$ , which was considered highly unlikely in our data interpretation. When we use calculated P2 to estimated expected number of events during which two cells could be labeled, we find:  $225 \times P2 = 225 \times 0.007 = 1.6$ . This is very close to 2, the recorded number in our experiment. This consistency confirms the validity of our initial assumption that no Tr2 cells start to divide prior to L3. When P1 and P2 are being compared, we find:  $P1/P2 = 0.12/0.007 = 17$ . So the possibility that clones observed in our experiments are derived from one single mother cell is:  $17/(17+1) = 0.94$ . So we have the confidence to say that the predominant clones we recorded are indeed derived from the same mother cell, which is essential for the estimation of the number of cell cycles Tr2 cells can possibly go through during the observation window.

## **II. Results**





## *1. A MARCM-BASED SCREEN AIMING TO IDENTIFY GENES FUNCTIONING IN THE PROCESS OF TRACHEAL CELL MIGRATION DURING ASP MORPHOGENESIS*

---

FGF-mediated cell migration plays an important role during *Drosophila* embryonic tracheal development, which also proves essential during ASP morphogenesis (Klambt et al. 1992; Sutherland et al. 1996; Affolter et al. 2003; Ghabrial et al. 2003; Uv et al. 2003; Sato and Kornberg, 2002; Cabernard and Affolter, 2005). Over the years, additional factors besides the FGF ligand, Branchless (Bnl)/FGF, and its receptor Breathless (Btl)/FGFR, have also been shown to be required for FGF-mediated cell migration, such as Sulfateless (Sfl) and Sugarless (Sgl), the FGFR coreceptors; Downstream-of-FGFR (Dof), the cytoplasmic adaptor; Corkscrew (Csw), a phosphatase recruited to FGFR upon its activation; and components of Ras/MAPK pathway (Michelson et al, 1998; Vincent et al. 1998; Imam et al. 1999; Lin et al. 1999; Pellegrini 2001; Petit et al. 2004; Cabernard and Affolter, 2005). Both EGFR and FGFR signaling pathways have been shown to play an important role during ASP morphogenesis, and interestingly, the ETS transcription factor Pointed appears to be exclusively required for FGF-mediated cell migration and to be dispensable for EGF-mediated cell division/survival (Cabernard and Affolter, 2005). To get a better understanding of: 1) how FGF ligand-receptor-coreceptor binding, which takes place at the cell surface, leads to the activation of Ras/MAPK pathway; 2) if and how Ras/MAPK activation leads to changes of cytoskeleton dynamics, finally resulting in the cell migrating behavior, additional players needed to be identified. For this purpose, we undertook a large-scale, MARCM-based genetic screen with fly lines carrying EMS-induced mutations.

### **1.1 Screening procedures**

Our screen started with EMS mutagenesis performed in the lab of Dr. Maria Leptin, our collaborator (Baer et al. 2007). A F<sub>3</sub> mutagenesis scheme was designed to establish mutant fly stocks carrying random EMS-induced mutations. Since our analysis focused on genes located on the left arm of the second chromosome, we used a *FRT40A* chromosome in the EMS-treated stock.

To induce MARCM mutant clones, ~10 males of each of these putative heterozygous mutant lines were crossed *en masse* to ~30 so-called *FRT40A* MARCM females; these females carry a *heat-shock-flippase* (*hs-flp*) source, a *FRT40A* chromosome recombined with a *tubulin-Gal80* (*tub-Gal80*) construct, and a third chromosome bearing a *breathless-Gal4* (*btl-Gal4*), a *UAS-CD8-*

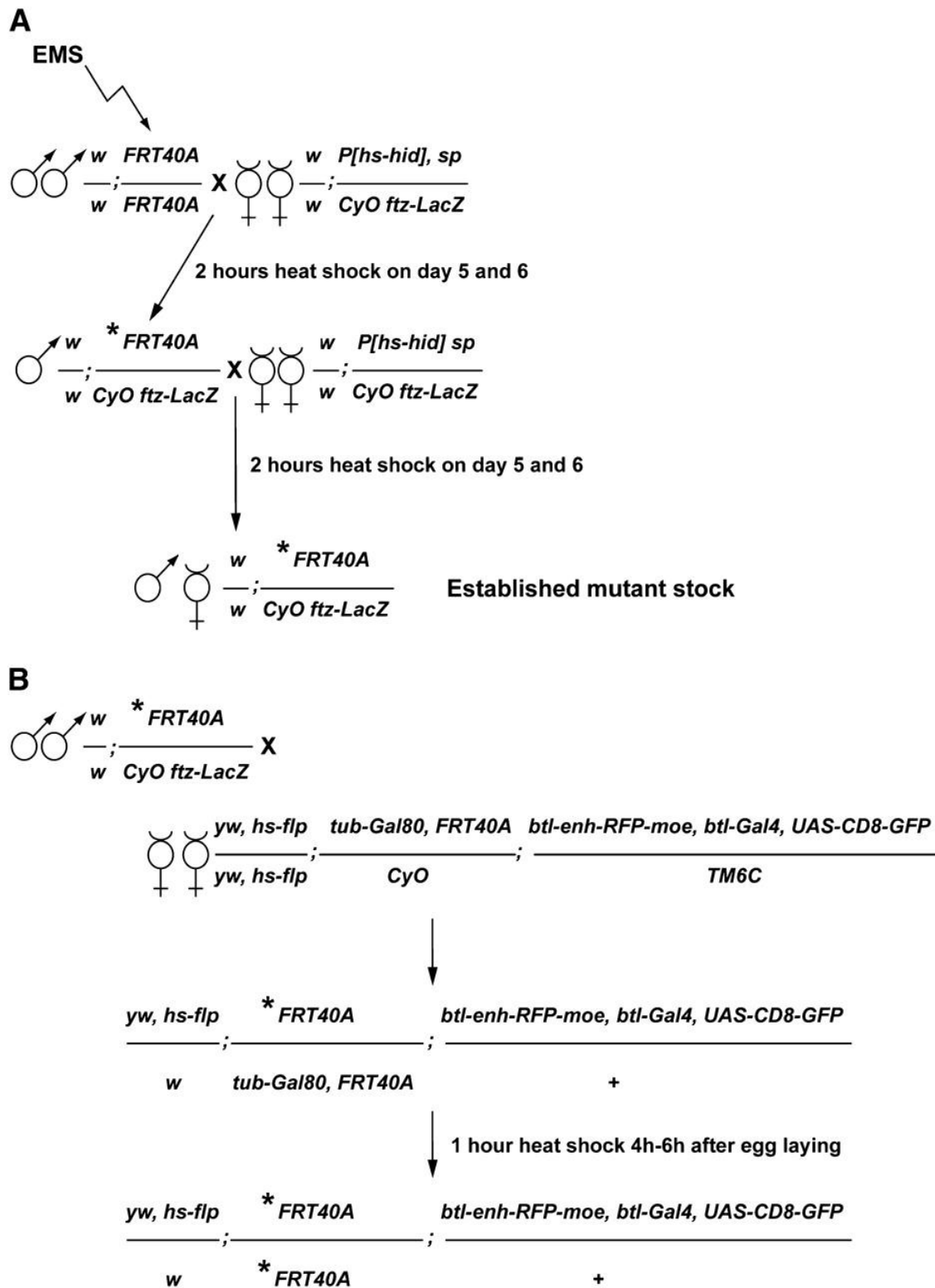


**Figure R1.** Mutagenesis and crossing scheme for generating MARCM clones of cells homozygous for mutations on chromosome 2L. (A) Scheme for the establishment of *Drosophila* stocks carrying mutations on the second chromosome. Ethyl methanesulfonate (EMS)-induced mutations were randomly generated in the genome of males bearing a

*FRT40A* chromosome. EMS-treated males were subsequently crossed to females carrying an *hs-hid* construct and a balancer chromosome. The asterisk represents the induced mutation. Balanced mutant stocks were established in two generations. A heat-shock regime applied to the progeny of the  $F_0$  and  $F_1$  generation induced the expression of the *hs-hid* construct and the death of animals due to ectopic apoptosis. Therefore, establishment of the heterozygous mutant stocks did not require virgin female collection. (B) Crossing scheme for inducing MARCM clones in the *Drosophila* larval tracheal system.  $F_2$  heterozygous mutant males were crossed to so-called MARCM females carrying a *heat-shock-flippase* (*hs-flp*) source, a *FRT40A* chromosome recombined with a *tubulin-Gal80* (*tub-Gal80*) construct, and a third chromosome bearing the *breathless-Gal4* (*btl-Gal4*), *UAS-CD8-green fluorescent protein* (*UAS-CD8-GFP*), and *breathless enhancer-red fluorescent protein-moesin* (*btl-enh-RFP-moe*) constructs. Heat-shock treatment of generation  $F_3$  induced the FLP-driven recombination at FRT sequences, which segregated the *tub-Gal80* construct away from the induced mutation. Therefore, the *btl-Gal4*-dependent expression of CD8-GFP was possible only in clones of cells homozygous for the induced mutation.

*green fluorescent protein* (*UAS-CD8-GFP*), and a *breathless enhancer-red fluorescent protein-moesin* (*btl-enh-RFP-moe*) construct (Cabernard and Affolter, 2005). Using this genetic setup, mutant clones can be induced via FLP-mediated recombination at *FRT40A* sites early in embryogenesis and visualized as GFP-positive groups of cells following the loss of Gal80. The Gal80-independent action of the *btl* enhancer enables the visualization of the entire tracheal system by the expression of the *RFP-moe* fusion construct. FLP-driven recombination was induced in early embryos according to the procedure described (Cabernard and Affolter, 2005).

Embryos were subsequently allowed to develop and third instar larvae displaying GFP-labeled patches of cells in the tracheal system were collected. Wing discs were dissected and ASPs bearing MARCM clones were analyzed using laser confocal microscopy in live tissues, without any fixation or staining treatment.

It has previously been reported that MARCM clones of wild-type cells contribute to the growing tip of ASP in ~70% of the observed cases (Cabernard and Affolter, 2005). It was also shown that the FGFR signaling pathway is crucial for tracheal cell migration, as MARCM clones mutant for

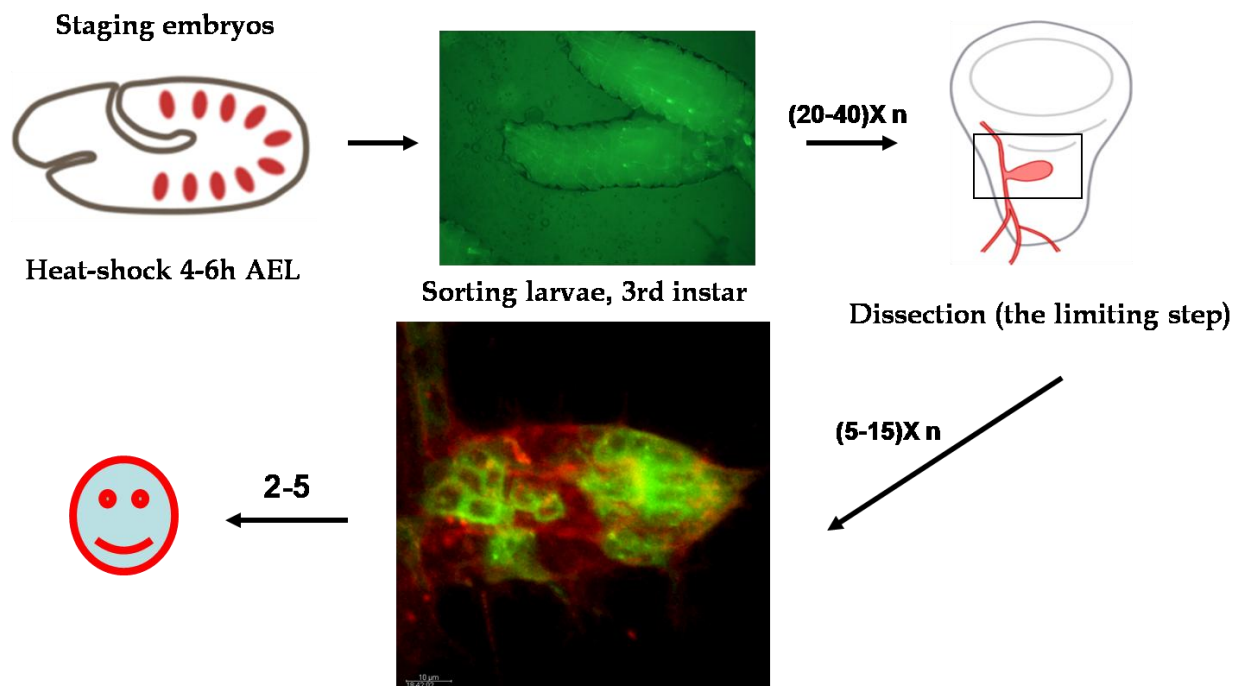


**Figure R2.** A description of screening procedures. MARCM clones were induced during early embryogenesis, which were then allowed to develop into L3 larval stage. Sorting, dissecting, and subsequent imaging procedures were performed to identify genes, once mutated, could give cell migration defect during ASP morphogenesis.

*Drosophila btl/FGFR* or for certain downstream effectors of the FGFR signaling pathway remained in the proximal region of ASP and never colonized the migrating tip. In our attempt to isolate genes necessary for tracheal cell migration during ASP morphogenesis, mutant lines displaying a migration defect, which was: with <40% of the MARCM clones present at the ASP distal tip, were kept for further analysis. Putative mutant lines were systematically retested a second and eventually a third time.

## 1.2 Summary of the screening outcome

As summarized in the following table R1, a total of 1123 mutant lines were tested. About 11% (122) of these lines produced no larvae bearing GFP-labeled MARCM clones in the trachea; about 8% (90) produced larvae bearing clones in the trachea but not in the ASP; about 77% (864) of these lines produced wild-type MARCM clones in the ASP; in the rest of about 4% (47) of these lines, ASP clones showing defects in cell migration were recovered. Lines displaying a tracheal cell migration phenotype were further classified into two

categories: class I showed a strict migration phenotype and class II showed a migration and/or proliferation phenotype. In

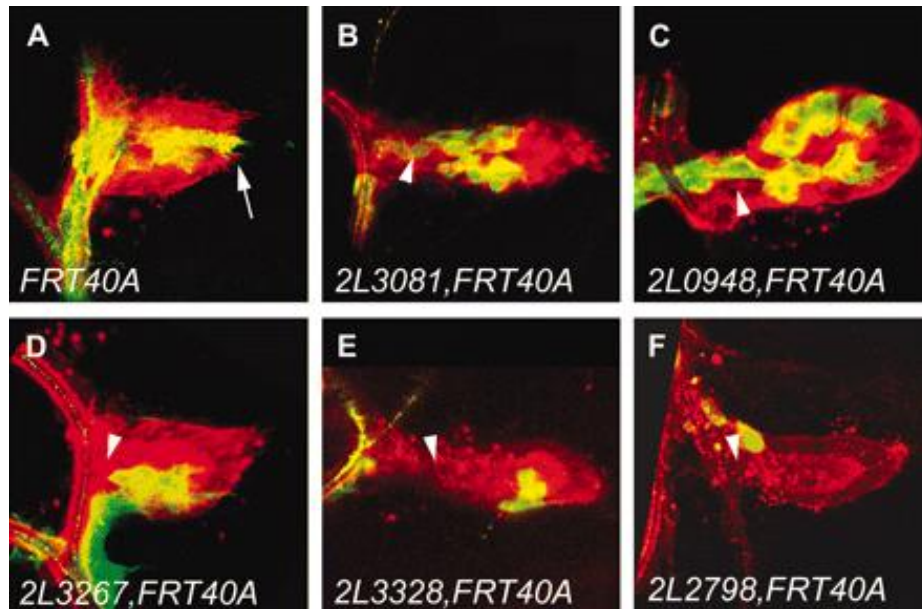


**Figure R3.** Migration defects of various mutants isolated during the screen. Confocal images of *Drosophila* ASPs during L3 are shown. All tracheal cells are labeled in red (RFP-moesin) and MARCM clones are labeled in green (CD8-GFP). The *FRT40A* chromosome (A) was used as a wild-type control. Isolated mutants were classified in two categories: class I mutants, characterized by a strict migration phenotype and displaying clones of normal size, such as observed in the lines *2L3081, FRT40A* (B), *2L0948, FRT40A* (C), and *2L3267, FRT40A* (D), and class II mutants, showing a migration defect and additionally a reduced size of MARCM clones, such as observed in lines *2L3328, FRT40A* (E) and *2L2798, FRT40A* (F). Arrows indicate the distal tip of the ASP. Arrow heads indicate the proximal region of the ASP.

both categories, homozygous lethal and viable alleles were recovered. In class I mutants, 34 out of a total of 38 lines are homozygous lethal; in class II mutants, 8 out of a total of 9 are homozygous lethal.

**Table R1. Summary of The Screening Outcome**

|   |                  |
|---|------------------|
| <b>Tested mutant lines</b>  | <b>1123</b>      |
| <b>Lines with larvae displaying no MARCM clones</b>                         | <b>122 (11%)</b> |
| <b>Lines with air sacs displaying no MARCM clones</b>                       | <b>90 (8%)</b>   |
| <b>Lines showing no tracheal cell migration and proliferation phenotype</b> | <b>864 (77%)</b> |
| <b>Lines showing a tracheal cell migration phenotype (class I)</b>          | <b>38</b>        |
| <b>Class I lethal lines</b>   | <b>34</b>        |
| <b>Class I not lethal lines</b>   | <b>4</b>         |
| <b>Lines showing a tracheal cell proliferation phenotype (class II)</b>     | <b>9</b>         |
| <b>Class II lethal lines</b>  | <b>8</b>         |
| <b>Class II not lethal lines</b>  | <b>1</b>         |

### **1.3 Mapping and complementation analysis**

To map lethal hits in candidate lines, we employed traditional complementation analysis. We took advantage of the Exelixis targeted deficiency kit, each line of which removed on average only ~25 genes in the fly genome (Parks et al., 2004). Exelixis deficiencies covered ~80% of transcription units on chromosomal arm 2L that had been described by the FlyBase Consortium. All the EMS candidate mutant lines were crossed to homozygous lethal Exelixis deficiency lines and progenies of these crosses were scored for the absence of viable *trans*-heterozygotes. This approach allowed us to map lethal hits in 20 mutant strains (Table R2). On the basis of these lethality tests, we found that 18 lines carried at least one lethal hit (no complementation between the lethal hit and either one deficiency or a group of overlapping deficiencies) and that 2 lines carried at least two lethal hits (no complementation between the lethal hit and two non-overlapping deficiencies) on the left arm of the second chromosome.

Mutant lines mapping to the same genomic area were crossed *inter se* to determine whether they belonged to the same complementation group. Using this procedure, we found that *2L1665* and *2L2475*, both carrying a lethal hit mapping to *Df(2L)exel6042*, as well as *2L2896* and *2L3297*, carrying a lethal hit mapping to *Df(2L)exel7049* and *Df(2L)exel8026*, did not complement each other's lethality (Table R2), suggesting that these mutations represent two independent alleles of the same gene.

To identify the affected loci in the 20 mapped mutant lines, we used available lethal mutations (previously isolated mutations or transposon insertions) in the region uncovered by the corresponding Exelixis deficiencies and tested whether these mutations complemented the lethality of the corresponding EMS-induced mutants. Alternatively, when no lethal mutation was available in the region of interest, a sequencing approach was used. These approaches led to the identification of two complementation groups responsible for lethality (see below).

Two candidate lines, 2L2896 and 2L3297, turned out to bear different mutations of the same gene, *stam* (*signal transducing adaptor molecule*). Line 2L2881 turned out to carry a mutation for the gene *mhc* (*myosin heavy chain*).

Note to Table R2:

Lines displaying a strict tracheal cell migration phenotype, characterized by the observation of <40% of MARCM clones reaching the distal tip of the ASP were retained for further analysis (class I mutants). We recovered 38 strains meeting this criterion (see also Table R1). For each candidate line, numbers refer to the amount of MARCM clones observed at the distal tip of the ASP (column 2) and in the proximal region (column 3), to the total number of observed clones (column 4), and to the percentage of MARCM clones localized at the ASP distal tip (column 5; Figure R3). We recovered 34 homozygous lethal lines and 4 homozygous viable lines. Exelixis deficiencies, other independent class I mutants or previously characterized alleles, and names of mutants belonging to the same complementation group as other class I mutants we isolated, are indicated in columns 7, 8, and 9, respectively.

**Table R2A. Overview of the phenotype and mapping of the isolated class I mutant lines**

| Candidate lines | Clones at the distal tip | Clones at the proximal region | Analyzed clones | % at the distal tip | Lethal line | Mapping to                 | Does not complement to | Identified gene |
|-----------------|--------------------------|-------------------------------|-----------------|---------------------|-------------|----------------------------|------------------------|-----------------|
| 2L.3267         | 0                        | 26                            | 26              | 0.0                 | Yes         | Df(2L)excl6039, 8036       |                        |                 |
| 2L.2870         | 0                        | 39                            | 39              | 0.0                 | Yes         |                            |                        |                 |
| 2L.2677         | 1                        | 29                            | 30              | 3.3                 | Yes         |                            |                        |                 |
| 2L.2436         | 1                        | 15                            | 16              | 6.3                 | Yes         | Df(2L)excl8012, 7021       |                        |                 |
| 2L.3186         | 1                        | 13                            | 14              | 7.1                 | Yes         | Df(2L)excl7038             |                        |                 |
| 2L.3189         | 1                        | 12                            | 13              | 7.7                 | Yes         |                            |                        |                 |
| 2L.3081         | 4                        | 31                            | 35              | 11.4                | Yes         | Df(2L)excl8038             |                        |                 |
| 2L.2881         | 2                        | 14                            | 16              | 12.5                | Yes         | Df(2L)excl6027, 7067       | <i>mhc1</i>            | <i>mhc</i>      |
| 2L.3298         | 1                        | 6                             | 7               | 14.3                | Yes         | Df(2L)excl7034             |                        |                 |
| 2L.2475         | 1                        | 6                             | 7               | 14.3                | Yes         | Df(2L)excl6042             | 2L.1665                |                 |
| 2L.2653         | 2                        | 11                            | 13              | 15.4                | Yes         | Df(2L)excl6047, 7055       |                        |                 |
| 2L.1683         | 2                        | 11                            | 13              | 15.4                | Yes         | Df(2L)excl7038             |                        |                 |
| 2L.3297         | 4                        | 21                            | 25              | 16.0                | Yes         | Df(2L)excl8026, 7049       | 2L.2896                | <i>stam</i>     |
| 2L.2896         | 5                        | 24                            | 29              | 17.2                | Yes         | Df(2L)excl7038, 8026, 7049 | 2L.3297                | <i>stam</i>     |



**Table R2B.** Overview of the phenotype and mapping of the isolated class I mutant lines

| Candidate lines | Clones at the distal tip | Clones at the proximal region | Analyzed clones | % at the distal tip | Lethal line | Mapping to     | Does not complement to | Identified gene |
|-----------------|--------------------------|-------------------------------|-----------------|---------------------|-------------|----------------|------------------------|-----------------|
| 2L.2828         | 6                        | 26                            | 32              | 18.8                | Yes         |                |                        |                 |
| 2L.2985         | 4                        | 15                            | 19              | 21.1                | Yes         |                |                        |                 |
| 2L.3073         | 3                        | 10                            | 13              | 23.1                | Yes         |                |                        |                 |
| 2L.2845         | 10                       | 32                            | 42              | 23.8                | Yes         |                |                        |                 |
| 2L.2853         | 8                        | 25                            | 33              | 24.2                | Yes         |                |                        |                 |
| 2L.2718         | 2                        | 5                             | 7               | 28.6                | Yes         |                |                        |                 |
| 2L.2775         | 7                        | 17                            | 24              | 29.2                | Yes         | Df(2L)exel6028 |                        |                 |
| 2L.1710         | 4                        | 9                             | 13              | 30.8                | Yes         |                |                        |                 |
| 2L.1685         | 7                        | 15                            | 22              | 31.8                | Yes         | Df(2L)exel8003 |                        |                 |
| 2L.948          | 9                        | 18                            | 27              | 33.3                | Yes         |                |                        |                 |
| 2L.2921         | 6                        | 12                            | 18              | 33.3                | Yes         |                |                        |                 |
| 2L.1561         | 3                        | 6                             | 9               | 33.3                | Yes         | Df(2L)exel6042 |                        |                 |
| 2L.1540         | 12                       | 22                            | 34              | 35.3                | Yes         | Df(2L)exel6044 |                        |                 |
| 2L.1809         | 10                       | 18                            | 28              | 35.7                | Yes         |                |                        |                 |

**Table R2C. Overview of the phenotype and mapping of the isolated class I mutant lines**

| Candidate lines | Clones at the distal tip | Clones at the proximal region | Analyzed clones | % at the distal tip | Lethal line | Mapping to           | Does not complement to | Identified gene |
|-----------------|--------------------------|-------------------------------|-----------------|---------------------|-------------|----------------------|------------------------|-----------------|
| 2L.2938         | 9                        | 16                            | 25              | 36.0                | Yes         | Df(2L)excl6277       |                        |                 |
| 2L.1665         | 9                        | 16                            | 25              | 36.0                | Yes         | Df(2L)excl6042       | 2L.2475                |                 |
| 2L.3179         | 8                        | 14                            | 22              | 36.4                | Yes         | Df(2L)excl7022       |                        |                 |
| 2L.2615         | 8                        | 14                            | 22              | 36.4                | Yes         | Df(2L)excl6031       |                        |                 |
| 2L.3011         | 13                       | 22                            | 35              | 37.1                | Yes         | Df(2L)excl6042, 8040 |                        |                 |
| 2L.1794         | 8                        | 13                            | 21              | 38.1                | Yes         |                      |                        |                 |
| 2L.2468         | 1                        | 7                             | 8               | 12.5                | No          |                      |                        |                 |
| 2L.2366         | 1                        | 7                             | 8               | 12.5                | No          |                      |                        |                 |
| 2L.883          | 4                        | 12                            | 16              | 25.0                | No          |                      |                        |                 |
| 2L.3064         | 7                        | 15                            | 22              | 31.8                | No          |                      |                        |                 |

## 2. A MARCM-based approach of direct candidate-testing to identify genes functioning in the process of tracheal cell migration during ASP morphogenesis

---

### 2.1 An overview

Let there be light.

Let there be cell migration.

Cell migration, an integrated process consisting of polarization, protrusion, traction, and retraction, keeps us company from life to death. It drives the morphogenetic processes of the embryo during its development. Failure of cells to migrate, or migration of cells to inappropriate locations, can result in life-threatening consequences such as the congenital brain defects. In the adult, cell migration plays a central role during homeostasis, without which such processes as mounting an effective immune response or repairing the injured tissues would not be possible. Moreover, pathological cell migration can cause vascular diseases, chronic inflammatory diseases, tumor formation and metastasis.

Cell migration is such a fundamental process that it has remained the focus of extensive investigation for decades, and at least five different systems have been developed in *Drosophila* alone to understand the basic mechanisms underlying it, such as the migration of primordial germ cells (PGC), of hemocytes, of border cells, of mesodermal cells, and of tracheal cells. Systems developed in other organisms, such as *Dictyostelium*, have also contributed greatly to our current understanding of cell migration. What has come into light is that different types of cells use diverse although overlapping molecular components for achieving their motility. Based on this emerging theme, I undertook an approach of direct candidate-testing, in order to identify those important players employed by tracheal cells for their migration during ASP formation.

To get started, I first established the fact that about 66% (out of a total of 32 recorded samples) of wild-type MARCM clones could occupy the tip (See Figure R4 for images of randomly-chosen clones). Bearing this in mind, I then went on to test selected candidates and examined if those mutant clones would demonstrate impaired ability of occupying the tip of ASP. The simple criterion used is to compare the percentage of mutant clones occupying the tip with that of wild-type clones. As summarized in table R3, 12 different alleles of 9 candidate genes were tested altogether.

Table R3 Summary of candidate-testing results

| Alleles tested                 | Number of samples recorded | Number of clones localized at ASP tip | Percentage of clones localized at ASP tip |
|--------------------------------|----------------------------|---------------------------------------|---|
| <i>wt</i>                      | 32                         | 21                                    | 66%                                       |
| <i>wasp3</i>                   | 15                         | 4                                     | 27%                                       |
| <i>scar-delta37</i>            | 22                         | 8                                     | 36%                                       |
| <i>scar-K13811</i>             | 29                         | 14                                    | 50%                                       |
| <i>sop-Q25st</i>               | 16                         | 4                                     | 25%                                       |
| <i>sop-W108R</i>               | 17                         | 6                                     | 35%                                       |
| <i>sop-Q25sd</i>               | 34                         | 19                                    | 56%                                       |
| <i>ena</i>                     | 25                         | 11                                    | 44%                                       |
| <i>th6</i>                     | 16                         | 5                                     | 31%                                       |
| <i>hrs</i>                     | 28                         | 1                                     | 4%  |
| <i>mmp1 (K07511)</i>           | 10                         | 8                                     | 80%                                       |
| <i>mmp1 (Q112)+mmp2 (W307)</i> | 8                          | 5                                     | 63%                                       |

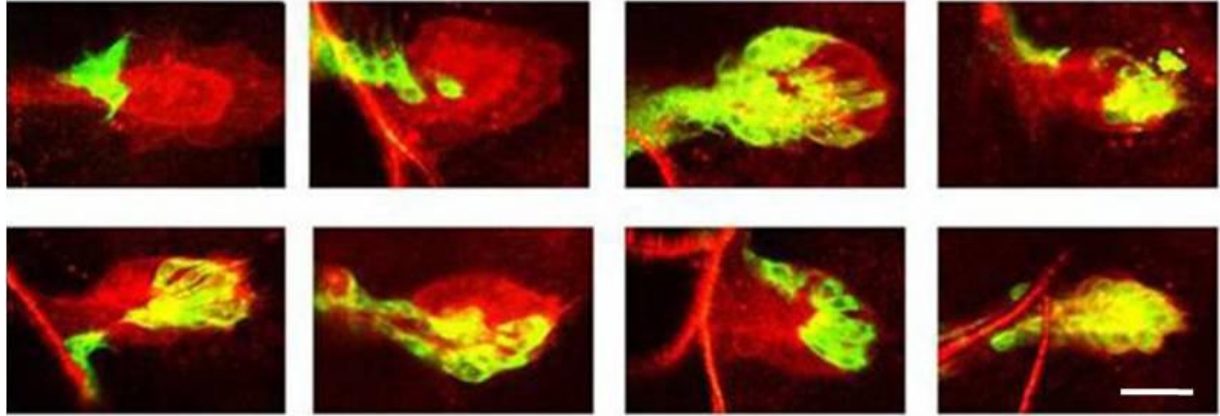


**Figure R4.** Randomly-chosen examples of wild-type MARCM clones, 66% (total =32) of which occupied the tip of ASP. (ASP labeled in red by *btlenh-RFPmoesin*, clones labeled in green by *UAS-CD8GFP*, scale bar=25  $\mu$ m)

## 2.2 *arp2/3*, *wasp*, and *scar* mutant clones

Actin related protein 2/3 (Arp 2/3) complex, consisting of seven different subunits, has been demonstrated to function in critical actin organization and all actin-dependent processes. It nucleates new actin filaments in response to upstream signals and cross-links newly formed filaments into Y-branched arrays characterized by a stereotypical branch angle of 70 degree.

To test if components of *Drosophila* Arp 2/3 complex would be required for ASP cell migration, MARCM clones of three distinct alleles of *sop* (encoding Arpc1, a subunit of Arp2/3 complex) were examined. 25% of (4 out of a total of 16) examined samples of *sop-Q25st*, 35% of (6 out of a total of 17) examined samples of *sop-w108R*, and 56% of (19 out of a total of 34) examined samples of *sop-Q25sd* were observed to populate the ASP tip. Compared with the percentage of 66% of *wt* clones, cells mutant for *sop* demonstrated a reduced ability to localize to the tip of ASP, the severity of phenotypes depending on the particular allele affected (See Figure R5).

Wasp (Wiskott-Aldrich syndrome protein) and Scar (Suppressor of cAR) have been described as actin nucleation-promoting factors (NPFs). *wasp*, the *Drosophila* gene homologue of the human *wasp* has been demonstrated to be required specifically for proper execution of asymmetric cell divisions in neural lineages. SCAR, on the other hand, has been shown to function as a primary regulator of Arp2/3-dependent morphological events in *Drosophila* and regulates predominantly the formation of both filopodia and lamellipodia (Ben-Yaacov, et al., 2001; Zallen et al., 2002).

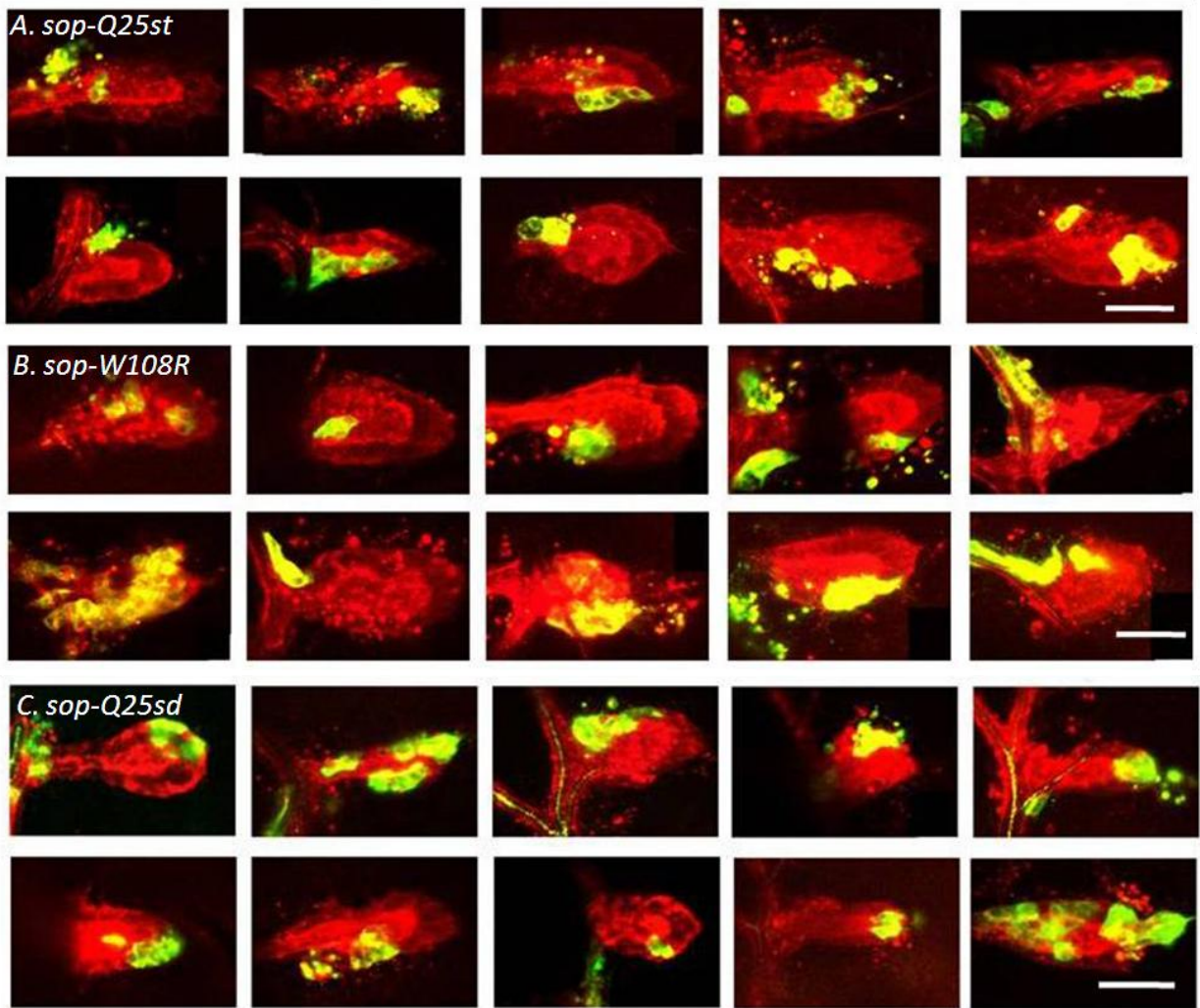


**Figure R5.** Randomly-chosen examples of *sop* (encoding Arpc1, a subunit of Arp2/3 complex) MARCM clones. Three alleles were tested. 25% (total =16) of *sop-Q25st* (A) occupied the tip of ASP; 35% (total =17) of *sop-w108R* (B) occupied the tip of ASP; 56% (total =34) of *sop-Q25sd* (C) occupied the tip of ASP. These data demonstrated a reduced ability of mutant clones to localize to the tip of ASP and the severity of phenotypes depended on alleles tested. (ASP labeled in red by *btlenh-RFPmoesin*, clones labeled in green by *UAS-CD8GFP*, scale bar=25  $\mu$ m)

To test if *Drosophila wasp* would be required for ASP cell migration, MARCM clones of the allele *wasp3* were examined. 27% of (4 out of a total of 15) examined samples were observed to populate the ASP tip. Compared with the percentage of 66% of *wt* clones capable of populating the ASP tip, cells mutant for *wasp3* demonstrated a reduced ability to localize to the tip of ASP (See Figure R6).

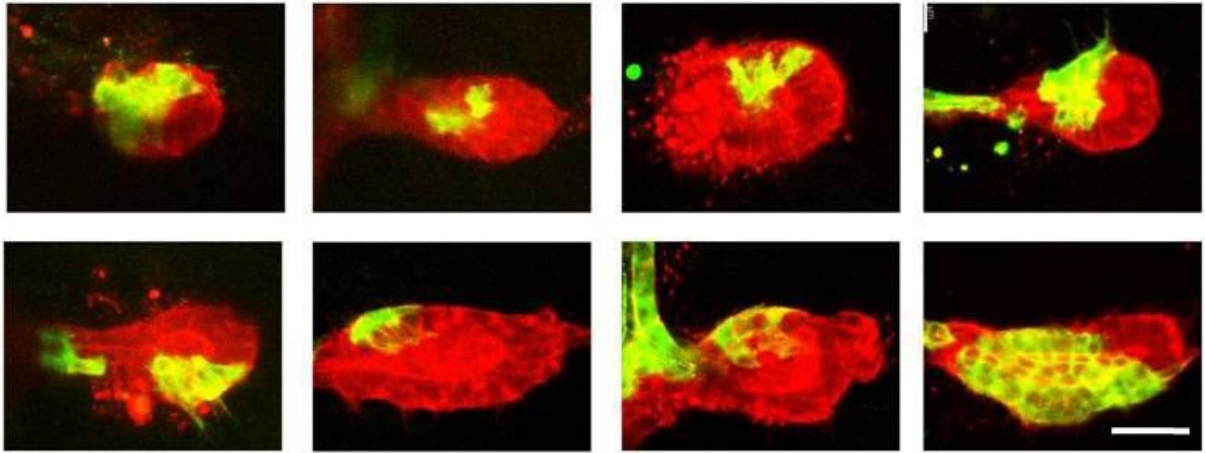


**Figure R6.** Randomly-chosen examples of *wasp3* MARCM clones, 27% (total =15) of which occupied the tip of ASP, demonstrating a reduced ability to localize to the tip of ASP. (ASP labeled in red by *btlenh-RFPmoesin*, clones labeled in green by *UAS-CD8GFP*, scale bar=25  $\mu$ m)

To test if *Drosophila scar* would be required for ASP cell migration, MARCM clones of two alleles of *scar* were examined. 36% of (8 out of a total of 22) examined samples of *scar-delta37* and 50% of (14 out of a total of 29) examined samples of *scar-K13811* were observed to populate the ASP tip. Compared with the percentage of 66% of *wt* clones, cells mutant for *scar* demonstrated a reduced ability to localize to the tip of ASP (See Figure R7).

### 2.3 *ena* mutant clones

Enabled (Ena) belongs to a conserved family of actin regulatory proteins, Ena/VASP proteins. It associates with barbed ends of actin filaments and antagonizes filament capping to help form long, unbranched actin filaments; it reduces the density of Arp2/3-dependent actin filament branches and bind profilin at sites of actin polymerization; it has been implicated in actin-based



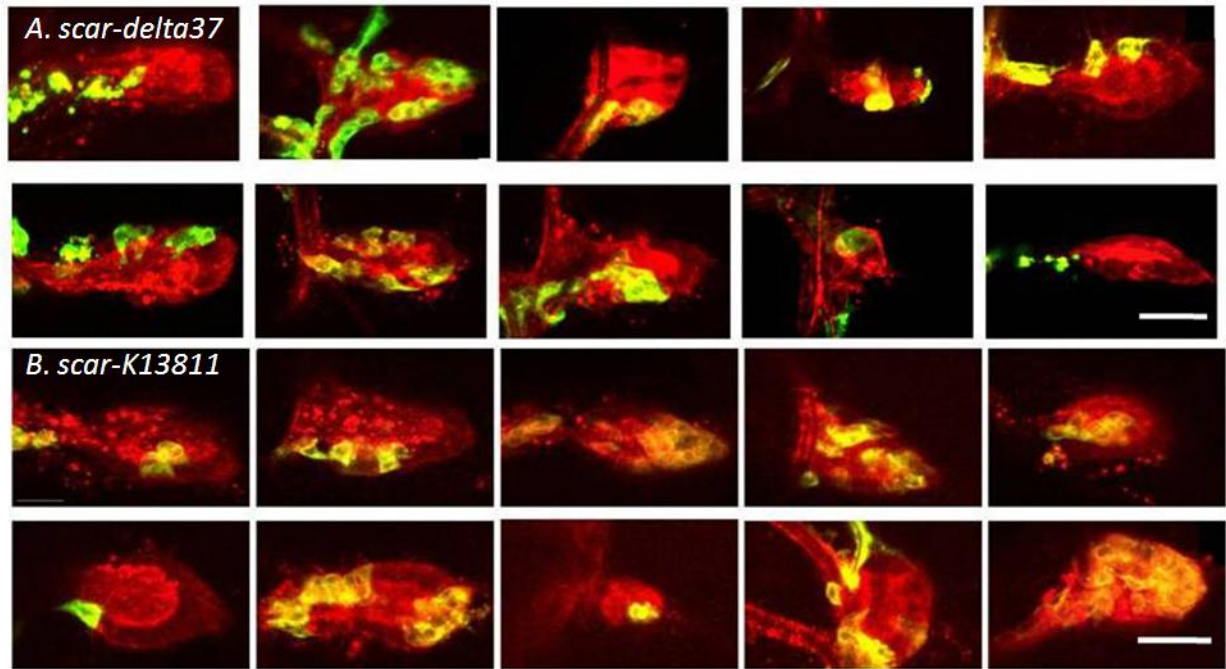


**Figure R7.** Randomly-chosen examples of *scar* MARCM clones. Two alleles were tested. 36% (total =22) of *scar-delta37* occupied the tip of ASP and 50% (total =29) of *scar-K1381* occupied the tip of ASP, demonstrating a reduced ability to localize to the tip of ASP. (ASP labeled in red by *btlenh-RFPmoesin*, clones labeled in green by *UAS-CD8GFP*, scale bar=25  $\mu$ m)

processes such as fibroblast migration, axon guidance, T cell polarization, epithelial morphogenesis, and the actin-based motility of the intracellular pathogen *Listeria monocytogenes*. In *Drosophila*, *Ena* has been shown to localize to the tip of filopodia, to localize to adherens junctions of most epithelial cells, to interact genetically with Arm and P-120 catenin, to interact physically with Netrin and Slit receptors (Fra and Robo), to interact with Receptor Phosphatase (Dlar) in axon guidance, and to interact directly with Khc (kinesin heavy chain), which functions in fast-axonal-transport (Forsthoefel et al., 2005; Li et al., 2005; Martin et al., 2005).

To test if *Drosophila ena* would be required for ASP cell migration, MARCM clones of *ena* were examined. 44% of (11 out of a total of 25) examined samples was observed to populate the ASP tip. Compared with the percentage of 66% of *wt* clones, cells mutant for *ena* demonstrated a slightly reduced ability to localize to the tip of ASP (See Figure R8).



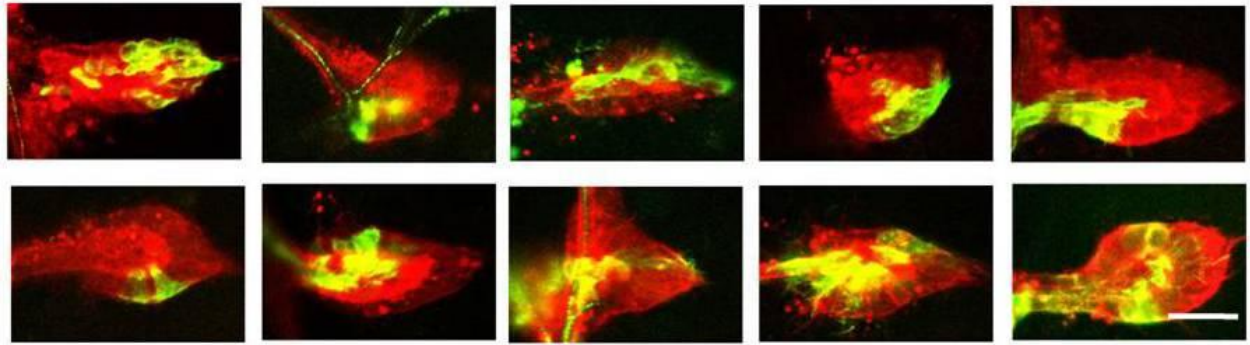


**Figure R8.** Randomly-chosen examples of *ena* MARCM clones, 44% (total =25) of which occupied the tip of ASP, demonstrating a reduced ability to localize to the tip of ASP. (ASP labeled in red by *btlenh-RFPmoesin*, clones labeled in green by *UAS-CD8GFP*, scale bar=25  $\mu$ m)

#### 2.4 *diap1* mutant clones

*Drosophila* inhibitor of apoptosis 1 (DIAP1), encoded by a gene called *thread* (*th*) has been identified in a screen searching for new genes that function in Rac-dependent cell motility during *Drosophila* border cell migration. The loss-of-function mutations in *th* caused migration defects, surprisingly, however, did not cause apoptosis. It has been shown that profilin and DIAP1 associated with Rac in a nucleotide-independent manner and therefore possibly regulated actin dynamics via protein-protein interaction within a complex (Geisbrecht and Montell, 2004).

To test if *Drosophila th* would be required for ASP cell migration, MARCM clones of the allele *th6B* were examined. 31% of (5 out of a total of 16) examined samples was observed to populate the ASP tip. Compared with the percentage of 66% of *wt* clones, cells mutant for *th6B* demonstrated a reduced ability to localize to the tip of ASP (See Figure R9).

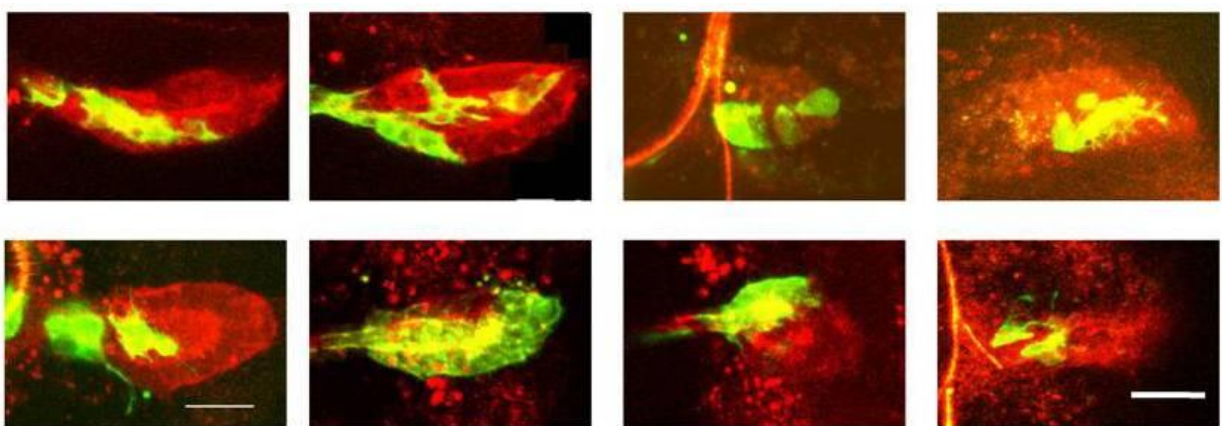


**Figure R9.** Randomly-chosen examples of *th* (encoding *Drosophila* inhibitor of apoptosis 1) MARCM clones, 31% (total =16) of which occupied the tip of ASP, demonstrating a reduced ability to localize to the tip of ASP. (ASP labeled in red by *btlenh-RFPmoesin*, clones labeled in green by *UAS-CD8GFP*, scale bar=25  $\mu$ m)

## 2.5 *hrs* mutant clones

Following endocytosis, an endosomal protein machinery capable of ubiquitin-binding is responsible for sorting endocytosed membrane proteins into intra-luminal vesicles of multi-vesicular endosomes (MVEs) for subsequent degradation in lysosomes. Hrs (Hepatocyte growth factor-regulated tyrosine kinase substrate) and endosomal sorting complex required for transport (ESCRT)-I, -II and -III are central components of this machinery. Hrs has been previously shown to down-regulate RTK signaling. And loss of *hrs* decreased RTK degradation, but it did not perturb the process of border cell migration (Lloyd et al., 2002; Jékely and Rørth, 2003; Jékely et al., 2005)

To test if *Drosophila hrs* would be required for ASP cell migration, MARCM clones of *hrs* were examined. 4% of (1 out of a total of 28) examined samples was observed to populate the ASP tip. Compared with the percentage of 66% of *wt* clones, cells mutant for *hrs* demonstrated a dramatically reduced ability to localize to the tip of ASP.

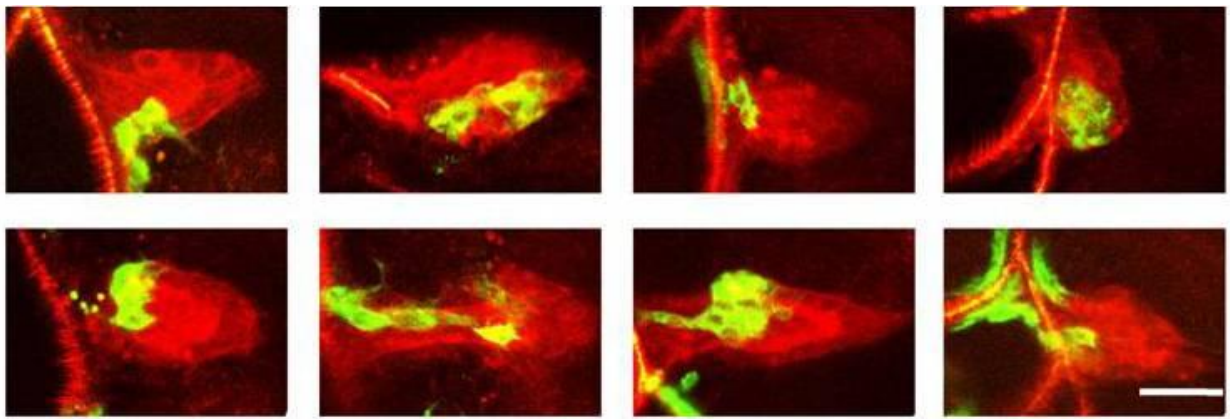


**Figure R10.** Randomly-chosen examples of *hrs* MARCM clones, 4% (total =28) of which occupied the tip of ASP, demonstrating a dramatically reduced ability to localize to the tip of ASP. (ASP labeled in red by *btlenh-RFPmoesin*, clones labeled in green by *UAS-CD8GFP*, scale bar=25  $\mu$ m)

## 2.6 *mmp* mutant clones

The matrix metalloproteinase (MMP) family of extracellular proteases is conserved throughout the animal kingdom. MMPs are zinc-dependent endo-peptidases and are capable of degrading all kinds of extracellular matrix proteins. In addition, they have also been shown to get involved in the cleavage of cell surface receptors, the release of apoptotic ligands (such as the FAS ligand), and chemokine in/activation. MMPs are also thought to play a role in cell proliferation, migration (adhesion/dispersion), differentiation, angiogenesis, apoptosis and host defense. In *Drosophila* there exist two *mmp* genes: *mmp1* and *mmp2*. *Drosophila* MMPs have been demonstrated to be required for tissue remodeling, axon guidance, dendritic remodeling, developmental tissue invasion, and tumor invasiveness (Page-McCaw et al., 2003; Page-McCaw, 2007).

To test if *Drosophila mmp* would be required for ASP cell migration, MARCM clones of *mmp* were examined. 80% of (8 out of a total of 10) examined samples for the *mmp2* allele *mmp2-K07511* was observed to populate the ASP tip, demonstrating an increased ability to localize to the tip of ASP, compared with *wt* clones. 63% of (5 out of a total of 8) examined samples of the double mutant, *mmp2-W307* and *mmp1-Q112*, was observed to populate the ASP tip, demonstrating a similar ability as *wt* clones to localize to the tip of ASP.

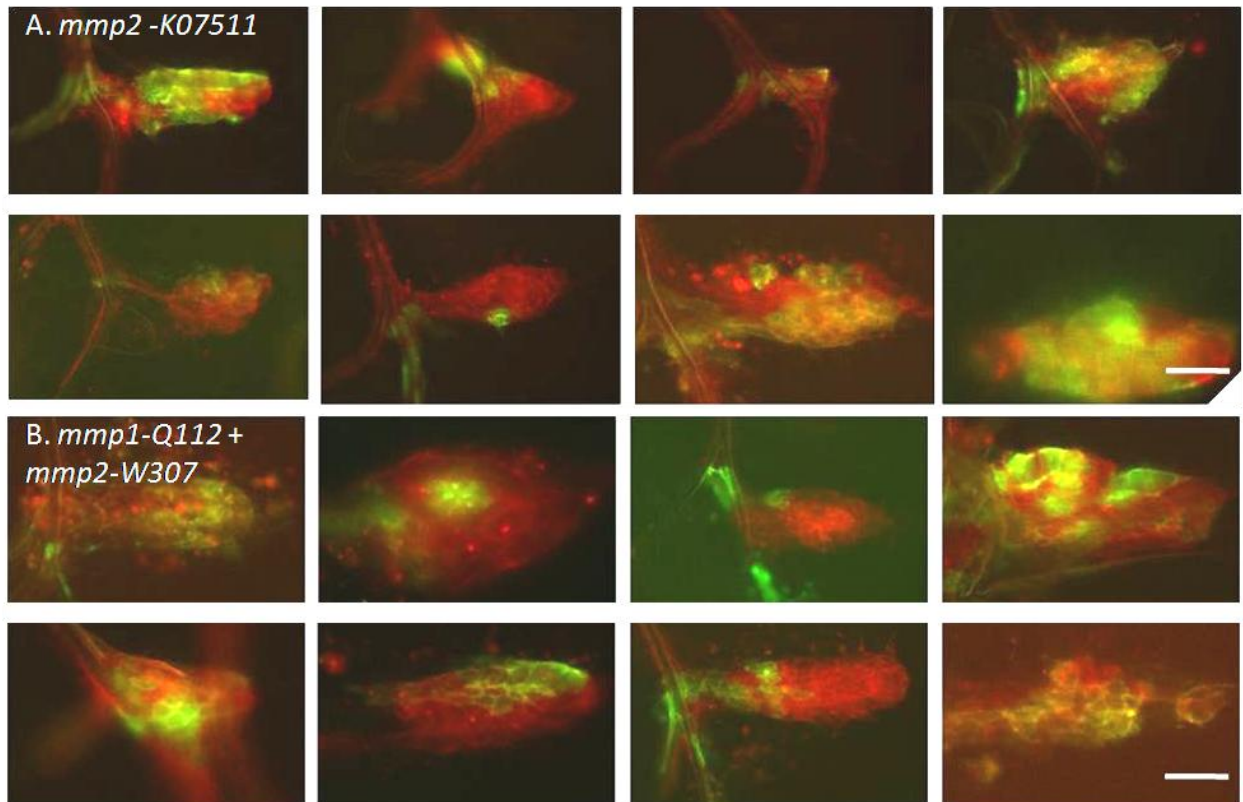


**Figure R11.** Randomly-chosen examples of *mmp* MARCM clones. 80% (total = 10) of *mmp2* -K07511 MARCM clones occupied the tip of ASP, demonstrating an increased ability to localize to the tip of ASP. 63% (total=8) of *mmp1*-Q112+*mmp2*-W307 double MARCM clones occupied the tip of ASP, demonstrating a similar ability as *wt* clones to localize to the tip of ASP. (ASP labeled in red by *btlenh-RFPmoesin*, clones labeled in green by *UAS-CD8GFP*, scale bar=25  $\mu$ m)

### 3. Clonal analysis of larval tracheal growth

---

#### 3.1 Different tracheal metameres are differentially sensitive to heat shock

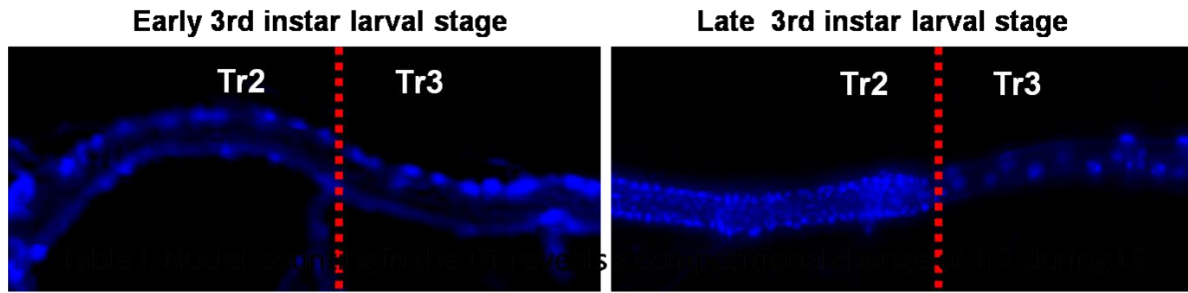
As demonstrated in recent studies (Guha et al, 2008; Sato et al, 2008), a previously described phenomenon coined as “repopulation” (Guha and Kornberg, 2005) embodies the unusual process during which fully differentiated larval tracheal cells in Tr2, arrested in cell cycle throughout L1 and L2 stage, revert back into proliferation and give rise to multi-potent progenies during L3, all happening without compromising the structural integrity and the air-conducting function of Tr2. In order to better understand how these Tr2 tracheal cells behave mitotically during L3, we have designed a scheme of clonal analysis, as diagramed in Figure 12B, and employed traditional flip-out clones (Theodosiou and Xu, 1998). Moderate heat shock was applied to late embryos for the purpose of inducing single-cell labeling event. These heat-shocked embryos were then allowed to develop under controlled temperature (23°C) and staged carefully to set aside 0-2L3 larvae. Subsequently, these staged animals would be allowed to grow for different periods of time before getting dissected at pre-chosen time points during L3 and identified clones were recorded. According to the time elapsed and the number of cells observed in the clones, we could then calculate the average cell cycling time and estimate how many cell cycles a cell had gone through during the defined period.

To get started, I first made sure that no spontaneous clone induction events would take place in the absence of heat shock. 102 un-heat-shocked DT were examined and none of them contained any GFP-positive cells. So we went on to look for optimal conditions for inducing single-cell labeling events.

During the process of experimenting with various heat-shock (HS) conditions, I noticed that cells localized in metameres more posterior to Tr2 often got labeled, whereas all Tr2 cells remained unlabeled. To confirm this initial observation that different tracheal metameres may be differently sensitive to heat shock, I performed experiments using a heat shock scheme that would not “over-label” cells (meaning that not all cells in the metamere would get labeled) and carefully recorded results found in the following three metameres: Tr2, Tr3, and Tr5, as summarized in table R4.

After calculation, the induction efficiency does appear to be higher in Tr5 and Tr3 than that in Tr2 (See table R4). To analyze the statistical significance of these values presented in table R4, Chi-Square Test was employed to calculate the possibility that Tr2 and Tr3 could be similar in

A



| Developmental Stage           |     | 0-2 L3<br>(n=7) | Late L3<br>(n=5) |
|-------------------------------|-----|-----------------|------------------|
| Metameres                     |     |                 |                  |
| Average cell number in the DT | Tr2 | 20±1            | 360±40           |
|                               | Tr3 | 15±1            | 15±1             |
|                               | Tr5 | 18±4            | 18±2             |

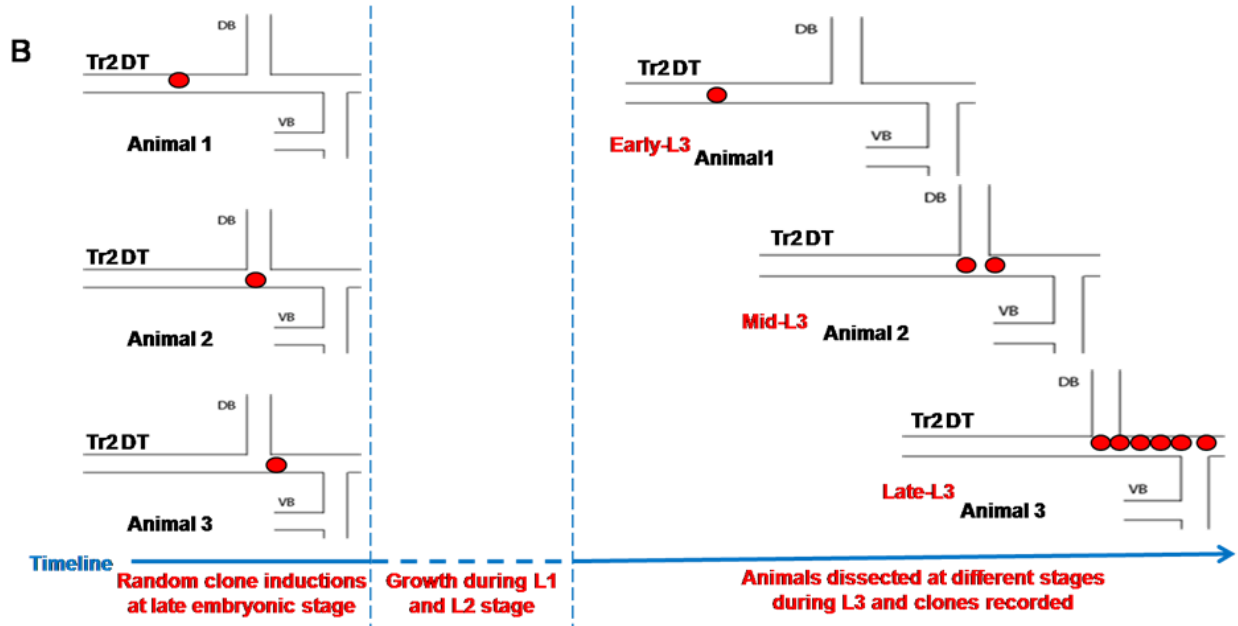


**Figure R12:** (A) Snapshots of “before” and “after” the repopulation process has taken place in the metamer Tr2 in L3, during which the cell composition of the Tr2 dramatically changes, whereas it remains more or less the same in Tr3. This can be easily reflected from a single counting of nuclei at two different time points in L3. In Tr2, the cell number has undergone a ten-fold increase; in Tr3, the cell number remains unchanged. (B) The experimental design of the clonal analysis aiming to describe mitotic behaviors of Tr2 cells



during L3. It requires emphasizing that the labeling of single-cells during clone induction is vital for the proper interpretation of our recorded data. After clone induction, different batches of animals were allowed to develop for different periods of time—theoretically, the longer a cell is allowed to divide, the more cell cycles it goes through, and therefore, the more progeny will be found. According to the time elapsed and the number of cells observed in recorded clones, we could then calculate the average cell cycling time and estimate how many cell cycles a cell had gone through during the defined periods.

properties. The resulted P equaled 0.0832, which is larger than 0.05. This means that Tr2 and Tr3 could be essentially the same. This statistical analysis was also applied to calculate the possibility that Tr2 and Tr5 could be similar in properties and the resulted P equaled 0.0001, which is smaller than 0.05. This means that Tr2 and Tr5 could be essentially distinct.

Our original goal was to perform a systematic clonal analysis for the entire metamere Tr2. However, the number of collected clones residing in other branches other than DT was extremely small. As summarized in table R5, we have calculated and compared the clone induction efficiencies in different branches of Tr2. It turned out that labeling cells localized in the dorsal branch (DB) or the transverse connective (TC)/lateral branch (LB) is much less efficient than labeling cells in the dorsal trunk (DT). This led us to focus on the clones available to us in the DT of Tr2. Therefore, the data to be presented, unless specified, were collected from Tr2 DT cells.

After testing various heat shock conditions and time points of clone induction during *Drosophila* development, we decided to apply heat shock at late embryonic stage. According to our experiences, embryos at late embryonic stage are relatively insensitive to heat and even labeling is easier to achieve. Moreover, cell division should be absent for tracheal cells around this period and the possibility of multi-labeling can be minimized. Time points of heat shock,

Table R4. Clone Induction Efficiencies of Metameres Tr2, Tr3 and Tr5

|  |  | Larvae dissected at 0-2 L3  |  |  | Larvae dissected at 48-50 L3   |  |   |
|--|--|---|--|--|--|--|---|
|  |  | Tr2   | Tr3  | Tr5  | Tr2  | Tr3  | Tr5   |
| Number of DT examined  |  | 349   |  |  | 366  |  |   |
| Total number of labeled DT and detailed descriptions of them                       |  | <b>Total:12</b><br>9 contain 1 labeled cell<br>1 contains 2 labeled cells<br>1 contains 4 labeled cells<br>1 contains 6 labeled cells | <b>Total:19</b><br>15 contain 1 labeled cell<br>2 contain 2 labeled cells<br>2 contain 4 labeled cells | <b>Total:40</b><br>19 contain 1 labeled cell<br>12 contain 2 labeled cells<br>5 contain 3 labeled cells<br>1 contains 4 labeled cells<br>2 contain 6 labeled cells<br>1 contains 8 labeled cells | <b>Total:16</b><br>3 contain 1 labeled cell<br>4 contain 2 labeled cells<br>1 contains 3 labeled cells<br>1 contains 4 labeled cells<br>1 contains 6 labeled cells<br>1 contains 7 labeled cells<br>2 contain 8 labeled cells<br>1 contains 16 labeled cells<br>1 contains 20 labeled cells<br>1 contains 24 labeled cells | <b>Total:25</b><br>13 contain 1 labeled cell<br>7 contain 2 labeled cells<br>5 contain 3 labeled cells | <b>Total:30</b><br>17 contain 1 labeled cell<br>7 contain 2 labeled cells<br>3 contain 4 labeled cells<br>3 contain 8 labeled cells |
| Total number of labeled cells=Σcell number in the clone (N) X number of clones (C) |  | <b>Total: 21=</b><br>1X21   | <b>Total: 27=</b><br>1X27  | <b>Total: 82=</b><br>1X82  | <b>Total: 107=</b><br>1X3+2X4+3X1+4X1<br>+6X4+7X1+8X6+10X1   | <b>Total: 42=</b><br>1X42  | <b>Total: 67=</b><br>1X67   |
| Clone induction efficiency (clone/metamere)  |  | 6%  | 8%   | 23%  | N.A.   | 11%  | 18%   |
| Clone induction efficiency adjusted by cell number in the metamere                 |  | 0.3%  | 0.5%   | 1.3%   | N.A.   | 0.8%   | 1.0%  |

**Table R5.Clone induction efficiencies in different branches of Tr2 at 0-2 L3**

**[12min HS ( 55 ) hrs prior to 0-2 L3, raised at 23° C.]**

|   | <b>DB</b>    | <b>DT</b>   | <b>Tc</b>    |
|---|--------------|-------------|--------------|
| <b>Number of DT examined</b>                                | <b>349</b>   | <b>349</b>  | <b>349</b>   |
| <b>Average number of cells of the branch being observed</b> | <b>4</b>     | <b>20</b>   | <b>7</b>     |
| <b>Total number of examined cells</b>                       | <b>1396</b>  | <b>6980</b> | <b>2443</b>  |
| <b>Number of labeled cells</b>                              | <b>1</b>     | <b>21</b>   | <b>1</b>     |
| <b>Clone induction efficiency</b>                           | <b>0.07%</b> | <b>0.3%</b> | <b>0.04%</b> |

time points of larval staging (to obtain a precise knowledge of larvae) and time points of sacrifice were carefully noted so that the exact growth period of clones could be calculated.

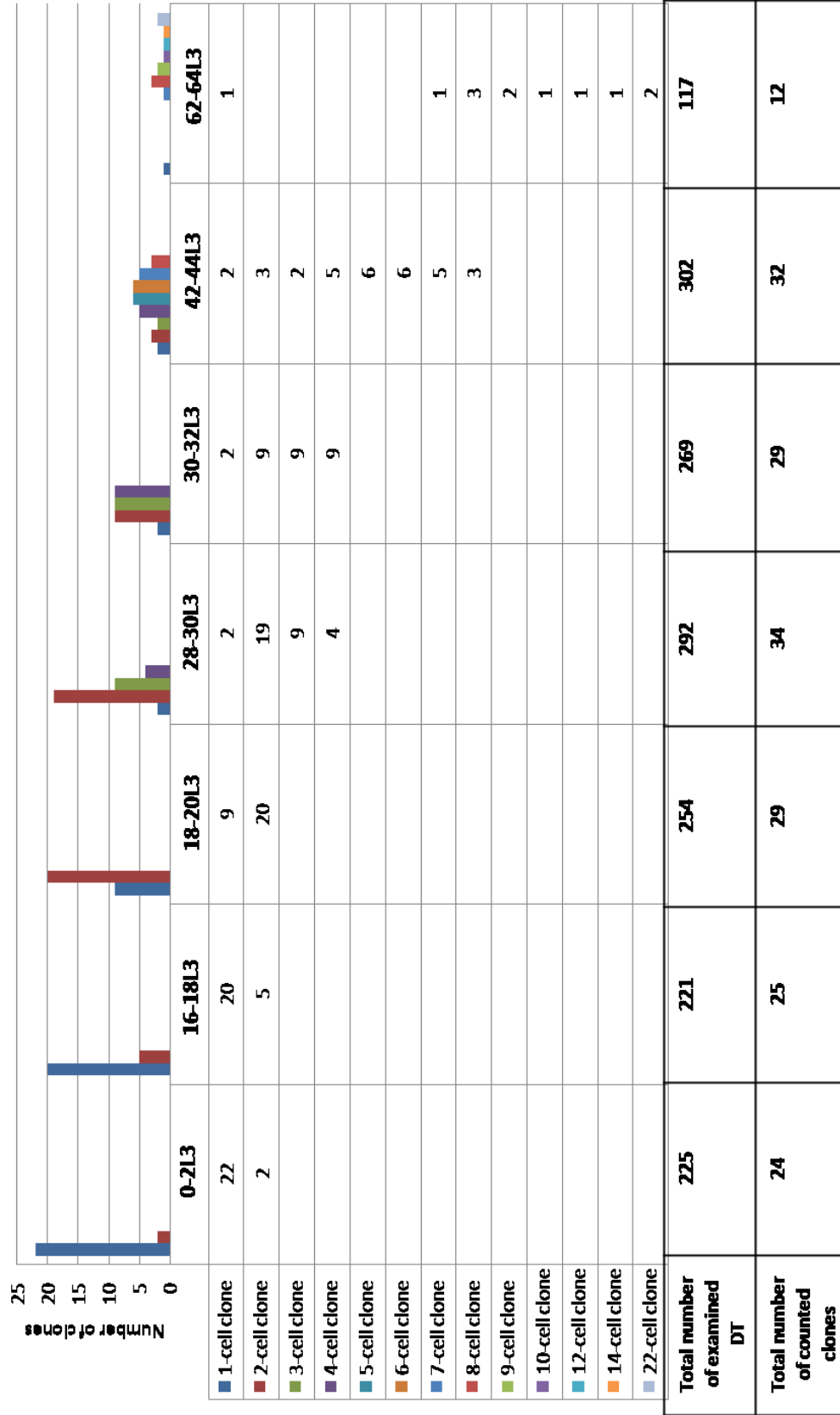
### **3.2 Non-synchronous mitotic behaviors of Tr2 cells during L3**

To correctly interpret the data of our clonal analysis and to obtain a clear picture of how many cells cycles a Tr2 cell went through during a certain time frame, labeling single cells during clone induction was vital. A control experiment was performed, as mentioned before, to make sure that no clone induction would take place in the absence of heat shock. This enabled us to temporally control the induction of clones. Since the promoter used for clone induction was *actin5C*, all cells in the animal body could get labeled without bias.

For the purpose of properly interpreting our data (see Figure R13A) collected in the clonal analysis aiming to understand mitotic behaviors of Tr2 cells, we calculated the probability of acquiring single-cell labeling using our heat shock scheme. Based on the assumption that no Tr2 cells would start to divide prior to the entry into L3 and multiple labeled cells within the same



## A Growth dynamics of Tr2 cells using clonal analysis



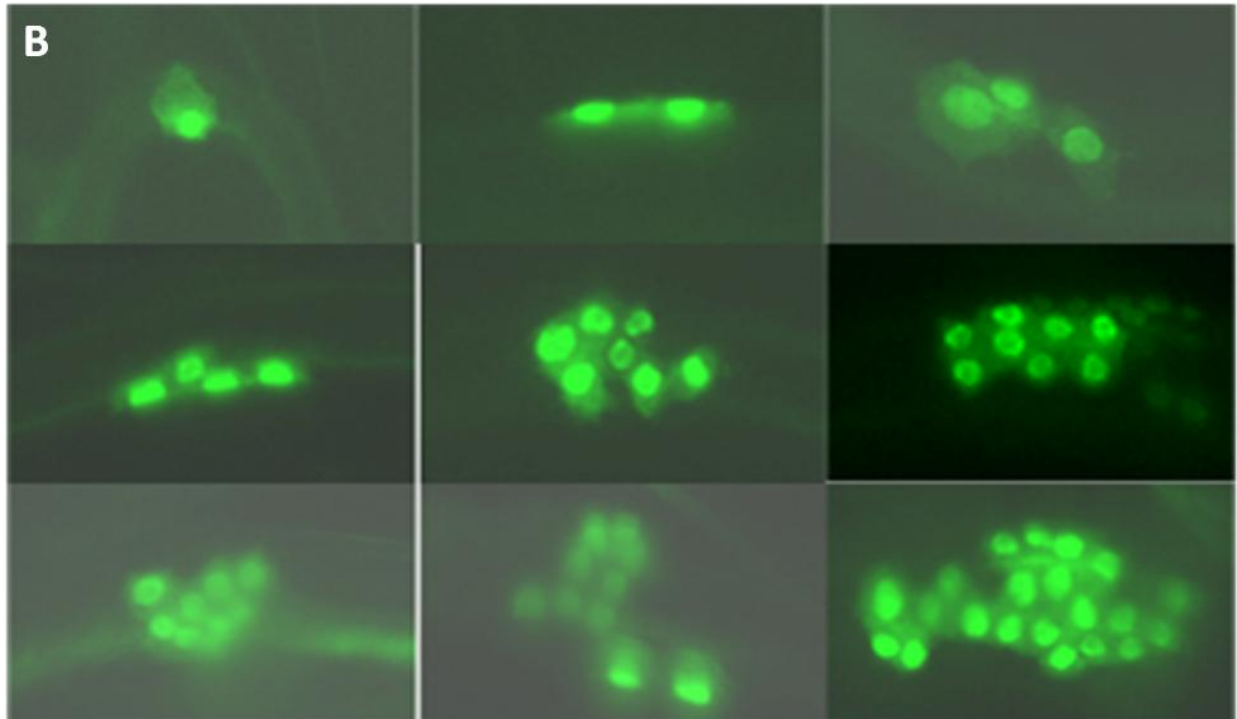


**Figure R13.** Summary of clonal analysis results and examples of collected clones. A. Most Tr2 cells appeared to divide continuously throughout L3, albeit not strictly synchronously. The longer time cells were allowed to develop into L3, the higher the number of cells found in a clone became, consistent with the idea that daughter cells from previous divisions continued to proliferate. B. As can be seen from the pictures, shapes of clones are generally compact and “patchy”, indicating little cell migration.

DT indicated independent events, the average clone induction efficiency was calculated as: number of labeled cells/total number of examined cells =  $(1 \times 22 + 2 \times 2) / (20 \times 225) = 0.006$ , since twenty-two 1-cell clones and two 2-cell clones were retrieved after 225 DT (of which the average cell number of was calculated as 20) had been examined. So the possibility of labeling one Tr2 cell at clone induction was  $P1 = 0.006 \times 20 = 0.12$ ; the possibility of labeling two cells at the same time during clone induction was:  $P2 = P1 \times P1 \times C_{20}^2 = 0.001$ . Similarly, the possibility of labeling three cells at the same time during clone induction was: 0.0001, which was considered highly unlikely in our data interpretation. When we used calculated P2 to estimated expected number of events during which two cells could be labeled, we found:  $225 \times P2 = 225 \times 0.01 = 2.25$ . This was very close to 2, the recorded number in our experiment. This consistency confirmed the validity of our initial assumption that no Tr2 cells started to divide prior to L3. When P1 and P2 were being compared, we found:  $P1/P2 = 0.12/0.01 = 12$ . So the possibility that clones observed in our experiments were derived from one single mother cell is:  $12/(12+1) = 0.92$ . So we have the confidence to say that the predominant majority of clones we recorded are indeed derived from the one and the same mother cell, which is essential for the correct estimation of the number of cell cycles Tr2 cells can possibly go through during the designated observation window.

To conclude, this statistic analysis enabled us to come to the conclusion that 92% of all clones recorded in our analysis should be the progeny of a single ancestor cell labeled during late embryonic stage.

As summarized in Figure R13A, most Tr2 cells appeared to divide continuously throughout L3, albeit not strictly synchronously. The longer time cells were allowed to develop into L3, the higher the number of cells found in a clone became, consistent with the idea that daughter cells from previous divisions continued to proliferate. After 20 hours of development into L3, the majority of Tr2 cells had finished their very first division in L3. This first round of mitosis seemed fairly synchronized, all taking place during 16-20L3. Subsequent cell cycle progression became less uniform, as revealed by the fact that clones having the same “age” didn’t always possess the same number of cells. This could result from growth variations in different animals, which happened persistently even if most external conditions were kept the same. Alternatively, the difference in cell number could also be caused by less synchronous, more individualistic cell cycle progression of Tr2 cells, whose number was gradually increasing. Based on our observation, a general correlation between the position of a cell and the number of cell cycles it would go through could not be established. However, the two or three cells localized right at the Tr2-Tr3 border did show a higher possibility of remaining undivided during our recording. From the fact that most clones demonstrated a compact, patchy appearance, we concluded that limited cell movement/migration was involved during DT repopulation process. The biggest clone we encountered consisted of 24 cells, which we interpreted as 8+16, meaning that after the first L3 division, one daughter cell went through another 3 cell cycles in the next 48 hours prior to pupation, whereas the other went through 4. In summary, we concluded that most Tr2 cells finished their first L3 cycle at 20L3; subsequent cell cycle took on average about 12-16 hours; most Tr2 cells went through about 4 cell cycles averagely.

### **3.3 Some Tr2 cells do not intermix, others do**

Our clonal analysis revealed that some cells in Tr2 appeared to have a strict “sense of territory”, meaning that they would remain localized and confined within the branch where they were born and would not trespass into its neighboring branch. This remained true, even if clones of big size were observed. As shown by examples displayed in Figure R14, cells of DB and cells of DT did not appear to intermix, and this feature consistently demonstrated itself in all the 8 cases we had collected.

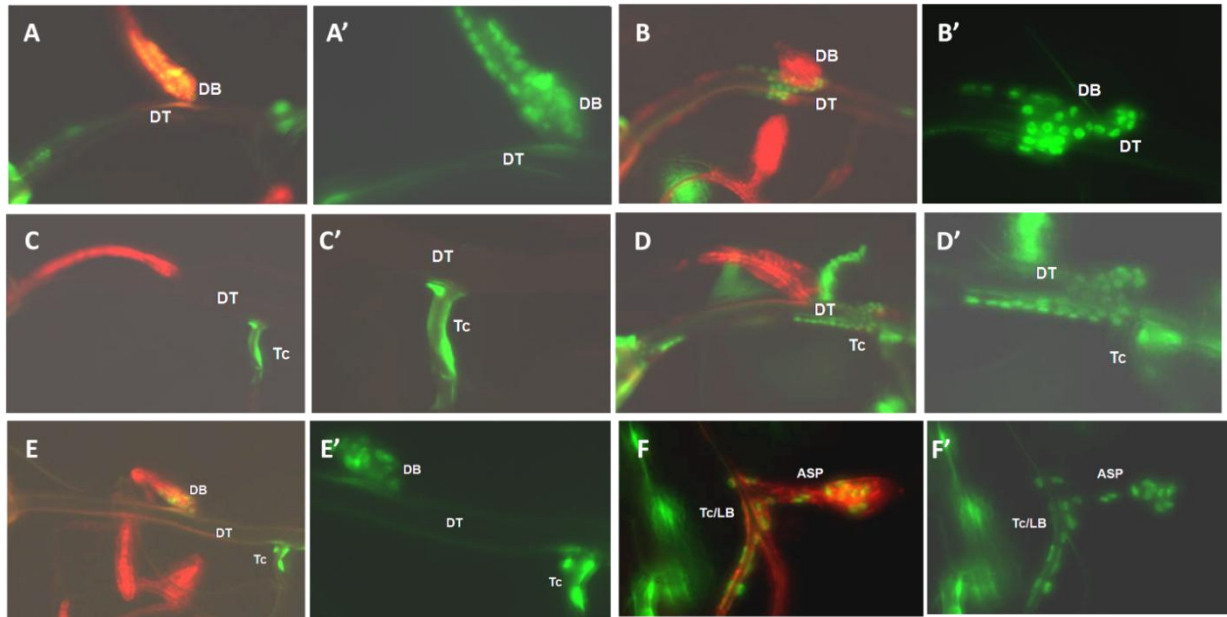


**Figure R14.** Clones demonstrating the phenomenon of “regionalization”: non-intermixing between DB and DT cells (A, A', B, B', E, E'), as big clones in the DB did not spread into DT, and *vice versa*; non-intermixing between DT and TC cells (C, C', D, D', E, E'); intermixing between TC and ASP cells (F, F'). Clones were labeled in green by nuclear GFP; DT, ASP, and some other parts of the trachea were labeled in red by RFP-moe driven by *btl* enhancer.

Neither did cells of DT appear to intermix with those of TC, for which we had also collected 8 examples. Interestingly, however, cells of TC and ASP did appear to intermix with another, for which we will provide an interesting explanation later in this report. We employ a term “regionalization” to describe such non-intermixing of cells bearing different branch identities.

### 3.4 *in vivo* tracking of the repopulation process

When I first started the clonal analysis, I wanted to find the mysterious Tr2 population of mitotic cells that would migrate out of their niche into different branches and replace the larval cells. However, I found no evidence which indicated the presence of such a population. The clone shapes were consistently compact, indicating little cell movement. Occasionally, clones were retrieved in which cell sizes could be approximately categorized into big, medium and small, indicating the presence of sequential cell cycle progression, which could result in serial cell size reduction. Repeated observation of such cases led us to seriously consider the possibility that the Tr2 larval tracheal cells could indeed re-enter mitosis and give rise to those mitotic cells observed during “repopulation”. About the same time, some other data in support of this proposed “de-differentiation” hypothesis also trickled in. For example, Tr2 cells were shown to have lower ploidy than cells of other metameres. Neither did they seem to replicate their DNA during L2 stage, as revealed by BrdU staining, whereas cells in other metameres did. All this seemed to point to the possibility that Tr2 cells were not really endo-replicating cells as they had been assumed to be. In addition, centrioles, an organelle maintained only by mitosis-competent cells, were

only detectable in the Tr2 cells during L2 and L3 stages but not in cells of other metameres, providing another clue that these Tr2 larval cells possessed the capacity to divide.

In an attempt to settle this issue, we devised a lineage-tracing method to track single tracheal cells in real time. This strategy is based on the expression of GFP after FLP-induced recombination (*hsflp; actin 5C>CD2>Gal4; UAS nuclear-GFP*). A brief heat shock during late embryogenesis induced GFP expression at a frequency low enough to mark single cells unambiguously. Importantly, this regimen restricted recombination to a short interval in the late embryo because we found no evidence that additional GFP-expressing cells were induced after the pulse of FLP expression. L3 larvae (0–2 h) that had been heat shocked as embryos were screened without dissection, and animals with GFP-labeled cells in Tr2 were set aside. These animals were examined again after 24 and 48 h. Of the 36 clones we identified with individually marked Tr2 cells, 29 increased the number of GFP-expressing cells (from 2 to 8 cells) during the period of examination; seven were quiescent. An example of apparent clonal proliferation is shown in Figure R19. In no case was GFP fluorescence lost, suggesting that none of the labeled cells was eliminated during this period. The persistence of these cells is consistent with the apparent absence of programmed cell death; their growth demonstrates that most of the post-mitotic Tr2 tracheal cells restart a mitotic program in L3. Because most of the labeled cells increased in number, the fraction of cells in Tr2 with proliferative potential is high. We conclude that the post-mitotic larval tracheal cells are the progenitors of the cells that proliferate and populate Tr2 tracheae during L3. Analysis of Tr2 clones induced at various times during embryonic and larval development indicates that the cell cycle is  $\approx 10$  h and that the increase in Tr2 cell number during L3 is driven entirely by larval Tr2 cell divisions.

Sato and Tabata had independently made similar observations concerning differences in cell size and came to the same conclusion (Sato and Tabata, 2008).

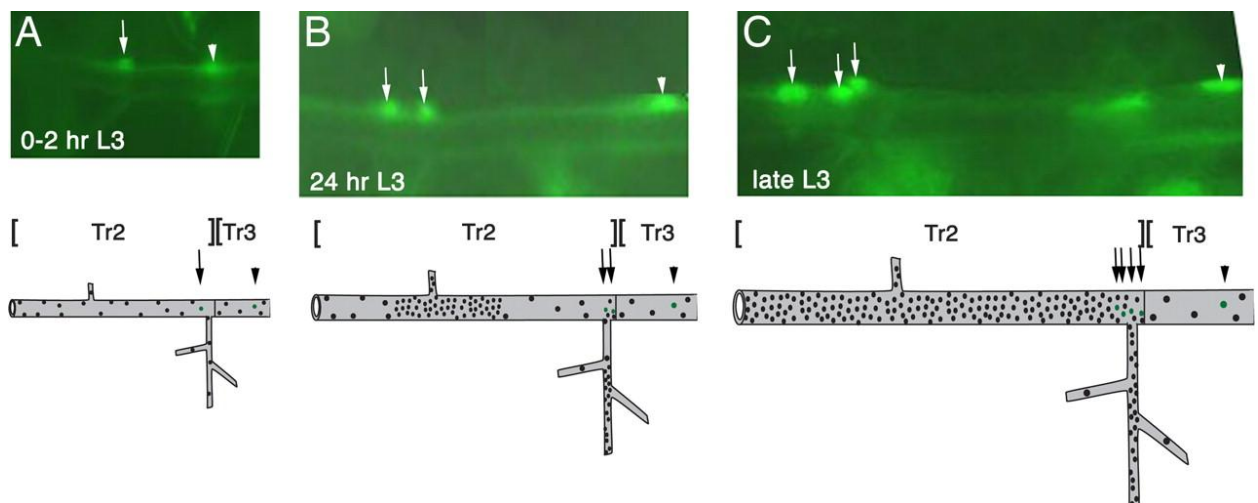


**Figure R15.** *in vivo* tracking of the process of repopulation. A one-cell clone identified in an early L3 larva has been tracked over time to visually observe how a Tr2 larval cell could indeed enter into mitosis and give rise to progenies. Clones are labeled by nuclear GFP (GFPnls).

## 4. Clonal analysis of ASP morphogenesis

---

### *Symmetry and asymmetry, which one is more dominant in nature?*

#### 4.1 ASP consists of two layers that are different in morphology and in mitotic activity

It came as an utter surprise, when it was observed for the very first time that the upper and the lower layer of ASP were not exactly the same in morphology, the opposite of which I had always assumed to be true.

To confirm this discovery, I designed a simple experiment. Crossing flies carrying *btl-gal4*, *UAS-nlsGFP* transgenes to those carrying *UAS-cherry-CD8*, I intended to label all cell nuclei in green in the ASP and all cell surfaces/contours in red, so as to compare the morphologies of cells located in the upper and the lower layers of ASP.

As shown in the Figure R20, all cell nuclei in the ASP were labeled in green by nuclear GFP.

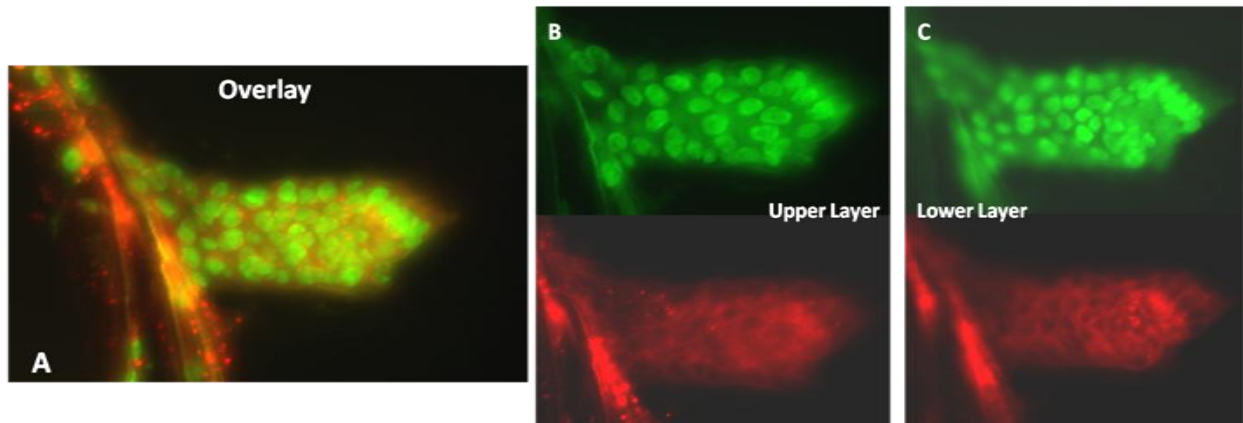


**Figure R16.** An asymmetry in morphology (nuclear and cellular) exists between the upper and the lower layer of ASP. As revealed by nuclear GFP (green) and cytoplasmic Cherry-CD8 (red) labeling, cells in the ASP upper layer possess bigger nuclei and are generally bigger in size, compared with those cells of the lower layer. In addition, the total number of cells comprising the upper layer seems smaller than that of the lower layer. A. Overlay; B. Upper layer; C. Lower layer.

However, instead of strictly labeling the cell contours, Cherry-CD8GFP tended to give a ubiquitous cytoplasm labeling. Differences between cells of the upper layer and those of the lower layer are clearly visible: in the ASP upper layer, cells possess bigger nuclei and are generally bigger in cell size, compared with those cells of the lower layer. In addition, the total number of cells comprising the upper layer seems smaller than that of the lower layer, which is exactly what one would expect, based on the assumption that the overall surface areas of the two ASP layers are about the same. The bigger sizes cells possess, the fewer of them are required to fill the same area. As demonstrated, an asymmetry in morphology (nuclear and cellular) exists between cells of the upper and lower layer of ASP. What struck as more surprising was the observation that cells of these two layers also differed in their mitotic activity. As revealed by BrdU staining, a method to selectively label



cells that are actively synthesizing DNA, only cells in the ASP upper layer could be detected to have incorporated BrdU (see Figure R21). The same experiment was repeated and the identical result obtained: BrdU staining was exclusively detectable in the ASP upper layer cells. This observation implied that only cells of the upper layer seemed to be replicating their DNA and thus be undergoing proliferation, whereas cells of the ASP lower layer seemed not to be taking part in DNA synthesis, an indispensable step for cell cycle progression, and were therefore mitotically quiescent.

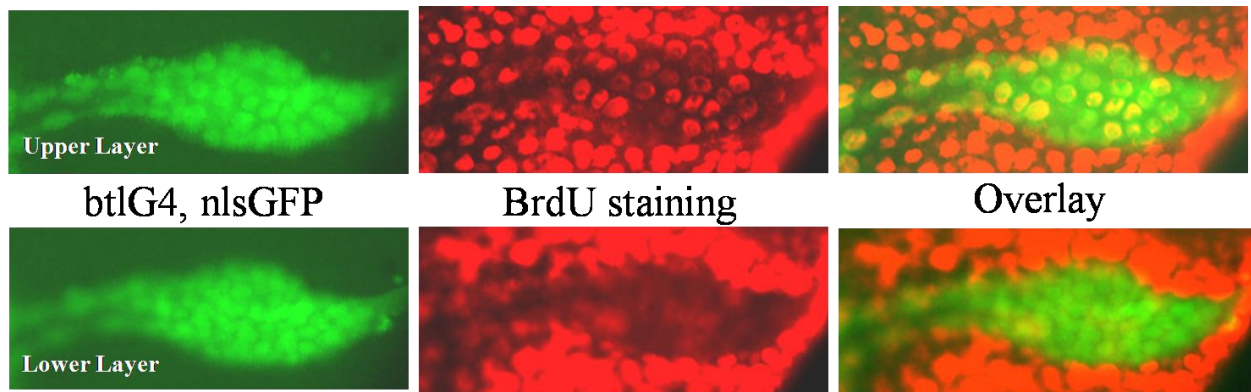


**Figure R17.** BrdU staining revealed an unexpected find: only cells of the ASP upper layer could be detected to have incorporated BrdU into their DNA and no cells of the lower layer seemed to do so.

#### **4.2 ASP lower layer grows through “cell replenishment” provided by ASP upper layer and neighboring TC/LB**

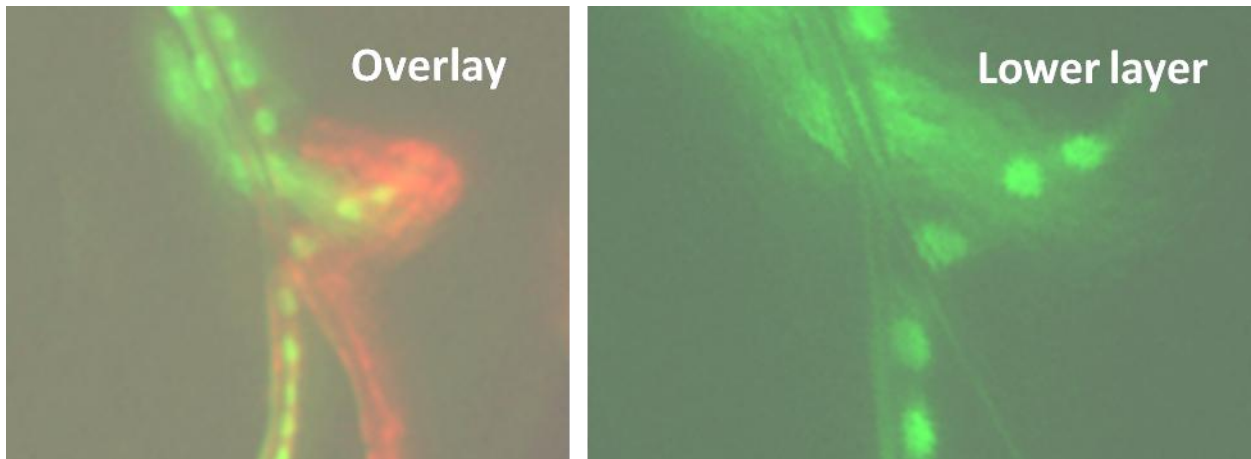
BrdU staining detectable solely in the upper layer of ASP immediately provoked the question of how the lower layer could grow in the absence of cell division— its lack of BrdU staining indicated the absence of DNA replication, a process indispensable for cell cycle progression. Three simplest hypotheses could be proposed: 1. ASP lower layer grows through cell replenishment provided by TC/LB; 2. it grows through cell replenishment provided by the upper layer; 3. it grows through both of the two aforementioned processes operating simultaneously.

Ideally, *in vivo* live imaging would be the most definite method to test our hypotheses. However, technical difficulties such as how to position living larvae in a way that ASP could be optimally imaged, how to prevent them from moving throughout the entire imaging course, how to keep the animals alive under the condition of being confined, and so on, prevented us from taking such an approach.

Neither could we test our hypotheses using live imaging of dissected samples due to problems of dehydration and tissue death. Therefore, we turned to flip-out clonal analysis, the second-best approach that we could employ. As mentioned before, (listed in table R5), it is extremely difficult to induce clones in TC/LB, from which ASP morphogenesis takes place during L3. And for the purpose of testing our hypothesis that cell relocation from ASP upper layer to the lower layer could take place, it was vital to make sure that all cells of such a recovered clone were derived from one and the same mother cell, which excluded the possibility of performing intensive heat shock so as to increase the labeling frequency

of ASP cells. So we used the heat shock condition that had been statistically analyzed for optimal single-cell labeling. After laborious effort, we acquired 3 clones confirming that cells can indeed move from TC/LB into ASP lower layer, one of which is shown in Figure R22, an Epi-fluorescence microscope image. We obtained 5 clones confirming that cells could indeed relocate from the ASP upper layer into the lower layer, one of which is shown in Figure R23, in which a series of confocal microscope images were assembled to demonstrate the cell behavior of moving from TC into the ASP upper layer, from where cells subsequently moved into the lower layer.

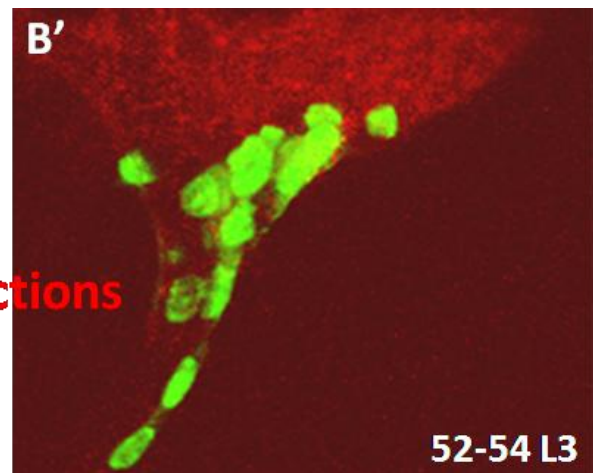
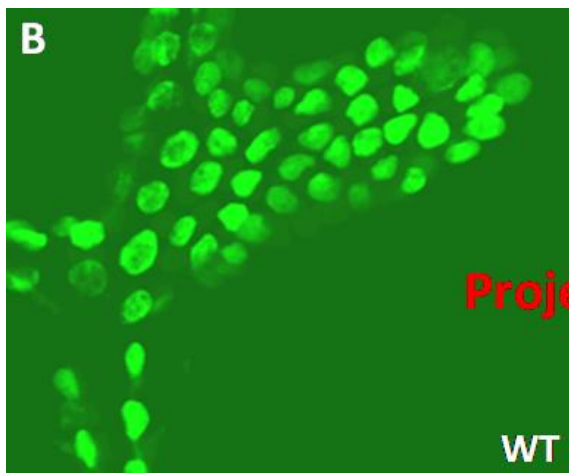
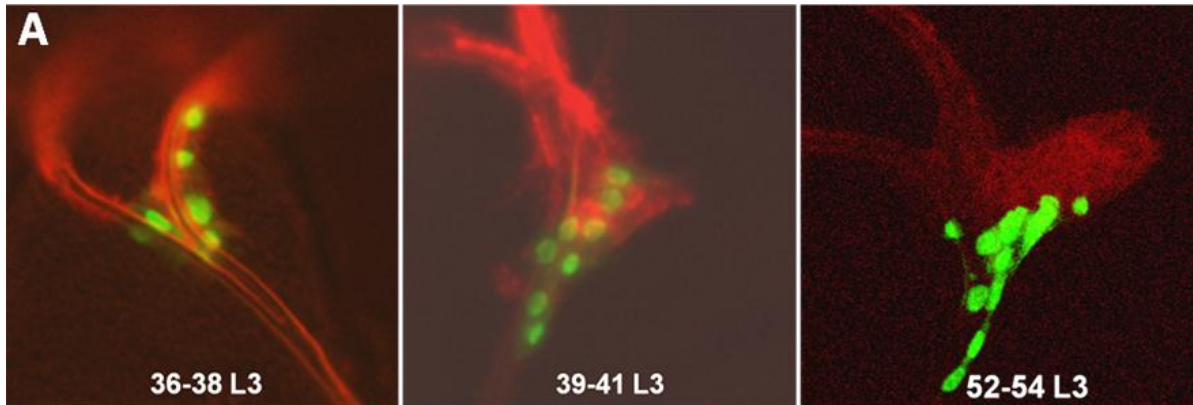
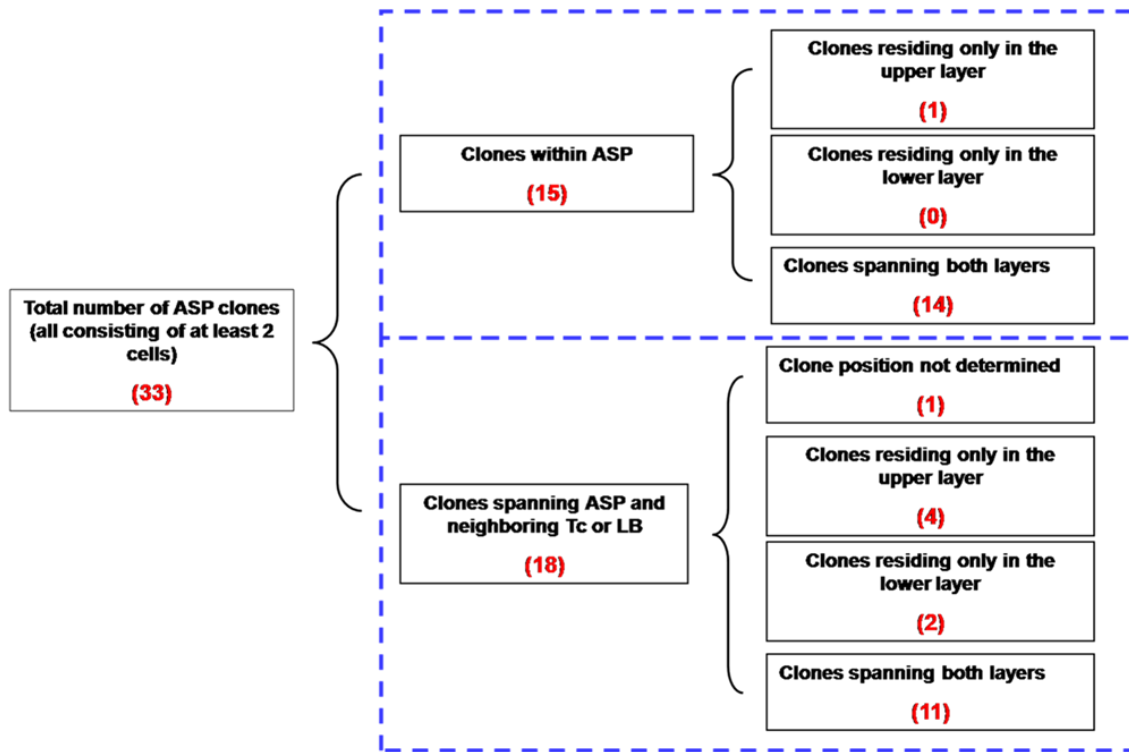
Our reasoning was the following: when the mother cell of the 52-54 L3 clone was labeled at late embryonic stage, it was localized somewhere in the TC, since there existed yet no ASP at such an early stage. With time passing, this mother cell underwent cell divisions during L3 and gave rise to progenies, which moved gradually from TC to the neighboring ASP upper layer. These progenies in the ASP upper layer continued to divide, forming a cluster of 15 cells, some of

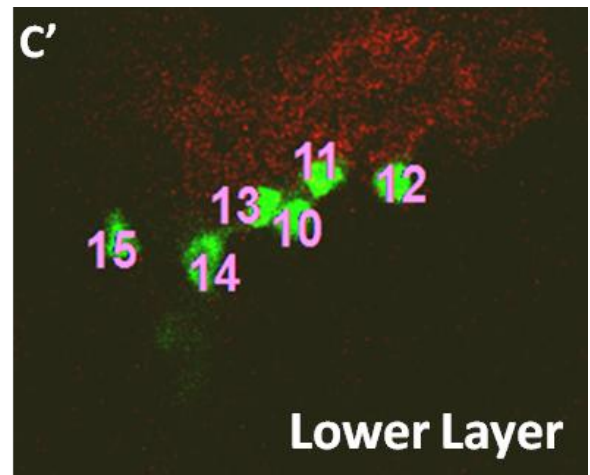
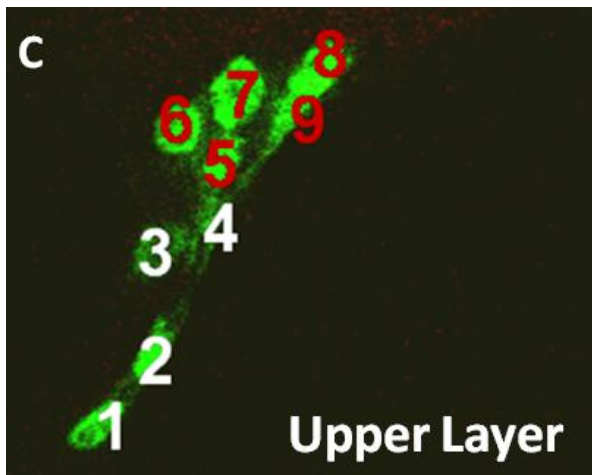


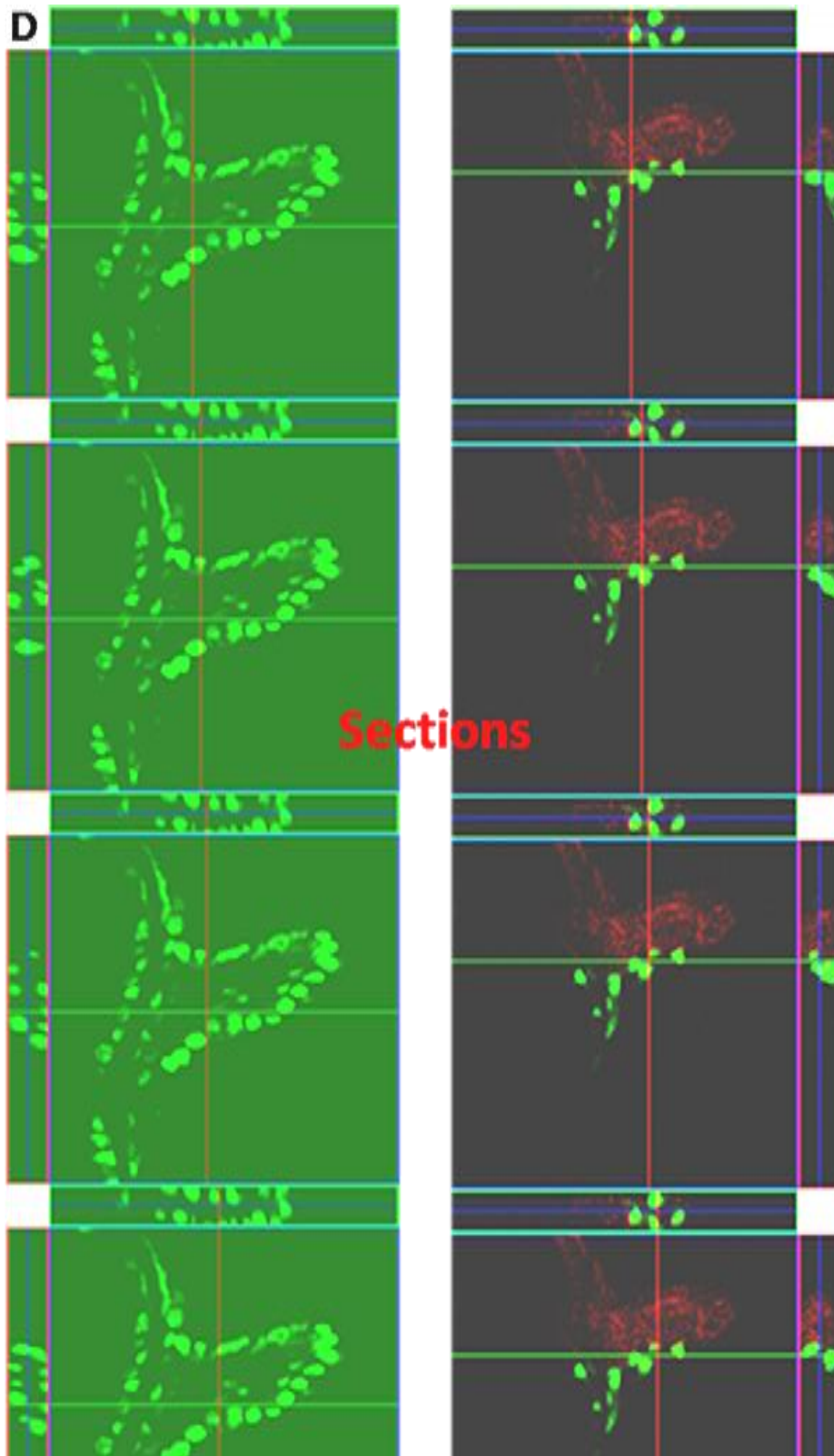
**Figure R18.** An example of a clone demonstrating movement from the lateral branch (LB) into the lower layer of the ASP, which is coined “cell-replenishing”, a model proposed to explain how the ASP lower layer could grow in size and cell number despite the absence of cell proliferation.

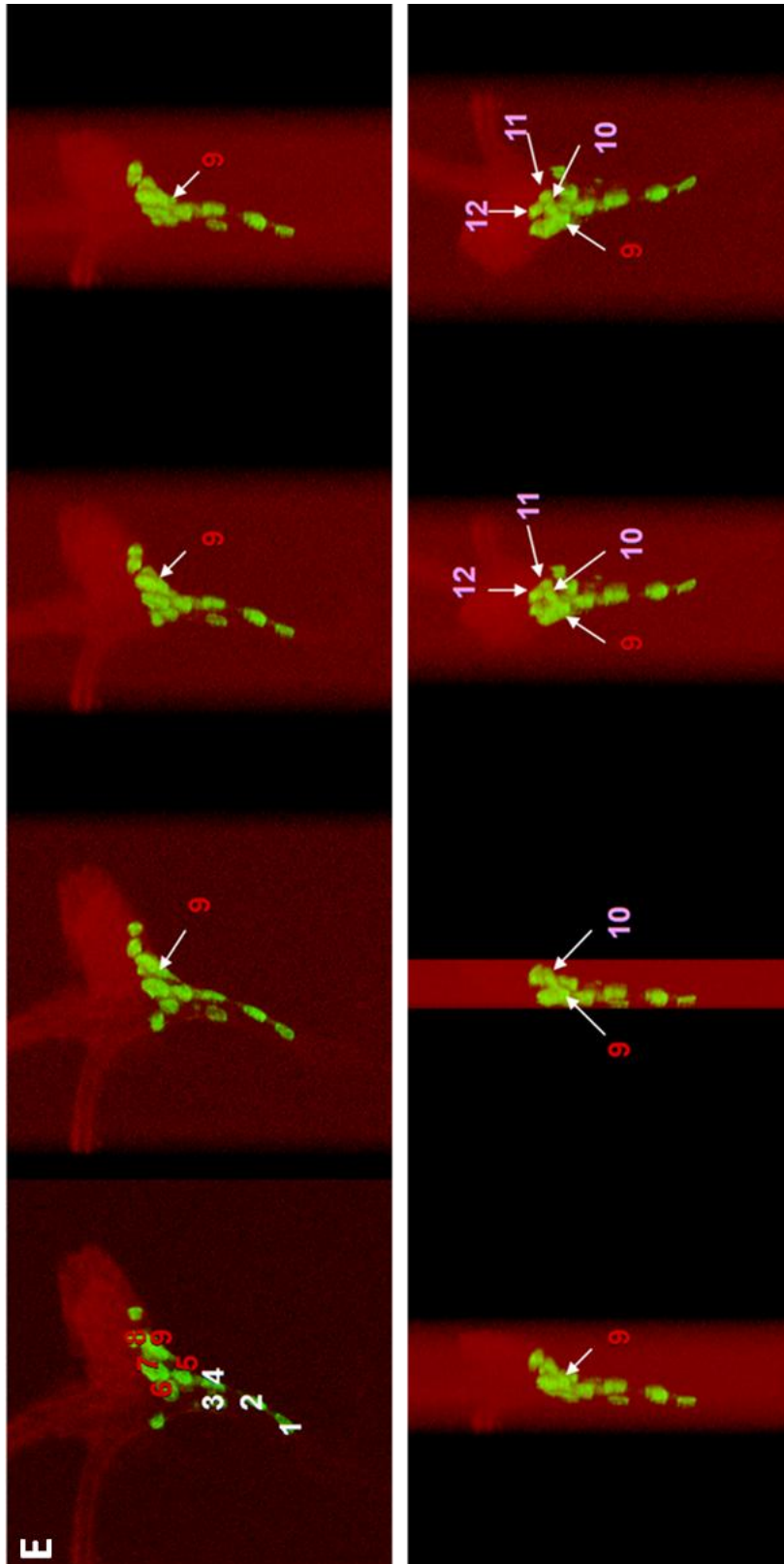


Table R6. Positional distribution of ASP clones is consistent with “cell-replenishment” hypothesis









**Figure R19.** An example of “cell replenishment”, a model proposed to be responsible for the growth of the ASP lower layer. In this clone (52-54L3), cells seemed to have moved from TC into the upper layer, and subsequently, into the lower layer.

A. A simple time course showing the growing process of a cell labeled during late embryonic stage. It aims to show that all cells of the 52-54 L3 clone have descended from

one and the same mother cell. This is an important prerequisite for the subsequent reasoning that cells can indeed relocate from the ASP upper layer to the lower.

B. and D. Projection and section images of a wild-type ASP (B and the left panel in D) and a 52-54 L3 clone (B' and the right panel in D) in the ASP. In the left column of D, a wild-type ASP was labeled by nuclear GFP and different sections of the ASP are shown to illustrate the relative spatial relationships between cells of the upper and lower layer. [One section that cut parallel to the proximal-distal (P-D) axis was kept constant, and 4 sections, cut parallel to the orthogonal axis (perpendicular to the P-D axis) and gradually moving along the P-D axis toward the distal tip of the ASP, were shown.] It can be seen that ASP, a flat tubular structure, consists of a lumen that is surrounded by a single-layered epithelium. In the right column, a 52-54 L3 clone (labeled in green by nuclear GFP) in the ASP (labeled in red by *btlenhRFP*, the dim labeling is caused by bleaching during the imaging process). (Sections were taken in exactly the same way as in the wild-type ASP on the left). From comparing these two columns of image assemblies, one can come to the conclusion that cells in this clone, all derived from the same mother, indeed occupy both the upper and the lower layers.

C. and C'. Numbering cells in the 52-54 L3 clone, C showing the upper layer and C' the lower. Cell 1-4 (labeled in white numbers) are localized in the Tc, cell 5-9 (labeled in red numbers) are localized in the upper layer, and cell 10-15 (labeled in purple numbers) are localized in the lower layer.

E. An assembly of a series frame-to-frame confocal images to show the relative spatial relationship of the 15 cells in the 52-54 L3 clone from all possible angles. Careful observation can lead to the conclusion that the cell 9 and the cell 10 are not strictly localized in the upper and the lower layer, respectively. Rather, they both seem to find themselves more at the 'lateral side' of the ASP, demonstrating the continuity of cells within the clone.

which relocated from the upper layer to the lower layer, possibly acting as a response to mechanical tension or signaling events (See also the detailed figure R23 legend).

As summarized in the table R6, the positional distribution of all ASP clones that we were able to collect over the years using various heat shock conditions was also consistent with our cell replenishment hypothesis. When ASP clones positioning strictly within ASP itself were recovered, no clones residing only in the lower layer could be found, since cells in the lower layer had to come from the upper. Only in clones spanning ASP and the neighboring TC/LB could cells residing only in the lower layer be found, in which case the cells in the lower layer came from TC/LB.

This "cell replenishment" phenomenon explains well why "regionalization" existing between DT and DB or between DT and TC is absent between TC/LB and ASP, because the normal growth of

ASP is dependent on the inflow of cells from TC/LB. Intermixing of TC/LB cells with those of ASP ensures the proper morphogenesis of ASP.

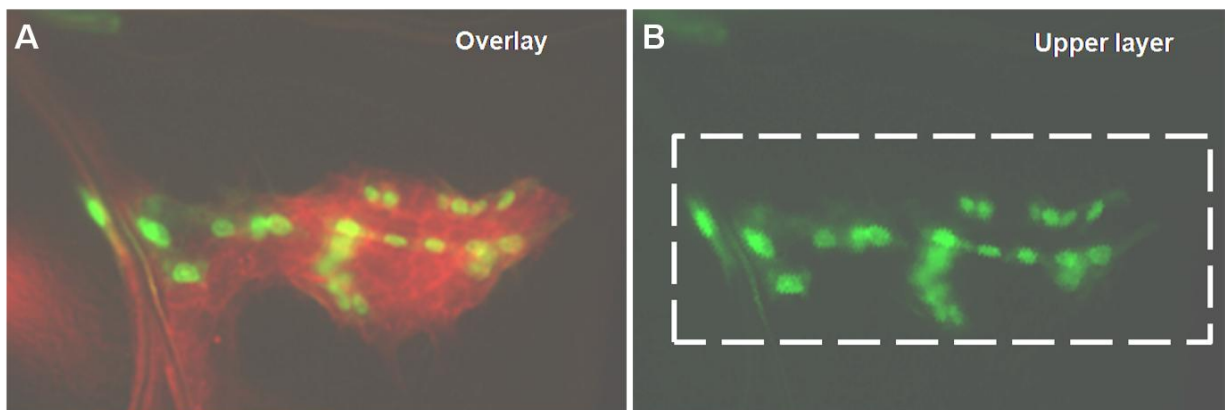
#### **4.3 Other possible behaviors involved during ASP morphogenesis: only guesses?**

The difficulty caused by the extremely low clone induction frequency of labeling cells in the TC/LB prevented me from performing any systematic clonal analysis for ASP, which may provide insight into what cell behaviors could contribute to the construction of ASP. Therefore, I could only depend on the occasional clones collected during all kinds of experimental conditions to gain some idea of what processes might be involved during this morphogenetic process.

Two interesting questions have arisen from this kind of “casual” observations:

1. Could oriented cell divisions along the proximal-distal (P-D) axis be involved?
2. Could cell intercalation/rearrangement be operating during ASP morphogenesis?

As presented in Figure R23, multiple clones, labeled in green with nuclear GFP, can be observed within the ASP, which was labeled in red with *breathless*-enhancer fused with *RFP-moesin* (*btlenhRFPmoe*). Attention should be given to the clone located on the upper layer of the ASP, as can be seen in (B), and in (C), in which each nucleus, altogether eight, is represented with a white dot. These eight cells, probably derived from the same mother cell, seem to be telling a story different from cell migration. Instead, they tell a story of oriented cell divisions along the P-D axis: it starts with one cell, which becomes two after one round of cell division. These two cells align themselves along the P-D axis, probably due to a FGF-dependent process that keeps the mitotic spindle in alignment with the P-D axis during the previous mitosis. Then the two cells give rise to four and subsequently eight cells, all of them aligning themselves according to the P-D axis dictated by the orientation of the mitotic spindle during cell division. The alignment of the white dots spans the entire length of the ASP, and this “growth” along the axis could simply be the outcome of the cell division process that splits one cell into two. Another possibility responsible for this longitudinal growth also exists.





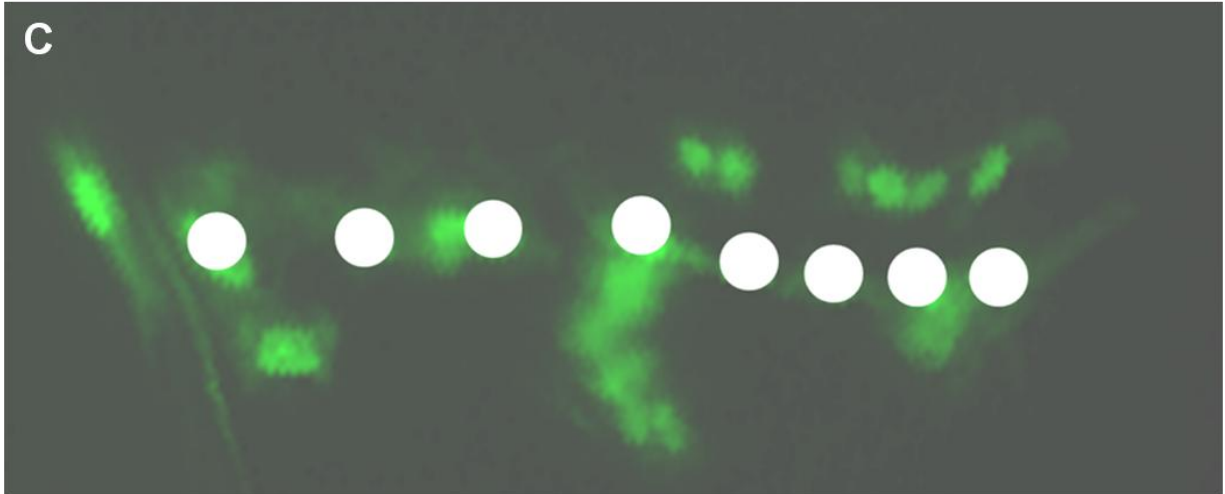


**Figure R20.** An ASP clone indicating the possible presence of oriented cell divisions along the proximal-distal (P-D) axis. A: the clones are in green (labeled by nuclear GFP) and the entire ASP in red (btlenhRFPmoe). B: clones localized in the upper layer of ASP. C: a modified version of the clone to be highlighted: each nucleus within the clone is represented by a white dot. The alignment of the white dots spans the entire length of the ASP.

Since the cells are labeled by nuclear GFP, it can't be determined exactly whether there exist additional cells in between the labeled ones. If there should be additional invisible cells present between the visible ones, this structural arrangement could result from another possible cell behavior involved during ASP morphogenesis: cell intercalation/rearrangement.

An example of the possible existence of cell intercalation/rearrangement during ASP morphogenesis is shown in Figure R24: again the ASP is labeled in red with BtlenhRFPmoe while the clone is labeled in green with GFP fused to Moesin (GFP-moe). The cell number in this particular clone is estimated to be eight and all these eight cells are believed to be the progenies of the same mother cell. Interestingly, these eight cells don't appear to be coherently connected with one another. Instead, they appear to be "evenly" divided into four two-cell groups, separated by gaps possibly consisting of one or two "invisible" cells. How does such cell arrangement form?

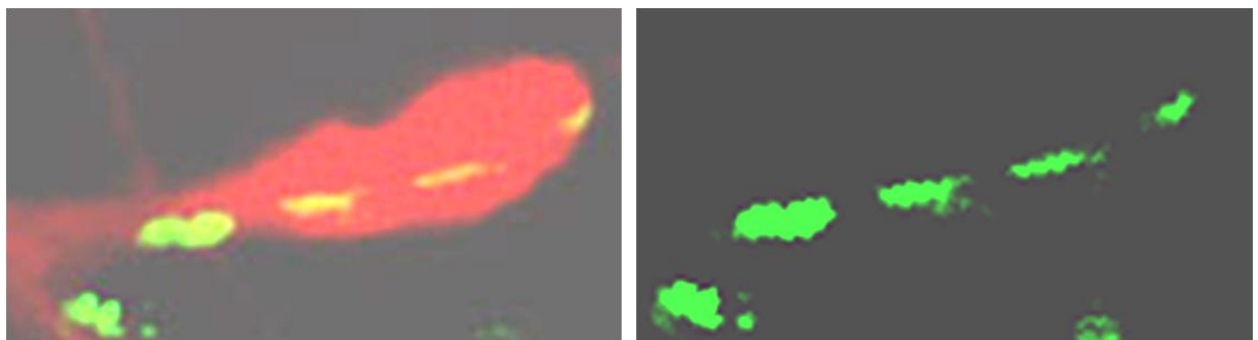


**Figure R21.** A clone indicating the possible involvement of cell intercalation/rearrangement, in which the clone is labeled in green (UAS-GFP-moesin) and the ASP is labeled in red (BtlenhRFPmoe). Cells of this clone seem to become evenly spaced out by the “squeezing-in” of unlabeled cells, leading to the speculation that cell intercalation/rearrangement may be responsible for the formation of this particular pattern.

This question immediately calls into mind a well-studied phenomenon called “convergent extension”, which takes place during gastrulation, in the course of which neighboring cells within the same epithelial sheet intercalate toward a mid-line to form a longer narrower structure.

It is tempting to propose that FGF-dependent cell intercalation could happen during ASP morphogenesis, since such a process has been observed for the dorsal branch (DB) during embryogenesis (Neumann and Affolter, 2006).

For now, the possible presence of oriented cell divisions and cell intercalation/rearrangement during ASP morphogenesis stay merely as interesting speculations. The verification awaits further investigation.



## **III. Discussion**

## 1. The genetic screen: did we find anything new and unexpected?

---

The most fascinating thing about genetic screens is that it offers an unbiased approach that can reveal utterly unknown or unexpected genes involved in a certain process of interest, because mutations are generally induced throughout the genome in a random manner.

Although we were aiming to find genes important for (FGF-mediated) cell migration during ASP morphogenesis, we did identify another different class of genes, whose mutations disrupt, directly or indirectly, ASP cell migration. These are genes that affect cell division.

### **1.1 Cell division and cell migration: two inseparable shaping forces for ASP morphogenesis?**

Cell division, through which the number of cells increases, and cell migration, through which cells can leave their “birth place” and move to a new position, are two indispensable shaping forces during embryonic morphogenesis.

Generally, these two processes are thought to be “separable”, meaning that a cell can either divide or migrate at a certain time point, but cannot do both at the same time, for both processes employ a heavy use of cell cytoskeletons and therefore the resulting competition tend to exclude each other. In *Drosophila*, for example, cell division is put on hold prior to the onset of gastrulation, during which intense cell movement, including cell migration, is involved.

Regulation of these two processes, however, is not strictly independent of each other. Ras-MAP kinase cascade downstream of RTK signaling pathways, for example, often proves important for both cell division and cell migration, even if the regulatory paths may diverge again further downstream, such as different transcription factors may mediate the final division or migration outcome (Cabernard and Affolter, 2005). In this light, mutations which we are yet to identify could turn out to affect common regulators of both cell division and cell migration, which would logically explain why clones containing such mutations are both small in size and incapable of populating the tip of ASP.

Interestingly, we have observed in our screen normal-sized clones that exhibited decreased ability to occupy the tip of ASP, a phenotype that we interpreted as cell migration defect, but we have never observed clones showing cell division defect to occupy the tip. In other words, in our experimental system, gene mutations affecting cell migration can be independent of cell division, whereas gene mutations affecting cell division always seem to inevitably affect cell migration simultaneously. How can we account for this observation?

The easiest explanation for the observation that defects in cell division always cause defect in cell migration in our system but not vice versa is that this observation is incomplete due to statistic error such as small sample size. However, we consider this unlikely.

A more plausible explanation is that during ASP morphogenesis cells undergo an initial proliferating phase to expand the population prior to the onset of migration. If a certain mutation affects a cell’s ability to divide, it produces less progeny and represents a smaller portion among the entire population compared to the neighboring wild-type cells. This will cause a disadvantage during the subsequent competition of cells for the role of “leading” the migration, which probably depends on the level of FGF signaling (Ghabrial and Krasnow,

2006). This scenario is consistent with the observation that at the early stage of ASP morphogenesis (the “budding stage”), its structure does look like a round-up ball and shows little directional growth implicating the presence of cell migration.

Another possibility is that genes affecting cell division somehow affect the general fitness of the cell. Therefore, cells containing such mutations will lose out in the migrating process to those fitter wild-type cells, ending up at the back of the ASP.

An important piece of information that we have learned from this screen is that both cell division and cell migration are indispensable processes that are intimately linked during ASP morphogenesis. Once cell division is affected, cell migration will become the “collateral damage”.

### **1.2 From cell signaling to cell skeleton: always the same story for cell migration?**

So far, two genes have been mapped in our screen to affect cell migration during ASP morphogenesis.

Two independent and distinct alleles of the gene encoding Stam (signal transducing adaptor molecule) have been identified. As will be mentioned later, the gene encoding Hrs (hepatocyte growth factor regulated substrate) had been identified as an essential player during ASP cell migration using the approach of direct candidate-testing before *stam* was mapped. In human and yeast, Hrs and Stam have been shown to bind to each other and function solely as a protein complex (Komada and Kitamura, 2004). Hrs/Stam complex has been demonstrated to be localized on the endosomal membrane, where it binds ubiquitin moieties and acts as sorting machinery that recognizes ubiquitinated receptors and subsequently transfers them to further lysosomal sorting/trafficking processes. In *Drosophila*, Hrs has been shown to be required for multi-vesicular body (MVB) maturation and down-regulation of several signaling receptors including RTK (Lloyd et al. 2002; Jekely and Rorth 2003). Prior to our study, no *stam* loss-of-function mutants had been reported, and its exact function remains to be explored.

The other gene that has been identified turns out to be *mhc*, which encodes a Myosin heavy chain protein belonging to the class of Myosin II molecules. Myosins constitute a large super-family of actin-dependent molecular motors; Myosin II, the conventional two-headed myosin that forms bipolar filaments in muscle and non-muscle cells, is directly involved in regulating cytokinesis, cell motility and cell morphology in non-muscle cells. In *Acanthamoeba*, the heavy chain phosphorylation of its myosin II has been shown to affect the activity of its actomyosin MgATPase; in the contrast, the heavy chain phosphorylation of *Dictyostelium* myosin II has no effect on MgATPase, instead, it markedly inhibits filament formation by stabilizing a polymerization-incompetent bent dimer (Brzeska and Korn, 1996). In *Drosophila*, *mhc* has been shown to be regulated in border cells by the transcription factor Slow border cells (Slbo), a key regulator of border cell migration during oogenesis (Borghese et al. 2006; Wang et al. 2006). And in the *mhc*<sup>3</sup> allele, border cell migration becomes impaired (Borghese et al. 2006).

As described above, neither of the two identified genes, one affecting cell signaling and the other affecting actin function, is an unexpected or surprising find. They fit well into the current understanding of how cell migration should take place. Further work is required to illustrate the detailed mechanisms of how these two players, Stam and Mhc, are acting during the process of ASP cell migration.

An interesting possibility is that Stam not only influences cell signaling. It might function, as part of protein sorting machinery, to maintain the apical-basal epithelial polarity of ASP cells, which gets maintained throughout ASP morphogenesis (Cabernard and Affolter, 2005). Since it has been reported for border cells that their epithelial properties, such as apical-basal polarity, are maintained and essential for their migration (Affolter and Weijer, 2005), it will be interesting to see if this would turn out to be true for ASP cells as well. It awaits further investigation.

Up to date, the majority of gene mutations identified in our screen still remain to be mapped. It will be interesting to see if any unexpected players will come into light.

If no unexpected genes should be found, this might indicate that most of the groundwork in the field of cell migration has already been accomplished and what remains is to work out exact details and to piece all the tiny bits of information together into a 4-dimensional understanding of this particular cell behavior using systematic biology approaches.

### **1.3 Oriented cell divisions (OCDs): an alternative explanation for ASP morphogenesis?**

“Build a model based on your data instead of fitting your data into a pre-conceived model!” This is an important lesson I have learned during my Ph.D. Another important lesson is to always ask myself: ““Have you exhausted all possible alternative hypotheses yet?” and to be the one who challenges my own conclusions most vigorously!

Now, three years after I was part of the screen team, I find myself emotionally less invested in the project and therefore in a better position to question the fundamental criterion that was used in our screen:

Is cell migration defect the only explanation for the observation that some mutations can reduce cells’ ability to populate the tip during ASP morphogenesis?

The answer is NO.

As mentioned earlier, gene mutations affecting the general “fitness” of cells could cause them to lose out in the competition for the leading position of a growing ASP, without directly impairing their ability to migrate.

As described in the result section, the observation of a clone consisting of eight cells that aligned themselves along the proximal-distal (P-D) axis and spanned the entire length of the ASP begs the question:

Could oriented cell divisions along the P-D axis be responsible for the longitudinal growth of ASP during its morphogenesis?

As pointed out by Ray Keller, without a change in volume, merely the cell division process of splitting one cell into two alone can theoretically produce a 60% elongation parallel to the spindle long axis (Keller, 2006). This provides a useful way to regulate the organization of cell populations within a certain tissue. The consistent systematic alignment of mitotic spindles within dividing populations could therefore lead to significant tissue elongation. For example, cell divisions in the zebrafish dorsal ectoderm is oriented parallel to the animal-vegetal axis at gastrulation (Concha and Adams, 1998; Gong et al., 2004). Mis-oriented divisions are associated with a failure to elongate the body axis in embryos with disrupted functions of Dishevelled, Wnt11/Silberblick, or Strabismus activity, important players mediating planar cell polarity (PCP) (Gong et al., 2004). Such oriented cell divisions also contribute to elongation of the *Drosophila* wing (Baena-Lopez et al., 2005) and the mammalian kidney (Fischer et al., 2006)

Planar cell polarity (PCP) describes a global tissue-level phenomenon that cells become coordinately polarized within a two-dimensional epithelial sheet, as revealed by the ability of some cells to orient hairs or cilia. It has been proposed that at least two independently acting processes should operate to regulate PCP, both utilizing directional cues provided locally by communication between neighboring cells (Lawrence et al, 2007).

There has yet been no report in the published literature concerning whether PCP plays a role during ASP morphogenesis. If oriented cell divisions (OCDs) should indeed contribute to the longitudinal growth of ASP, it would be fascinating to find out if such OCDs should be regulated by the PCP pathways, which probably would function downstream of FGF. Whatever the conclusion would be, it would deepen our understanding of how to use different strategies for constructing a polarized tissue.

#### **1.4 What are the possible roles of FGF signaling during ASP morphogenesis?**

It has been well established that FGF/Bnl functions as a chemoattractant for guiding migrating tracheal cells during embryonic tracheal development (Sutherland et al., 1996). The absence of cell proliferation in the tracheal system during embryogenesis after the onset of branching morphogenesis simplifies the analysis. ASP morphogenesis during the 3<sup>rd</sup> *instar* larval stage (L3), however, clearly involves both cell proliferation and cell migration (Sato and Kornberg, 2002; Cabernard and Affolter, 2005), which complicates the analysis of the exact roles played by FGF.

In 2002, Sato and Kornberg, in their cardinal publication which opened the field of ASP morphogenesis, proposed that FGF functioned as both a mitogen and a motogen, responsible for cell proliferation and cell migration. Cabernard and Affolter, on the other hand, presented a hypothesis in their 2005 paper that FGF signaling directed cell migration at the tip of the structure, while EGF signaling was instrumental for cell division and cell survival in the growing epithelial structure. Both publications have come to the conclusion that FGF is indispensable for ASP cell migration. What remains controversial is the following question:

Is FGF signaling required for cell proliferation during ASP morphogenesis?

Sato and Kornberg answered “yes” to this question, because when they expressed a dominant-negative form of *btl* (*UAS-btl<sup>DN</sup>*) driven by *btl-Gal4*, the formation of ASP became completely abolished, which should not be the case if the cell proliferation had remained unimpaired (in which case, an abnormal, un-elongated ASP would have been seen). In addition, when they used the same *btl-Gal4* driver to express a constitutively active *btl* (*UAS-λbtl*), they observed an increase in the number of ASP cells, consistent with the idea that FGF should function as a mitogen.

Cabernard and Affolter answered “no” to this question, because MARCM clones of an amorph allele of *breathless (btl)*, the encoder of *Drosophila* FGFR, showed mere defect in cell migration but unaffected cell proliferation, as *btl* clones retrieved exhibited sizes comparable to wild-type clones, an observation contradictory to the idea that FGF could work as a mitogen. Instead, they discovered that clones mutant for EGFR showed decreased size and viability. Hence, they came to the conclusion that EGF, but not FGF, was required to stimulate ASP cell proliferation.

Is there any way that we could reconcile these two conflicting conclusions?

Personally, I think one key experiment to be repeated is to drive *UAS-btl<sup>DN</sup>* expression using *btl-Gal4* again and to record the penetrance of the phenotype that no ASP forms. This will provide a crucial piece of data for interpreting the possible roles of FGF during ASP morphogenesis. In addition, it may be interesting to test if over-expression of *UAS-btl<sup>DN</sup>* would in any way block EGFR signaling simultaneously—this would show if the absence of ASP with *UAS-btl<sup>DN</sup>* over-expression could be due to disrupted EGFR signaling. It also remains to be tested if FGF –mediated cell intercalation and FGF-regulated planar cell polarity (PCP) could also be operating during ASP morphogenesis.

## 2. The approach of direct candidate-testing: oh that —did not I know already?

---

In contrast to the screening approach, which could uncover totally unexpected players, the approach of direct candidate-testing often provides no surprises. As revealed by the name, “direct candidate-testing”, some clues must already be available that lead to the determination why a certain gene should get chosen as a candidate.

### 2.1 Redundancy: the best way to provide robustness?

As presented in the Results section, some well-known genes regulating actin dynamics or genes demonstrated to be essential for other types of cell migration were tested for their possible roles during tracheal cell migration in the course of ASP morphogenesis.

Not surprisingly, key regulators of actin nucleation process, such as SCAR, Wasp and Arp2/3, do affect ASP cell migration— the stronger the allele, the worse the phenotype becomes. Similarly, Ena, an important actin regulatory protein, also seems to be involved. A mutation in *diap1*, a protein important for border cell migration, reduces ASP cells’ ability to populate the tip, possibly due to the disrupted function of Rac, another important regulator of actin dynamics.

*Drosophila* Mmps, a family of proteases that have been hailed to be indispensable for cell migration/invasion, appear to have no significant effect on the behavior of mutant clones, possibly because that Mmps may function non-cell-autonomously in the wild-type situation. Interestingly, mutations in *mmp2*, the encoder of a membrane-tethered Mmp, somehow increased the ability of clones to occupy the tip. This could possibly indicate that it functions as a negative regulator for FGF signaling during ASP morphogenesis. It may be worthwhile to invest further effort into confirming this preliminary observation and to pinpoint how this could happen, if this hypothesis should be true. Does Mmp2 normally function to cleave the FGF-FGFR-HSPG signaling complexes and down-regulate FGF signaling? Or does it function in a more unexpected way?

One important message that I have extracted from these candidate-testing experiments is that tremendous redundancy exists in the interacting network which mediates the cell migratory behavior. Visually speaking, I would like to imagine a pyramid-shaped diagram which depicts all possible relationships among the molecular participants taking part in the maneuver of leading a cell to migrate. It may all start at the cell surface, where only a few kinds of specific signals could “convince” a cell to re-distribute its cellular resources and to initiate downstream actions that will ultimately lead to modified activities of cell skeletons. The closer a link is to the modification of cytoskeletons, the more redundancy there might exist. This is as if that during evolution a cell has learned not to easily succumb itself to external commands, but once it has “decided” to follow an order, it will do its very best to ensure that such an order will get executed. Therefore, both specificity and robustness can be achieved. In this light, it will be plain to see why different actin regulators, which are at the bottom of the pyramid-shaped network, each alone has relatively mild effect on cell migration, since abundant back-up personnel are available to compensate its mal-function. On the contrary, once a defect strikes a player high “up” in the pyramid-shaped network,

its effect on cell migration will be much worse. And *hrs* may exactly be such an upstream regulator.

## **2.2 *hrs* and *stam*: two pieces of the same puzzle?**

Serendipity happens in Science. And I seem to have experienced it at a tiny scale. As mentioned earlier, I had identified *hrs*, the gene encoding Hrs (hepatocyte growth factor regulated substrate) as an essential player during ASP cell migration, using the approach of direct candidate-testing. This was prior to the final mapping of *stam* mutations identified in our MARCM-based screen. When we found out in the literature that Hrs and Stam had been shown, in human and yeast cells, to bind to each other via their coiled-coil domains and possibly function as a complex, we were feeling elated. Two utterly different approaches, a genetic screen and candidate-testing, have brought our attention to the two important players of the same pathway, two pieces of the same puzzle:

How does the endocytic machinery have a hold over the cell migratory behavior?

In mammalian cells, a process called “receptor down-regulation” has been well studied, during which, upon stimulation by growth factors, the growth factor/receptor tyrosine kinase (RTK) complex becomes rapidly internalized via clathrin-coated vesicle-mediated endocytosis and gets eventually transported into lysosomes for acid hydrolases-mediated degradation. This provides a cellular strategy to attenuate cell proliferation triggered by growth factors and to prevent the overgrowth of the cell. Conjugation of ubiquitin (Ub) to RTKs has been shown to play an essential role in their down-regulation. This ubiquitination, rather interestingly, does not serve as a signal for proteasomal degradation. Instead, it serves as a sorting signal for transport to the lysosome.

Following endocytosis, ligand-activated RTKs become incorporated into luminal vesicles of the endosome that bud inward to form the so-called multi-vesicular body (MVB), giving this trafficking route its name as the MVB pathway, which is conserved from yeasts to higher eukaryotes. These MVBs either mature into or fuse with late endosomes, and subsequent fusion of late endosomes with lysosomes results in the release of luminal vesicles containing activated RTKs into the lumen of lysosomes, where complete degradation of RTKs take place.

In the mammalian cells, the Hrs/Stam complex, localized on the cytoplasmic surface of early endosomes, has been shown to function as the key players during RTK down-regulation via the MVB pathway (For review, see Komada and Kitamura, 2005). Hrs has a FYVE (Fab1/YOTB/Vac1/EEA1) domain, which specifically binds phosphatidylinositol 3-phosphate (PtdIns3P). PtdIns3P is especially enriched in the endosomal membrane, thereby functioning to anchor Hrs on the endosome. Stam, however, does not have such a lipid-binding domain and is shown to be indirectly localized on the early endosome by binding to Hrs. On the early endosomal membrane, specific areas exist to which a flat clathrin coat is attached. Localization of Hrs is restricted to this micro-domain of the endosome, although the function of the clathrin coat still remains elusive. Hrs binds the clathrin heavy chain via a clathrin box, a short peptide motif located at the C-terminus of Hrs. It has been speculated, therefore, that the Hrs/Stam complex might recruit the clathrin coat to the micro-domain of the endosome, or *vice versa*, through direct protein-protein interaction.



Both Hrs and Stam possess a Ub-interacting motif (UIM) and have been shown to bind Ub directly. In Hrs, the UIM serves as the major Ub-binding site, whereas in Stam, the N-terminally-located VHS (Vps27/Hrs/Stam) domain plays an essential role in Ub binding, cooperating with the following downstream UIM. In the yeast, the Hrs/Stam complex has been shown to recruit ESCRT-I (endosomal sorting complex required for transport-I), one of the complexes that serve as the sorting machinery for ubiquitinated cargoes on the endosomal membrane. In addition, the Hrs/Stam complex is also required for MVB formation (*i.e.*, invagination and budding of the endosomal limiting membrane into its lumen).

In *Drosophila*, Hrs has been shown to be required for MVB maturation and down-regulation of several signaling receptors, including RTKs (Lloyd et al. 2002; Jekely and Rorth 2003), consistent with the findings obtained for Hrs in other systems. Prior to our study, no *stam* loss-of-function mutants had been isolated or studied in *Drosophila*.

Recently, it has been shown that *Drosophila* Hrs/Stam complex does function in the same way as its counterparts in yeast or mammalian cells do, namely, it indeed functions to down-regulate FGF signaling during ASP cell migration (H.C. et al, unpublished results). However, the question still remains: how does mutated *hrs* or *stam* results in cell migration defect?

The answer is not instinctively clear.

If the Hrs/Stam complex normally down-regulates RTK signaling, a mutant *hrs* or *stam* allele will abolish this attenuating effect and probably results in prolonged and/or over-activated signaling mediated by cell surface receptors, including RTKs. But why should prolonged and/or over-activated signaling activities cause cell migration effect? Do prolonged and/or over-activated signaling activities somehow blur the directionality contained in the original message, such as by disrupting the polarized distribution of signaling receptors, and cause the cells confusion about where to go? What are other possible explanations?

Or, alternatively, in addition to its role in regulating signaling receptors, does the Hrs/Stam complex possibly carry out other functions as well? For example, does it help to maintain epithelial properties, such as the apical-basal polarity, of the ASP cells? Is it possible that the proper epithelial properties are required for ASP cells to migrate normally, which become impaired in the *hrs* or *stam* mutants?

What is also worth pointing out is that *hrs* or *stam* clones in the ASP do not seem to become over-grown, which should have been the case if RTK signaling such as EGFR signaling was prolonged and/or over-activated. Rather, these clones appear to be comparable or even smaller in size than wild-type clones. How should this be explained?

As it has become clear now, the exact mechanism of how defected endocytosis could disrupt cell migration during ASP morphogenesis still remains elusive. Further investigation is required to solve this puzzle.

### 3. Clonal analysis

---

#### 3.1 Origin of L3 mitotic cells in Tr2: new hope for regenerative medicine?

To our own surprise, the origin of Tr2 mitotic cells found during the “repopulation” turns out to be the Tr2 larval tracheal cells, which were presumed to be terminally differentiated, endo-replicated and unable to re-enter the cell cycle. Indeed, we were ourselves favoring the “replacement” hypothesis, in which a mitosis-competent population, distinct from the larval tracheal cells, would proliferate upon stimulation, migrate out of its niche, possibly the spiracular branch (SB), and replace the Tr2 larval tracheal cells. This scenario, as it has turned out, indeed applies well to other tracheal metameres, except for the Tr2 (Weaver and Krasnow, 2008).

At the beginning of our clonal analysis, I was looking for even the slightest trace of evidence that could indicate the presence of cell migration. Disappointingly, I found no such evidence at all. The shapes of clones tend to be compact and “patchy”, indicating little cell movement; the cell sizes within a clone can sometimes be roughly categorized into being “big”, “medium” and “small”, indicating a possible, daring idea that sequential mitoses starting with Tr2 larval tracheal cells may be operating and these terminally differentiated cells may indeed be capable of dividing after all—Sato and Tabata made similar observations, which led them to the same conclusion (Sato and Tabata, 2008).

In summary, the discovery of the provenance of Tr2 mitotic cells observed during the “repopulation” offers several insights relevant to cell proliferation in differentiated organs undergoing repair or renewal. First, some of the cells that make up the larval tracheal system retain their capacity for proliferation. The ability of cells of the Tr2 metamere to restart their mitotic program revealed that expression of a fully differentiated state does not prohibit subsequent proliferation. For such cells, the term “terminal differentiation,” with its implication that the cells lack growth potential, is inappropriate. Second, the process that reconstitutes the Tr2 metamere, increasing the number of constituent cells by  $\approx 10$ -fold and entirely transforming its cellular composition, does so without compromising function. This metamere retains its multipartite structure [e.g., apical taenidial cuticle, cellular core, and basal lamina (Guha and Kornberg, unpublished data)] and functions as an air-filled conduit throughout the period of reconstitution. The term “dedifferentiation” may also therefore be inappropriate. Third, the larval cells of Tr2 show developmental plasticity, a property they manifest by contributing not only to the preexisting tracheal branches, but by also populating the ASP. In this context, they are multipotent. The dorsal air sacs that the ASP generates are arguably distinct organs, lacking the taenidial cuticle and radial symmetry that are characteristic of all tracheal branches (Guha and Kornberg, unpublished data). Fourth, the ancestry of the cells that proliferate and renew the larval tracheal system is not the same in all of the metameres. Although proliferating cells that rebuild the tracheal network in Tr2 are derived from the cells that constitute Tr2 tracheal branches in the embryo, L1, L2, and early L3 larva, the polyploid state of the cells that constitute the other tracheal metameres makes it unlikely that these cells return to a mitotic program. Indeed, renewal of the tracheal branches in the abdominal metameres is

reported to involve replacement of larval cells by a distinct population of imaginal tracheoblast precursors. Thus, within this single organ, the *Drosophila* tracheal system, mechanisms of remodeling vary. It has been shown that the Bithorax Complex (BX-C) functions in the Tr3 metamere to block cell proliferation and tubulogenesis, establishing that such differences are regulated, in part, by the mechanisms that determine segmental pattern and identity (Guha and Kornberg, 2005).

The mechanisms of organ renewal and neogenesis in animals are of both fundamental and clinical importance. Although the involvement of pluripotent stem cells has been established for many vertebrate and invertebrate organ systems, contributions may also come from dedicated pools of precursors or from differentiated cells that revert to a proliferative state. The cells of the imaginal discs of holometabolous insects such as *Drosophila* are examples of precursors that are dedicated to a particular epidermal fate and differentiate structures only after the larval epidermis has been eliminated at metamorphosis. These imaginal disc cells proliferate in an undifferentiated state throughout the foraging stages of larval development. There are also cases of cells that both express a differentiated state yet retain the capacity for growth. In the larval abdomen of *Drosophila*, larval cells occupy most of the epidermal surface and secrete most of the cuticle, but the imaginal histoblasts that will replace the larval cells at metamorphosis and make the adult abdominal cuticle occupy a small portion of the larval epidermis and secrete cuticle during the larval stages. Examples of differentiated cells that contribute to renewal or neogenesis in vertebrates include the insulin-producing beta cells in the mouse pancreas that may be a source of beta cells during adult life (Dor et al, 2004) and proliferating cardiomyocytes in regenerating the zebrafish heart (Poss et al, 2002).

Our work has demonstrated again a stem cell-independent mechanism of organ renewal and possibly expands the strategies that Regenerative Medicine could employ and explore for the benefit of patients.

### **3.2 When do different metameres become different from each other?**

The observation that different tracheal metameres are not equally sensitive to heat shock have led us to a simplest explanation, which is that metameres Tr2, Tr3 and Tr5 are already essentially different at late embryonic stage when clones get induced. Although the physical diameter of DT does increase from anterior to posterior, we think the essential difference of these metameres lies in the ploidy of cells that constitute them, respectively. The higher the ploidy, the more copies of *hs-flp*, *Act>CD2>Gal4*, and *UAS-GFPnls* can be found within a cell; even if the induction condition of heat shock remains the same, more copies of these genes can lead to more functional flippase protein molecules producing more flip-out events, therefore increasing the efficiency of cell labeling. Our recent study (Guha et al, 2008) shows that the ploidy of Tr2, Tr3 and Tr5 are dramatically different during L2 and L3 stage, which can be explained by the fact that Tr3 and Tr5 undergo endo-replication whereas Tr2 does not. However, when the endo-replication program starts exactly, remains unknown. The essential difference between Tr2 and Tr5 indicates that Tr5 probably has started its endo-replication process even prior to entering L1 larval stage. The difference between Tr2 and Tr3 is not statistically significant. The small sample size we collected may not be enough to reveal their difference, if they should be indeed

different. Or, it could also indicate that Tr3 hasn't entered into endo-replication yet at the time of clone induction. Therefore, it possesses the same ploidy as Tr2 does. It requires further research to investigate what drives tracheal cells into endo-replication, when this program starts, what prevents Tr2 from entering into such a program, and if the remaining metameres all start endo—replication simultaneously.

### **3.3 What regulates the mitotic behaviors of Tr2 cells during larval stage?**

The DNA content data presented in our recent study (Guha et al, 2008) shows an interesting shift toward lower ploidy in wandering L3 larvae, at which stage Tr2 cells are actively dividing, compared with L2 larvae, at which stage Tr2 cells still remain mitotically quiescent. This shift to lower ploidy indicates a possibility that these Tr2 cells could be arrested at G2, or S/G2 prior to re-entering into proliferation during L3, namely, they could have at least partially replicated their DNA, and as a consequence, be bearing a ploidy number higher than 2N, the predominant ploidy number of Tr2 cells at the wandering L3 stage. This possibility is also supported by the fact that over-expression of *string*, which encodes a G2/M regulator Cdc25 phosphatase, can push Tr2 cells into mitosis during L2 stage (Guha and Kornberg, unpublished data). Is there any factor that keeps these Tr2 cells arrested prior to L3 stage? If so, what releases them from the growth inhibition and allows them to enter into a proliferative state? Do these cells require different signals for initiating proliferation and for maintaining its proliferative state? Or do they require sequential signals for these tasks?

In order to answer such questions, we need to have an assay which can enable us to tell if the mitotic activity of Tr2 cells proceeds normally or if it gets disturbed. Our clonal analysis data presented here has enabled us to attain a picture of wild-type mitotic landscape of Tr2 cells during L3 and allowed us to screen for possible regulators that could potentially regulate their mitotic behaviors.

*Drosophila* histoblasts, founder imaginal cells specified during embryonic stages as small incorporated groups organized in nests and from which the adult epidermis is formed, were reported to be mitotically quiescent and arrested in G2 (Madhavan and Schneiderman, 1977) during larval stages. In wild type, the abdominal histoblasts arrest in G2 of the cell cycle through most of larval development and then re-enter the cell cycle after puparium formation. In Cdk1 and escargot mutants, histoblasts fail to arrest in G2 and instead enter an endocycle (Hayashi, 1996; Hayashi et al., 1993). It has been shown that extrinsic Ecdysone hormones are responsible for histoblast proliferation (Ninov et al, 2007).

So far, the signals regulating the mitotic behaviors during larval stage have not been identified. Ecdysone, Jak-Stat, Hh, EGF and FGF each alone is not sufficient. It remains to be elucidated if a signaling pathway or multiple signaling pathways will turn out to regulate this process.

### **3.4 Is Tr2 regionalized?**

During embryonic tracheal development, different signaling pathways take place in different branches within a metamere, endowing these branches with their unique

identities. For example, Dpp is expressed in ectodermal stripes dorsal and ventral to the tracheal placode, giving rise to DB and lateral trunk (LT) (Vincent et al., 1997). Rhomboid (rho)-mediated EGFR signaling pathway and Wingless (Wg) pathway determine a central domain that gives rise to DT and visceral branch (VB) (Wappner et al., 1997; Chihara and Hayashi, 2000; Llimargas, 2000). Activities of these signaling pathways promote territorial differentiation of these tracheal cells, which exhibits itself through branch-specific expression of transcription factors, such as Knirps (Kni) and Knirps related (Knrl) in the DB and LT (Chen et al., 1998), and spalt major (Salm) in the DT and VB (Kuhnlein and Schuh, 1996; Franch-Marro and Casanova, 2002). In the light of these reports, it seems easy to explain why cells in the DB and DT, or cells in the DT and TC don't mix with another. On the other hand, ASP buds out from TC during L3. Or, put differently, TC gives rise to ASP. So it is not at all surprising that TC cells can "intermix" with those of ASP, and they will, since this intermixing, this replenishment, is indispensable for the proper growth of ASP. It is worth noting that cells of different branches in Tr2 may be dissimilar due to their distinct signaling histories, but they all demonstrate the same developmental behaviors: staying mitotically quiescent throughout the rest of embryonic stage after their specification, throughout L1 and L2 larval stage, and then reverting back into a proliferative state to give rise to progenies for the remodeling of its tracheal structure.

### **3.5 What cell behaviors are involved during ASP morphogenesis?**

Cell proliferation and cell migration are the first two cell behaviors that were recognized immediately upon the discovery of ASP, as reported in detail in the cardinal paper of Sato and Kornberg in 2002.

Using clonal analysis, a method to randomly label one cell and its progeny among a large population, we seem to have gained a more "close and personal" look at how cells may behave in their natural habitat during a morphogenetic process such as ASP formation. What we have found is that cells seem to be more active and more versatile in terms of "internal movement" (movement within a certain structure) than previously conceived. In the context of ASP morphogenesis, cells may take up the following behaviors in addition to cell proliferation (un-oriented) and cell migration (longitudinal, from the base to the tip of ASP):

Lateral movement, in which cells don't move "forward" but "around", allowing them to relocate themselves from the upper layer to the lower layer, possibly in part due to mechanical tension;

Oriented cell division, during which a cell and its daughter cells keep orienting their mitotic spindles along the proximal-distal axis, contributing to the efficient longitudinal growth of the structure. This process very likely depends on the FGF signaling;

Cell intercalation/rearrangement, during which cells within the same epithelial layer move toward an imaginary mid-line, "squeeze" into each other, and possibly remodel cell-cell adhesion actively while they are doing so. This also contributes to the longitudinal growth of the structure.

With more systematic recordings, and especially when live-imaging of ASP morphogenesis in dissected wing discs becomes possible, more yet-to-be-discovered cell behaviors will probably continue to get uncovered, enriching our in-depth knowledge about cells' private and social lives during morphogenesis.

### 3.6 Open questions

If we consider 2002 as the year that the field of ASP is initiated, we have gained much understanding about how ASP develops, seven years down the road. Still more, however, remains to be investigated.

Some of the most intriguing questions are the following:

What makes Tr2, from which ASP develops, so different from the rest of the metameres? Hox gene control apparently plays a role, but is that all? And evolutionarily speaking, does the distinction between Tr2 and other metameres teach us anything about evolution?

If we ask smaller, more concrete questions instead of the previous conceptual ones, many things come to mind:

What are the exact roles played by FGF signaling pathway? Is it possible that FGF could function as a morphogen? For example, is it possible that the cells experiencing the highest concentration of FGF migrate, those experiencing the medium concentration proliferate, and those experiencing the least does neither of the two? Does FGF signaling cross-talk to any other pathways?

As described previously, two rounds of cell divisions take place during embryonic tracheal development prior to the onset of branching. Some preliminary evidence indicates that Tr2 cells are arrested in G2 before executing the first mitosis in L3 and probably remain so throughout L2, which means that they have finished replicating their genome already before entering into L2. If this should really be the case, what signal drives the Tr2 cells to replicate their DNA and when? What keeps these cells arrested through L2 and the beginning of L3 stage? What is the signal or the combination of signals that release the Tr2 cells from their G2 arrest? Does the same signal or the combination of signals also persist to maintain their proliferating ability or does/do some new regulator(s) come into play? Do these cells continue proliferating in the pupal stage? What happens to them afterward? All these fascinating questions concerning how developmental control of cell cycle takes place remain to be explored.

It has been well demonstrated now that the Tr2 larval tracheal cells, upon stimulation by yet-to-identified signals, probably in L3 or late L2, will go into mitosis and produce progenies that are about 10-fold more in number at the end of L3. What happens, during the pupal stage or at metamorphosis, to these mitosis-competent cells observed in late L3? Are these cells going to give rise to the adult air sacs? Or are they going to be replaced by some other cells, out of which adult air sacs will develop?

What cell behaviors are taking place during ASP morphogenesis? Can oriented cell divisions and cell intercalation/rearrangement get confirmed to take part in the process of ASP construction?

Endocytosis seems to play a role during ASP morphogenesis, possibly through its effect on cell migration. How does this work exactly? Does endocytosis regulate cell polarity, cell signaling, or some other processes?

It is surprising and intriguing that the ASP upper and lower layers are different in morphology and in mitotic activity, since these kinds of asymmetry of a tube have not been previously reported, according to our knowledge. The presence of asymmetry in mitotic activity creates a special problem for the growth of the overall structure of ASP, which gets solved ingeniously by a strategy of cell movement, commonly employed during morphogenetic processes throughout species, possibly engendered by a need to balance the mechanical tension within the growing or shape-changing structure itself. It yet remains a mystery how this asymmetry is initiated and maintained, what signaling pathways or molecules are involved, and if this asymmetry has any functional implications in the adults.

And what about adult air sacs? How do they function? How are they regulated? Do they, like human lungs, have additional functions besides providing oxygen for the organism, such as immune defense?

Abundant exciting questions still await exploration.

## **V. Short description of other projects**





***A life spent making mistakes is not only more honorable but more useful than a life spent in doing nothing.***

**--George Bernard Shaw**

Everything started when I stumbled into a paper (Sørensen, V. et. al., 2006), which described how secreted FGF-2 in the mammalian system had been found to reach the cytosol and nucleus of target cells and how nuclear translocation of FGF-2 was required for a full mitogenic response, although not for differentiation. A question immediately rose to my mind: “How about the FGF in flies? Could it behave in a similar way?”

No answer to this question could be found in the available literature. Biochemical characterization of Bnl had not been reported. In *Drosophila*, it had been known that FGF/Bnl was the ligand of FGFR/Btl and FGFR signaling was essential for tracheal morphogenesis, both at embryonic and later stages. It had always been assumed that Bnl proteins would get produced in *bnl*-expressing cells and then secreted into their surroundings, where they could work both as a mitogen and a motogen. Nobody, however, had presented any solid data to backup this assumption. Neither did people know exactly how FGF/Bnl and FGFR/Btl interacted with each other *in vivo*, and what would take place after the binding of FGF/Bnl to its receptor FGFR/Btl on the surface of target cells. Does Bnl/Btl complex get internalized after signaling initiation and then end up destroyed in lysosomes? Or does FGF/Bnl perhaps also go into the cytosol and then into the nucleus of its receiving cells, just as its mammalian counterpart FGF2 does? To try to answer these questions, I decided to give a try studying FGF/Bnl trafficking in Schneider (S2) cells.

To get started, I chose to tag Bnl with HA, assuming that a small tag like HA would probably not interfere with the normal function of Bnl. Being aware of previously failed effort of adding a tag to the C-terminus of Bnl and the presence of signal peptide for secretion at its N-terminus, I decided to put HA tag internally. To increase my chance of success, I selected four different tag insertion sites along the protein sequence, with two locating upstream of Bnl FGF core domain (the only part of this *Drosophila* protein that shows some homology with FGF proteins in other organisms) and two downstream of it (See Figure V1). At the same time, I also took up the project of making antibodies against Bnl, which would provide a useful tool for my own studies (with S2 cells or with fly tissues) and for the *Drosophila* community at large. I chopped the Bnl sequence into three fragments: F1

denotes the N-terminus of the protein preceding the FGF core domain, F2 denotes the FGF core domain, and F3 denotes the C-terminus of Bnl downstream of the core domain (See Figure V2).

### 1. Purification of Bnl core domain for antibody production

By regular cloning, I inserted the encoding sequences of all three fragments into an expression vector called pGEX-KG (containing the sequence encoding a GST tag, which helps purification and could also increase the solubility of tagged proteins). After being introduced into bacteria, all three constructs showed similar expression levels. Assuming that it would make better sense to produce antibodies against the most conserved part of the Bnl protein, I decided to focus my effort on the purification of the F2 fragment containing the FGF core domain.

A major problem showing up already at the very beginning of the purification process was that the bacteria-produced F2 peptide remained insoluble and ended up in inclusion bodies. This made it difficult to obtain pure and active protein molecules preferred for the purpose of antibody production. Different Optical Density (OD) values of growing bacteria, different IPTG (isopropyl  $\beta$ -D-1-thiogalactopyranoside) concentrations for inducing protein expression, different induction/expression temperatures, different protein expression durations, different lysis buffers and methods were tried out to increase the solubility of the product. Nothing worked. 8M urea and subsequent dialysis were also tested, but the denatured protein products crashed out of solution during the last step of re-naturation (going from 0.5M urea into PBS).

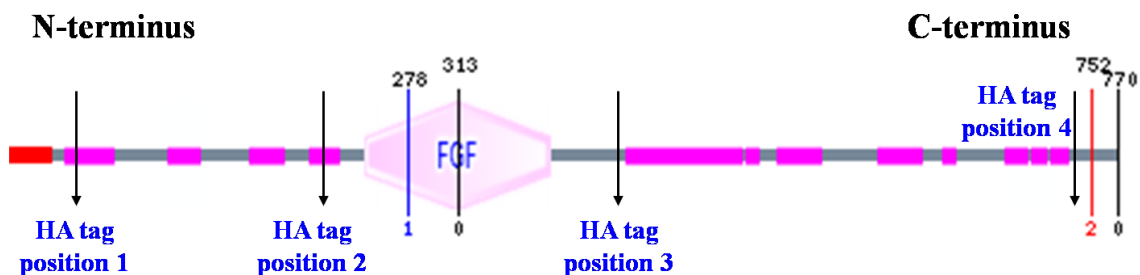


**Figure V1.** A graph indicating the 4 positions used for HA tag insertion, and subsequently for GFP tagging.

## bn1 Open Reading Frame (ORF)

1 ATGCGAAGAA ACCTGCGCTT AGACTGGAGG GCCCTGGCGC TGCTGGGCGC  
51 CCTCCTCTCG TTCATCATCG CCTGGCGGGG CTTGTATCT GCGATGCCCC  
101 TCATGGCCAT GGACAACAAC TTGACAGACT CATCCGGATC CACAAACACA  
151 TCCACATCCT CCACATCAAA ATACAACAGC ACGAACAATA GTAATCTGTT  
201 TAGTAATAGT TATCTACAAA GTGATCATAG TCGTAGTAGT TTAGTGCCGA  
251 GCGCAGTGAG TGAACGTAGT GTAAATCAAC CCACAAATCA AAGTATTAAT  
301 GCTGAATTTA ATCAGAGCTT AAGCACGCAT CCAACTGCCA TAACAAGCAC  
351 ACCACAAACC CAAACTCAAA CCCAAATCCA ATCCCAATAC CCATCGCAGG  
401 CGGAGGATTC CGATCAGCTG GAGGAGCCGC TGGGATTCGT CATCTCAGCG  
451 ATGCCGAACG AGCATCTGGC GGTCTGTGCG CGTACCGAAC GCAGCATTGCG  
501 TCACCAGAAT CAGCAGCAGC AGAAGAAGCA TCACCATCAT CACCAACAAC  
551 AGCAACAGCA ACAGCATCAG CAGCAGCAAC CAATGTCGCC CGCTGACAAT  
601 AATTTTCATTG GTTCGAAATC GAAAAGACTG AGCAACCCTA GAAGTAGTCT  
651 TAACATAAAT AGCAGTAGCA GTAACACGCC CATCAGCAAT CTGGACCCTA  
701 ACGAACGATC CACGGTGCCA CAGTCCCATT TGGCCTGGAC **CTCGCGCAAG**  
**751 ATCCAGCTGT ACATCAAAA TCGCATCCTT CAGATATTGC GGGATGGCGT**  
**801 TGTCAACGGA ACCCAGGACG AGAATAGTGA ATTCACAATT CTCCAGCGAT**  
**851 CCACGGTGGA TGTGGGACGC ATCAAGTTGC AGAGTGTGGC CACTTGCCTG**  
**901 TATCTCTGCA TGGACGCGTG CGGTGTTCCT TACGGCTCGA AAGACTTCAC**  
**951 CGACGACTGC GTCTTCAACG AGAACATGGG TCTTCAGAAC TACAACACTT**  
**1001 ACTCCTCCAC GTACCACTCT CAGGCGCGGC GGGTCTTCTA CCTGGCCCTG**  
**1051 AATGGCAGTG GCCAGCCCCG GCGTACCCAG ATCCCGGCCA GCCGATCGCT**  
**1101 GGGCAAGCTG AGCACCTACA CGAACGCCAT CACGGAGACG GTGCCGCAGG**  
1151 AGCGGGTCGA GCAGCTGATC GCCAAGAATT TTGGGGCCAA TCGCGTCAAG  
1201 CACGGCGTGC GGCAACTCTG TGATACGGGC AAGCCGCTGA TCGAGCTGAT  
1251 CGATGTGGCC AGATTCAAGG CGCCGCCACA TTGCAGCAGC AAC**ACTAGTG**  
1301 GCAGCAGCAG CAGCATCAGC AGCAGCAGTA GTAGCAGTAG CAAAAGTAGT  
1351 AGCAATAGCA GTAGCAGTTA CGTTCCTGTG TCTGCGATCA GCAGCCTGAG  
1401 TAGTATTAGT AACAGTAGTC AAAGCGAGAG CGGCCATATT AGCAGTAGCC  
1451 TTAGCGGTAG CAGTAACAGT AATAGTAGTA GCAATAGTAG TAGCAGTAAC  
1501 AGTAGCAGTA ATAGTAGTAG ACCAAGTGGT AGCAAGGCCA ACAAGAAGAA  
1551 GAAGCCCAAG TGCAAGCCGC ACGAGCAGGA GGACACTCAC AATTGCCAGA  
1601 AGCGCGGTGG CGCCGGAGCG GGAGCATTGC GAAAACCTTG TCCCAAGGCG  
1651 AAGAGGTGCA AGGAGCTGCG GGAGAAGGCG GCCGCCGAGA AGCGAGCGCC  
1701 GCCCAATTGT GGCAAGAAGA ATGGGGCCAG GAAGAATCCT ACAGAGGCAG  
1751 CCAAGGCGGT GCAACAGCGA CCCAAGGGAA ACATCCAGCA CGGAGGCAAG  
1801 AAGAAGCCGA ACAAGGCTGG TAAACAGCGC CAAAATGGGG GCAAAAAGCA  
1851 GCAGCAGCAG CAACAGCATC AGTTGCAACA ACAGCCGCTG CAACATCAGG  
1901 CCAAATCCAT TTCCGGTGGC AAGAGGAAGC ATCGGAAATT GGATGCAAGT  
1951 ACCACCACCA CCATGGCCAC CAGCCTGGGC ACGCCCCCAA GTAGCCACTG



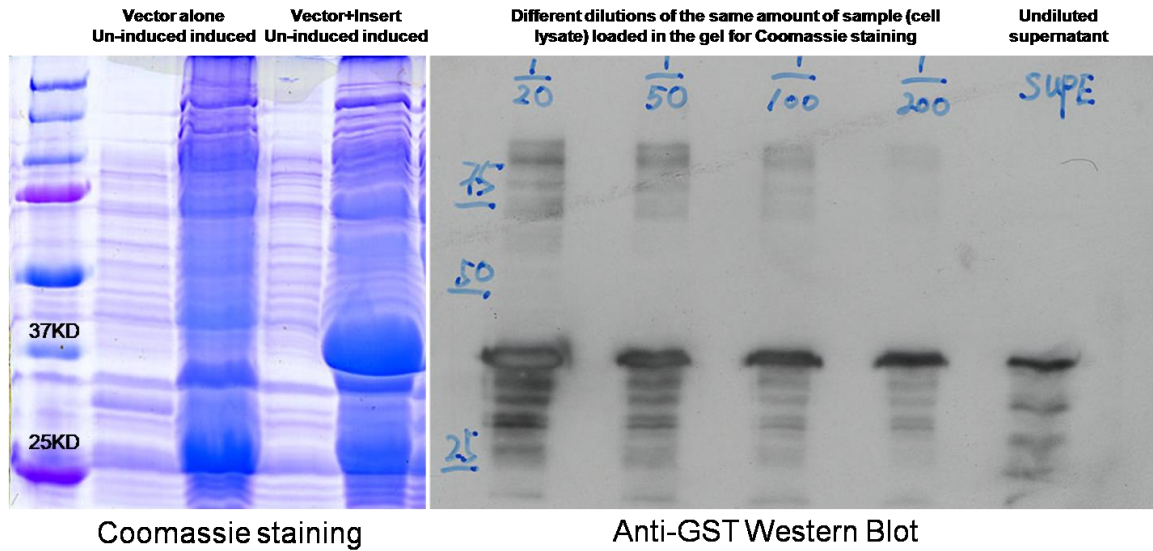


**Figure V3.** Comparative Coomassie staining and anti-GST Western blot data revealed the insolubility of the GST-tagged Bnl core domain (on the left panel) and the fact that the core domain was indeed GST- tagged and got expressed only after induction.

suspended in protein loading buffer, boiled, and loaded into a gel. A reversible protein staining kit (Pierce) was used for staining the gel after electrophoresis and the band possessing the right size was cut out and sent away for antibody production (Aves lab, Oregon).

As shown in Figure V3, proper quality control was performed to ensure that I was working with the right peptide during the purification process. In Figure V4, “before” and “after” the final cutting-out procedure, prior to sending off the cut-out peptide for antibody production, is shown on the left and right panel, respectively.

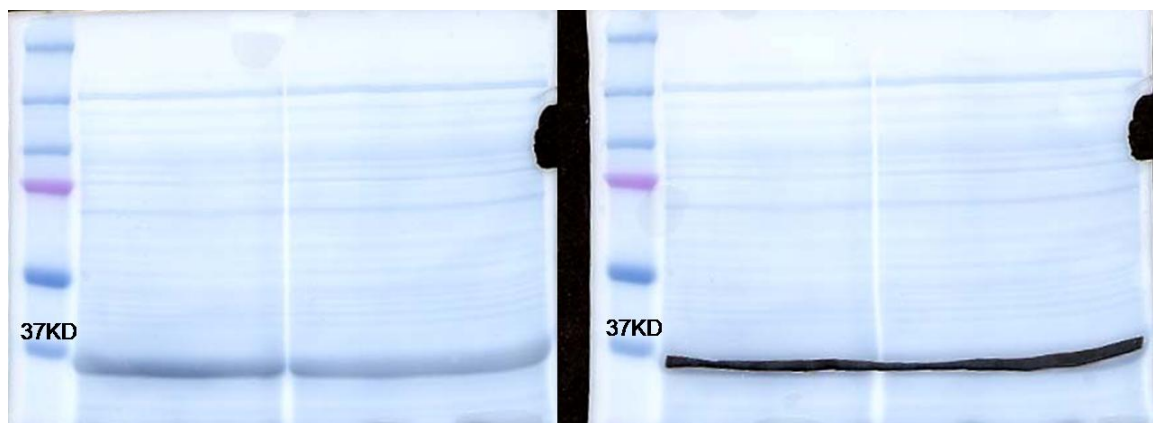


**Figure V4.** Purified F2 fragment was cut out and sent for antibody production. “Before” and “after” the final cutting-out procedure is shown on the left and right panel, respectively.

Disappointingly, when the polyclonal antibodies (produced in chicken) were tested, they failed to recognize in Western blot even the very protein fragment originally used for their production; they did not work for fly tissues, either.

## **2. Generation of Bnl-GFP for *in vivo* imaging of FGF-FGFR interaction**

After the successful cloning of four different *HA-bnl* constructs, S2 cells were transfected with all of them. HA antibody staining was then performed and the sub-cellular localization of HA-Bnl was observed. NOT in the nucleus—was what I found out. Instead, the sub-cellular localization of HA-Bnl appeared to be everywhere but in the nucleus.

My next attempt was to take advantage of the restriction sites introduced by HA tagging and inserted GFP-encoding sequence into the four different tagging locations. Originally, the ultimate goal of this GFP-tagging was to replace the wild-type *bnl* locus by a *bnl-GFP* transgene, which could be achieved by gene targeting. Ideally, all endogeneous Bnl protein molecules would then become labeled by GFP in this way and *in vivo* studies of this important signaling molecule could then be pursued. Interesting questions such as “How does Bnl disperse?”, “How do Btl-expressing cells come into contact with Bnl?”, “Is it achieved by cytonemes, maybe?”, and “How does Bnl interact with Bnl?” could then be asked.

After cloning, all four *bnl-GFP* constructs were transfected into S2 cells and their products were detected by Western blotting using anti-GFP antibodies. Unfortunately, almost all constructs displayed multiple cleavage products except BTP3 (Bnl tag position 3). So I continued further work only with BTP3. Repeated anti-GFP Western blot were performed and the absence of cleavage products was confirmed. From these experiments, I learned that Bnl was indeed secreted into the medium by transfected cells and the protein seemed not to get cleaved before secretion.

The next step was to test if BTP3 (referred to as Bnl-GFP from here on) was functional. This was achieved by incubating *btl-GFP*-transfected cells with medium containing products secreted by *bnl-GFP*-transfected cells and by performing dp-ERK antibody staining and subsequent anti-dpERK Western blotting. Data from above-mentioned studies indicated that Bnl-GFP protein produced by S2 cells could well be functional, and the ultimate test was to make transgenic flies and to examine the function of Bnl-GFP *in vivo*.

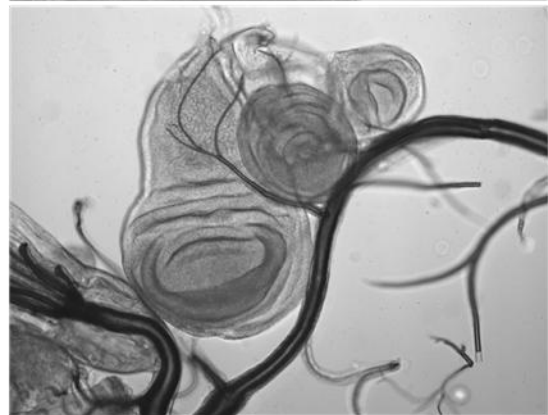
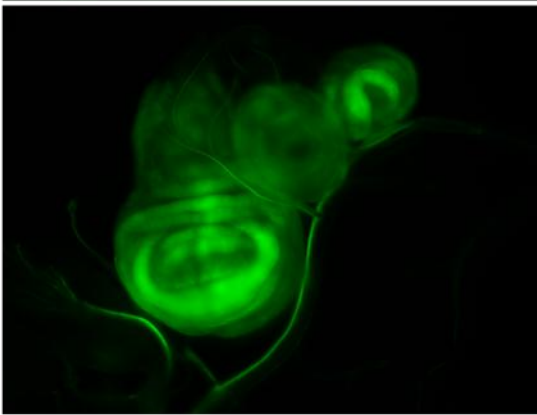
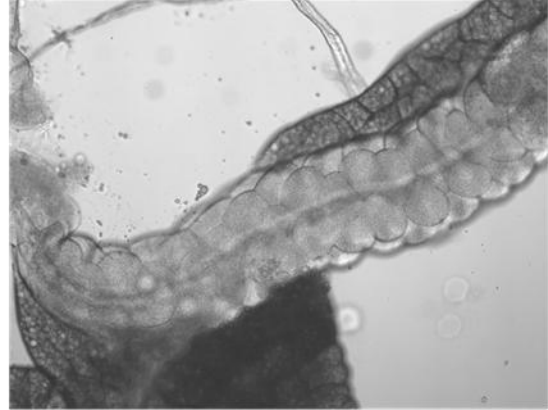
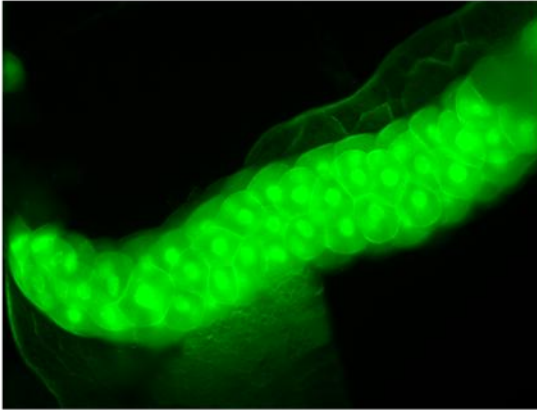
Luckily, Bnl-GFP turned out to be indeed functional *in vivo*, as could be demonstrated by the overgrowth of the tracheal tissue and ectopic tracheal outgrowth into salivary glands and wing imaginal discs (See Figure V5).

Despite its functionality, however, it turned out that Bnl-GFP fluorescence was too weak to be visible, using the microscopic settings available in the lab, even when this construct was over-expressed by Bnl-GAL4 driver (See Figure V6). This invisibility problem immediately posed a vital question: if this Bnl-GFP fusion protein could not be observed at the level of over-expression, would it be wise to pursue the gene targeting project? If the gene targeting project aiming to replace the wild type *bnl* locus by a modified *bnl-GFP* transgene should succeed, the expression level of this fusion construct under the endogenous transcriptional



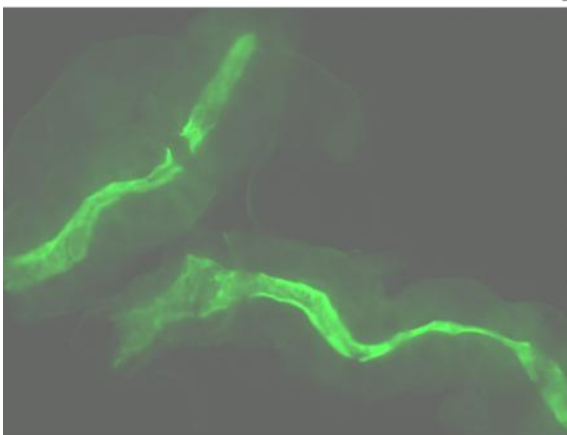
**A**

**Control: C765 X UASGFP**

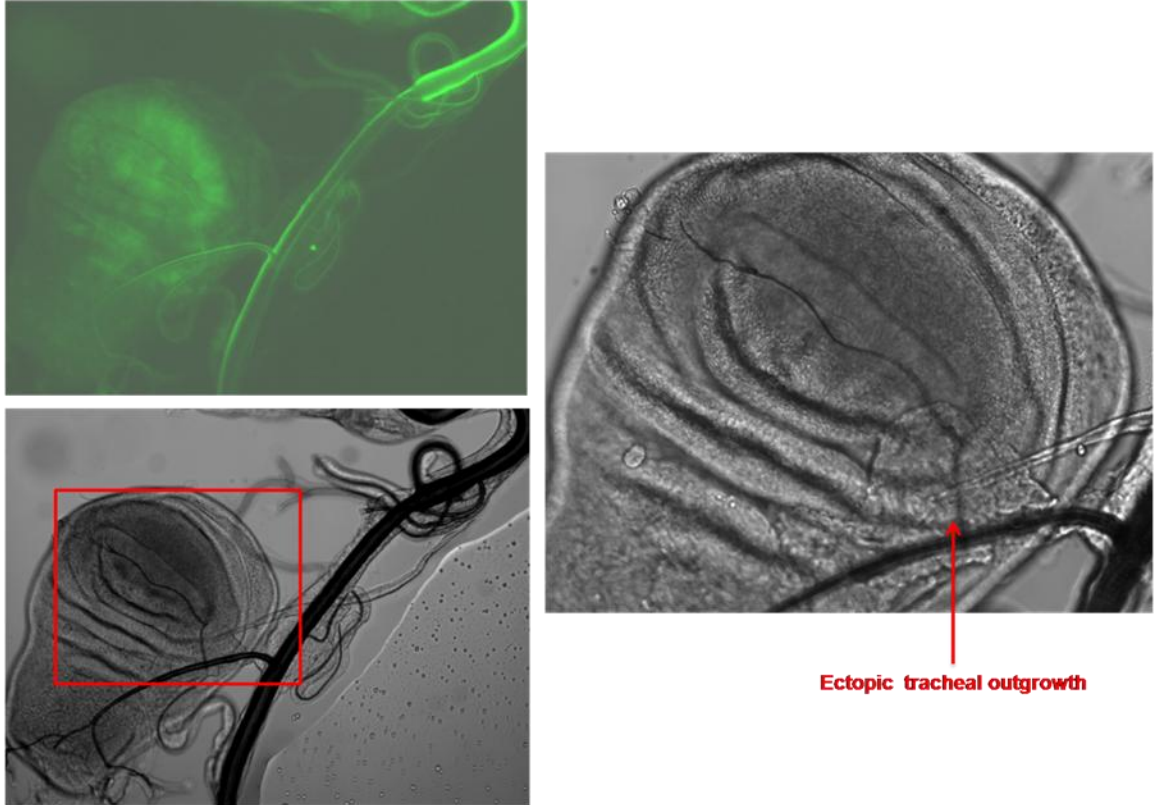


**B**

**C765 X UAS dFGF/Bnl-EGFP  
Salivary Gland**



**C** C765 X UAS FGF/Bnl-EGFP, Wing imaginal disc



**D** C765 X UAS dFGF/Bnl-EGFP, overgrowth of tracheal tissue could be observed



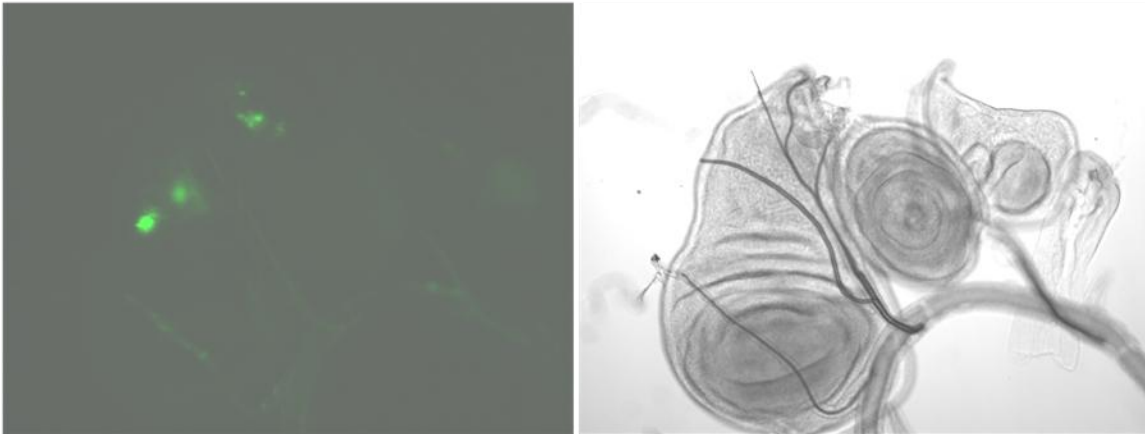
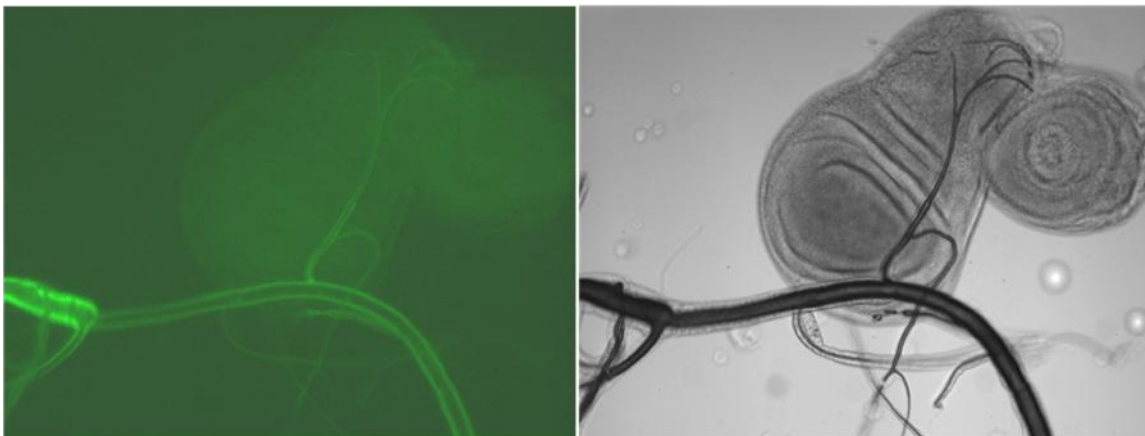
**Figure V5.** Data demonstrating that Bnl-GFP fusion protein is functional and capable of inducing tracheal tissue overgrowth and ectopic tracheal outgrowth into the salivary gland and wing imaginal disc. C765 is a GAL driver expressed in salivary glands and in wing imaginal discs. A. An control experiment showing the expression domain of the C765 driver, in salivary glands and in wing discs. B. When Bnl-GFP was expressed in salivary glands, it could be observed to be secreted into the lumen, which resulted in ectopic tracheal growth. C. and D. are showing the ectopic growth phenotype (in C) and overgrowth phenotype (in D.) when Bnl-GFP was expressed in wing discs by the C765 driver.

control, would unlikely be higher than that achieved by UAS/GAL4 over-expression system. Therefore, it would probably also be invisible *in vivo*.

In an attempt to boost the protein level of Bnl-GFP and make its fluorescence visible, I inserted an endogeneous intron into the fusion construct, since it had been reported, both in flies and mammals, that the presence of an intron could increase the expression level of a protein by 500 fold. This strategy did not seem to work for Bnl-GFP, because cells transfected with *bnl-GFP-intron* appeared even dimmer in fluorescence than those transfected with *bnl-GFP*.

Genetic manipulations such as crossing transgenes of *UAS-bnl-GFP*, *bnlGAL4* and *UAS-GAL4* into the same fly also failed to increase the fluorescence of the Bnl-GFP fusion protein.

Currently, the project of *in vivo* imaging of FGF-FGFR interaction is put on hold.

**A**Control: *bnlGal4XUASnlsGFP***B***bnlGal4XUASbnlGFP*

**Figure V6.** Invisibility of Bnl-GFP under the control of *bnl*-GAL4. A. In the control, the GFP fluorescence of a nuclear GFP (nlsGFP) driven by *bnl*-GAL4 was well visible, whereas the GFP fluorescence of Bnl-GFP driven by the same driver could not be observed (in B).

## VI. References

- Adryan, B., Decker, H.J., Papas, T.S., Hsu, T., 2000. Tracheal development and the von Hippel–Lindau tumor suppressor homolog in *Drosophila*. *Oncogene* 19, 2803–2811.
- Affolter, M., Montagne, J., Walldorf, U., Groppe, J., Kloter, U., LaRosa, M., Gehring, W.J., 1994. The *Drosophila* SRF homolog is expressed in a subset of tracheal cells and maps within a genomic region required for tracheal development. *Development* 120, 743–753.
- Affolter, M., Nellen, D., Nussbaumer, U., Basler, K., 1994. Multiple requirements for the receptor serine/threonine kinase thick veins reveal novel functions of TGF beta homologs during *Drosophila* embryogenesis. *Development* 120, 3105–3117.
- Affolter M, Shilo BZ, 2000. Genetic control of branching morphogenesis during *Drosophila* tracheal development. *Curr Opin Cell Biol.* 12, 731-735.
- Affolter, M., S. Bellusci, N. Itoh, B. Shilo, J. P. Thiery *et al.*, 2003. Tube or not tube: remodeling epithelial tissues by branching morphogenesis. *Dev. Cell* 4, 11–18.
- Affolter, M., and C. J. Weijer, 2005. Signaling to cytoskeletal dynamics during chemotaxis. *Dev. Cell* 9, 19–34.
- Affolter M, Caussinus E, 2008. Tracheal branching morphogenesis in *Drosophila*: new insights into cell behaviour and organ architecture. *Development.* 135, 2055-2064.
- Anderson, M.G., Certel, S.J., Certel, K., Lee, T., Montell, D.J., Johnson, W.A., 1996. Function of the *Drosophila* POU domain transcription factor drifter as an upstream regulator of breathless receptor tyrosine kinase expression in developing trachea. *Development* 122, 4169–4178.
- Anderson, M.G., Perkins, G.L., Chittick, P., Shrigley, R.J., Johnson, W.A., 1995. drifter, a *Drosophila* POU-domain transcription factor, is required for correct differentiation and migration of tracheal cells and midline glia. *Genes Devel.* 9, 123–137.
- Aso, T., Yamazaki, K., Aigaki, T., Kitajima, S., 2000. *Drosophila* von Hippel–Lindau tumor suppressor complex possesses E3 ubiquitin ligase activity. *Biochem. Biophys. Res. Commun.* 276, 355–361.
- Bache, K. G., C. Raiborg, A. Mehlum and H. Stenmark, 2003. STAM and Hrs are subunits of a multivalent ubiquitin-binding complex on early endosomes. *J. Biol. Chem.* 278, 12513–12521.

Beitel, G.J., Krasnow, M.A., 2000. Genetic control of epithelial tube size in the *Drosophila* tracheal system. *Development* 127, 3271–3282.

Ben-Yaacov S, Le Borgne R, Abramson I, Schweisguth F, Schejter ED, 2001. Wasp, the *Drosophila* Wiskott-Aldrich syndrome gene homologue, is required for cell fate decisions mediated by Notch signaling. *J Cell Biol.* 152, 1-13.

Blake, K.J., Myette, G., Jack, J., 1999. ribbon, raw, and zipper have distinct functions in reshaping the *Drosophila* cytoskeleton. *Devel. Genes Evol.* 209, 555–559.

Blochlinger, K., Bodmer, R., Jan, L.Y., Jan, Y.N., 1990. Patterns of expression of cut, a protein required for external sensory organ development in wild-type and cut mutant *Drosophila* embryos. *Genes Devel.* 4, 1322–1331.

Böttcher RT, Niehrs C, 2005. Fibroblast growth factor signaling during early vertebrate development. *Endocr Rev.* 26, 63-77.

Borghese, L., G. Fletcher, J. Mathieu, A. Atzberger, W. C. Eades *et al.*, 2006. Systematic analysis of the transcriptional switch inducing migration of border cells. *Dev. Cell* 10, 497–508.

Boube, M., Llimargas, M., Casanova, J., 2000. Cross-regulatory interactions among tracheal genes support a co-operative model for the induction of tracheal fates in the *Drosophila* embryo. *Mech. Devel.* 91, 271–278.

Boube, M., Martin-Bermudo, M.D., Brown, N.H., Casanova, J., 2001. Specific tracheal migration is mediated by complementary expression of cell surface proteins. *Genes Devel.* 15, 1554–1562.

Bradley, P.L., Andrew, D.J., 2001. ribbon encodes a novel BTB/POZ protein required for directed cell migration in *Drosophila melanogaster*. *Development* 128, 3001–3015.

Bray, S.J., Kafatos, F.C., 1991. Developmental function of Elf-1: an essential transcription factor during embryogenesis in *Drosophila*. *Genes Devel.* 5, 1672–1683.

Brown, S., Hu, N., Hombria, J.C., 2001. Identification of the first invertebrate interleukin JAK/STATreceptor, the *Drosophila* gene domeless. *Curr. Biol.* 11, 1700–1705.

Bruick, R.K., McKnight, S.L., 2001. A conserved family of prolyl-4-hydroxylases that modify HIF. *Science* 294, 1337–1340.

Brzeska H, Korn ED, 1996. Regulation of class I and class II myosins by heavy chain phosphorylation. *J Biol Chem.* 271, 16983-16986.

- Buechner, M., 2002. Tubes and the single *C. elegans* excretory cell. *Trends Cell Biol.* 12, 479–484.
- Cabernard C, Affolter M, 2005. Distinct roles for two receptor tyrosine kinases in epithelial branching morphogenesis in *Drosophila*. *Dev Cell.* 9, 831–42.
- Campos-Ortega, J.A., Hartenstein, V., 1985. *The Embryonic Development of Drosophila melanogaster*. Springer-Verlag, New York.
- Casci, T., Vinos, J., Freeman, M., 1999. Sprouty, an intracellular inhibitor of Ras signaling. *Cell* 96, 655–665.
- Chen, C.K., Kuhnlein, R.P., Eulenberg, K.G., Vincent, S., Affolter, M., Schuh, R., 1998. The transcription factors Knirps and Knirps Related control cell migration and branch morphogenesis during *Drosophila* tracheal development. *Development* 125, 4959–4968.
- Chen, H.W., Chen, X., Oh, S.W., Marinissen, M.J., Gutkind, J.S., Hou, S.X., 2002. mom identifies a receptor for the *Drosophila* JAK/STAT signal transduction pathway and encodes a protein distantly related to the mammalian cytokine receptor family. *Genes Devel.* 16, 388–398.
- Chiang, C., Young, K.E., Beachy, P.A., 1995. Control of *Drosophila* tracheal branching by the novel homeodomain gene unplugged, a regulatory target for genes of the bithorax complex. *Development* 121, 3901–3912.
- Chihara, T., Hayashi, S., 2000. Control of tracheal tubulogenesis by Wingless signaling. *Development* 127, 4433–4442.
- Chihara, T., Kato, K., Taniguchi, M., Ng, J., Hayashi, S., 2003. Rac promotes epithelial cell rearrangement during tracheal tubulogenesis in *Drosophila*. *Development* 130, 1419–1428.
- Cohen, E., 2001. Chitin synthesis and inhibition: a revisit. *Pest Mgt Sci.* 57, 946–950.
- Colvin JS, Green RP, Schmahl J, Capel B, Ornitz DM, 2001. Male-to-female sex reversal in mice lacking fibroblast growth factor 9. *Cell.* 104, 875–889.
- Crick FH, Lawrence PA, 1975. Compartments and polyclones in insect development. *Science.* 189, 340–347.
- de Celis, J.F., Llimargas, M., Casanova, J., 1995. ventral veinless, the gene encoding the Cfla transcription factor, links positional information and cell differentiation during embryonic and imaginal development in *Drosophila melanogaster*. *Development* 121, 3405–3416.

Dorfman, R., Glazer, L., Weihe, U., Wernet, M.F., Shilo, B.Z., 2002a. Elbow and Noc define a family of zinc finger proteins controlling morphogenesis of specific tracheal branches. *Development* 129, 3585–3596.

Dorfman, R., Shilo, B.Z., Volk, T., 2002b. Stripe provides cues synergizing with branchless to direct tracheal cell migration. *Devel. Biol.* 252, 119–126.

Dor Y, Brown J, Martinez OI, Melton DA, 2004. Adult pancreatic beta-cells are formed by self-duplication rather than stem-cell differentiation. *Nature.* 429, 41–46.

Dossenbach, C., Rock, S., Affolter, M., 2001. Specificity of FGF signaling in cell migration in *Drosophila*. *Development* 128, 4563–4572.

Englund, C., Steneberg, P., Falileeva, L., Xylourgidis, N., Samakovlis, C., 2002. Attractive and repulsive functions of Slit are mediated by different receptors in the *Drosophila* trachea. *Development* 129, 4941–4951.

Englund, C., Uv, A.E., Cantera, R., Mathies, L.D., Krasnow, M.A., Samakovlis, C., 1999. *adrift*, a novel *bnl*-induced *Drosophila* gene, required for tracheal path-finding into the CNS. *Development* 126, 1505–1514.

Eswarakumar VP, Lax I, Schlessinger J, 2005. Cellular signaling by fibroblast growth factor receptors. *Cytokine Growth Factor Rev.* 16, 139-149.

Eulenberg, K.G., Schuh, R., 1997. The tracheae defective gene encodes a bZIP protein that controls tracheal cell movement during *Drosophila* embryogenesis. *EMBO J.* 16, 7156–7165.

Forsthoefel DJ, Liebl EC, Kolodziej PA, Seeger MA, 2005. The Abelson tyrosine kinase, the Trio GEF and Enabled interact with the Netrin receptor Frazzled in *Drosophila*. *Development.* 132, 1983-94.

Franch-Marro, X., Casanova, J., 2000. The alternative migratory pathways of the *Drosophila* tracheal cells are associated with distinct subsets of mesodermal cells. *Devel. Biol.* 227, 80–90.

Franch-Marro, X., Casanova, J., 2002. *spalt*-induced specification of distinct dorsal and ventral domains is required for *Drosophila* tracheal patterning. *Devel. Biol.* 250, 374–382.

Fulga TA, Rørth P, 2002. Invasive cell migration is initiated by guided growth of long cellular extensions. *Nat Cell Biol.* 4, 715-9.

Gabay, L., Seger, R., Shilo, B.Z., 1997. MAP kinase in situ activation atlas during *Drosophila* embryogenesis. *Development* 124, 3535–3541.



Geisbrecht ER, Montell DJ, 2004. A role for *Drosophila* IAP1-mediated caspase inhibition in Rac-dependent cell migration. *Cell*. 118, 111-25.

Gerhart J., 1999. 1998 Warkany lecture: signaling pathways in development. *Teratology*. 1999, 60, 226-39.

Ghabrial A, Luschnig S, Metzstein MM, Krasnow MA, 2003. Branching morphogenesis of the *Drosophila* tracheal system. *Annu Rev Cell Dev Biol*. 19, 623-647.

Gagou, M.E., Kapsetaki, M., Turberg, A., Kafetzopoulos, D., 2002. Stage-specific expression of the chitin synthase *DmeChSA* and *DmeChSB* genes during the onset of *Drosophila* metamorphosis. *Insect Biochem. Mol. Biol.* 32, 141–146.

Glazer, L., Shilo, B.Z., 1991. The *Drosophila* FGF-R homolog is expressed in the embryonic tracheal system and appears to be required for directed tracheal cell extension. *Genes Devel.* 5, 697–705.

Glazer, L., Shilo, B.Z., 2001. Hedgehog signaling patterns the tracheal branches. *Development* 128, 1599–1606.

Guha A, Kornberg TB, 2005. Tracheal branch repopulation precedes induction of the *Drosophila* dorsal air sac primordium. *Dev Biol*. 287, 192-200.

Guha A, Lin L, Kornberg TB, 2008. Organ renewal and cell divisions by differentiated cells in *Drosophila*. *Proc Natl Acad Sci U S A*. 105, 10832-10836.

Guillemin, K., Groppe, J., Ducker, K., Treisman, R., Hafen, E., Affolter, M., Krasnow, M.A., 1996. The pruned gene encodes the *Drosophila* serum response factor and regulates cytoplasmic outgrowth during terminal branching of the tracheal system. *Development* 122, 1353–1362.

Guillemin, K., Williams, T., Krasnow, M.A., 2001. A nuclear lamin is required for cytoplasmic organization and egg polarity in *Drosophila*. *Nature Cell Biol.* 3, 848–851.

Hacohen, N., Kramer, S., Sutherland, D., Hiromi, Y., Krasnow, M.A., 1998. *sprouty* encodes a novel antagonist of FGF signaling that patterns apical branching of the *Drosophila* airways. *Cell* 92, 253–263.

Hartenstein, K., Sinha, P., Mishra, A., Schenkel, H., Torok, I., Mechler, B.M., 1997. The congested-like tracheae gene of *Drosophila melanogaster* encodes a member of the mitochondrial carrier family required for gas-filling of the tracheal system and expansion of the wings after eclosion. *Genetics* 147, 1755–1768.

Hayashi, S., Hirose, S., Metcalfe, T. and Shirras, A. D., 1993. Control of imaginal cell development by the escargot gene of *Drosophila*. *Development* 118, 105 -115.

Hayashi, S. 1996. A Cdc2 dependent checkpoint maintains diploidy in *Drosophila*. *Development* 122,1051 -1058.

Hemphala, J., Uv, A., Cantera, R., Bray, S., Samakovlis, C., 2003. Grainy head controls apical membrane growth and tube elongation in response to Branchless/FGF signaling. *Development* 130, 249–258.

Huang P, Stern MJ, 2005. FGF signaling in flies and worms: more and more relevant to vertebrate biology. *Cytokine Growth Factor Rev.* 16, 151-158.

Huff, J.L., Kingsley, K.L., Miller, J.M., Hoshizaki, D.K., 2002. *Drosophila* windpipe codes for a leucine-rich repeat protein expressed in the developing trachea. *Mech. Devel.* 111, 173–176.

Ikeya, T., Hayashi, S., 1999. Interplay of Notch and FGF signaling restricts cell fate and MAPK activation in the *Drosophila* trachea. *Development* 126, 4455–4463.

Imam, F., Sutherland, D., Huang, W., Krasnow, M.A., 1999. stumps, a *Drosophila* gene required for fibroblast growth factor (FGF)-directed migrations of tracheal and mesodermal cells. *Genetics* 152, 307–318.

Isaac, D.D., Andrew, D.J., 1996. Tubulogenesis in *Drosophila*: a requirement for the trachealess gene product. *Genes Devel.* 10, 103–117.

Itoh N, Ornitz DM, 2004. Evolution of the Fgf and Fgfr gene families. *Trends Genet.* 20, 563-569.

Jack, J., Myette, G., 1997. The genes raw and ribbon are required for proper shape of tubular epithelial tissues in *Drosophila*. *Genetics* 147, 243–253.

Jarecki, J., Johnson, E., Krasnow, M.A., 1999. Oxygen regulation of airway branching in *Drosophila* is mediated by branchless FGF. *Cell* 99, 211–220.

Jékely G, Rørth P, 2003. Hrs mediates downregulation of multiple signalling receptors in *Drosophila*. *EMBO Rep.* 4, 1163-8.

Jékely G, Sung HH, Luque CM, Rørth P, 2005. Regulators of endocytosis maintain localized receptor tyrosine kinase signaling in guided migration. *Dev Cell.* 9, 197-207.

Jiang, L., Crews, S.T., 2003. The *Drosophila* dysfusion basic helix–loop–helix (bHLH)-PAS gene controls tracheal fusion and levels of the trachealess bHLH-PAS protein. *Mol. Cell Biol.* 23, 5625–5637.

Jin, J., Anthopoulos, N., Wetsch, B., Binari, R.C., Isaac, D.D., Andrew, D.J., Woodgett, J.R., Manoukian, A.S., 2001. Regulation of *Drosophila* tracheal system development by protein kinase B. *Devel. Cell* 1, 817–827.

Jin T, Xu X, Fang J, Isik N, Yan J, Brzostowski JA, Hereld D, 2008. How human leukocytes track down and destroy pathogens: lessons learned from the model organism *Dictyostelium discoideum*. *Immunol Res.* 2008 Oct 1.

Kamimura, K., Fujise, M., Villa, F., Izumi, S., Habuchi, H., Kimata, K., Nakato, H., 2001. *Drosophila* heparin sulfate 6-O-sulfotransferase (dHS6ST) gene: structure, expression, and function in the formation of the tracheal system. *J. Biol. Chem.* 276, 17014–17021.

Kerman BE, Cheshire AM, Andrew DJ, 2006. From fate to function: the *Drosophila* trachea and salivary gland as models for tubulogenesis. *Differentiation.* 74, 326-348.

Klambt, C., Glazer, L., Shilo, B.Z., 1992. *breathless*, a *Drosophila* FGF receptor homolog, is essential for migration of tracheal and specific midline glial cells. *Genes Devel.* 6, 1668–1678.

Komada M, Kitamura N, 2005. The Hrs/STAM complex in the downregulation of receptor tyrosine kinases. *J Biochem.* 137, 1-8.

Kramer, S., Okabe, M., Hacohen, N., Krasnow, M.A., Hiromi, Y., 1999. *Sprouty*: a common antagonist of FGF and EGF signaling pathways in *Drosophila*. *Development* 126, 2515–2525.

Kuhnlein, R.P., Schuh, R., 1996. Dual function of the region-specific homeotic gene *spalt* during *Drosophila* tracheal system development. *Development* 122, 2215–2223.

Lane, M.E., Sauer, K., Wallace, K., Jan, Y.N., Lehner, C.F., Vaessin, H., 1996. *Dacapo*, a cyclin-dependent kinase inhibitor, stops cell proliferation during *Drosophila* development. *Cell* 87, 1225–1235.

Lavista-Llanos, S., Centanin, L., Irisarri, M., Russo, D.M., Gleadle, J.M., Bocca, S.N., Muzzopappa, M., Ratcliffe, P.J., Wappner, P., 2002. Control of the hypoxic response in *Drosophila melanogaster* by the basic helix–loop–helix PAS protein similar. *Mol. Cell Biol.* 22, 6842–6853.

Lawrence PA, Struhl G, Casal J, 2007. Planar cell polarity: one or two pathways? *Nat Rev Genet.* 8, 555-563.

Lee LA, Orr-Weaver TL, 2003. Regulation of cell cycles in *Drosophila* development: intrinsic and extrinsic cues. *Annu Rev Genet.* 37, 545-578.

- Lee, S., Kolodziej, P.A., 2002. The plakin Short Stop and the RhoAGTPase are required for E-cadherin-dependent apical surface remodeling during tracheal tube fusion. *Development* 129, 1509–1520.
- Lee, T., Hacohen, N., Krasnow, M., Montell, D.J., 1996. Regulated Breathless receptor tyrosine kinase activity required to pattern cell migration and branching in the *Drosophila* tracheal system. *Genes Devel.* 10, 2912–2921.
- Lee, T., and L. Luo, 1999. Mosaic analysis with a repressible cell marker for studies of gene function in neuronal morphogenesis. *Neuron.* 22, 451–46.
- Lin, X., Buff, E.M., Perrimon, N., Michelson, A.M., 1999. Heparan sulfate proteoglycans are essential for FGF receptor signaling during *Drosophila* embryonic development. *Development* 126, 3715–3723.
- Liu, L., Johnson, W.A., Welsh, M.J., 2003. *Drosophila* DEG/ENaC pickpocket genes are expressed in the tracheal system, where they may be involved in liquid clearance. *Proc. Natl Acad. Sci. USA* 100, 2128–2133.
- Liu, Q.X., Jindra, M., Ueda, H., Hiromi, Y., Hirose, S., 2003. *Drosophila* MBF1 is a co-activator for Tracheae Defective and contributes to the formation of tracheal and nervous systems. *Development* 130, 719–728.
- Li W, Li Y, Gao FB, 2005. Abelson, enabled, and p120 catenin exert distinct effects on dendritic morphogenesis in *Drosophila*. *Dev Dyn.* 234, 512–22.
- Liu, X., Kiss, I., Lengyel, J.A., 1999. Identification of genes controlling Malpighian tubule and other epithelial morphogenesis in *Drosophila melanogaster*. *Genetics* 151, 685–695.
- Llimargas, M., 1999. The Notch pathway helps to pattern the tips of the *Drosophila* tracheal branches by selecting cell fates. *Development* 126, 2355–2364.
- Llimargas, M., 2000. Wingless and its signalling pathway have common and separable functions during tracheal development. *Development* 127, 4407–4417.
- Llimargas, M., Casanova, J., 1997. ventral veinless, a POU domain transcription factor, regulates different transduction pathways required for tracheal branching in *Drosophila*. *Development* 124, 3273–3281.
- Llimargas, M., Casanova, J., 1999. EGF signaling regulates cell invagination as well as cell migration during formation of tracheal system in *Drosophila*. *Devel. Genes Evol.* 209, 174–179.

- Llimargas, M., Lawrence, P.A., 2001. Seven Wnt homologues in *Drosophila*: a case study of the developing tracheae. *Proc. Natl Acad. Sci. USA* 98, 14487–14492.
- Lloyd, T. E., R. Atkinson, M. N. Wu, Y. Zhou, G. Pennetta G, Bellen HJ, 2002. Hrs regulates endosome membrane invagination and tyrosine kinase receptor signaling in *Drosophila*. *Cell* 108, 261–269.
- Madhavan MM, Schneiderman HA, 1977. Histological analysis of the dynamics of growth of imaginal discs and histoblast nests during the larval development of *Drosophila melanogaster*. *Roux's Archiv Dev Biol.* 183, 269–305.
- Manning, G., Krasnow, M.A., 1993. Development of the *Drosophila* tracheal system. In: Bate, M., Martinez Arias, A. (Eds.), *The Development of Drosophila melanogaster*, vol. X. Cold Spring Harbor Laboratory Press, Cold Spring Harbor, NY, pp. 609–686.
- Martin M, Ahern-Djamali SM, Hoffmann FM, Saxton WM, 2005. Abl tyrosine kinase and its substrate Ena/VASP have functional interactions with kinesin-1. *Mol Biol Cell.* 16, 4225-30.
- Michelson, A.M., Gisselbrecht, S., Buff, E., Skeath, J.B., 1998. Heartbroken is a specific downstream mediator of FGF receptor signalling in *Drosophila*. *Development* 125, 4379–4389.
- Montagne, J., Groppe, J., Guillemin, K., Krasnow, M.A., Gehring, W.J., Affolter, M., 1996. The *Drosophila* serum response factor gene is required for the formation of intervein tissue of the wing and is allelic to blistered. *Development* 122, 2589–2597.
- Montell DJ, 2003. Border-cell migration: the race is on. *Nat Rev Mol Cell Biol.* 4, 13-24.
- Montell DJ, 2006. The social lives of migrating cells in *Drosophila*. *Curr Opin Genet Dev.* 16, 374-383.
- Mukouyama, Y.S., Shin, D., Britsch, S., Taniguchi, M., Anderson, D.J., 2002. Sensory nerves determine the pattern of arterial differentiation and blood vessel branching in the skin. *Cell* 109, 693–705.
- Nagao, M., Ebert, B.L., Ratcliffe, P.J., Pugh, C.W., 1996. *Drosophila melanogaster* SL2 cells contain a hypoxically inducible DNA binding complex which recognizes mammalian HIF-binding sites. *FEBS Lett.* 387, 161–166.
- Newfeld, S.J., Mehra, A., Singer, M.A., Wrana, J.L., Attisano, L., Gelbart, W.M., 1997. Mothers against dpp participates in a DDP/TGF-beta responsive serine/threonine kinase signal transduction cascade. *Development* 124, 3167–3176.

- Ninov N, Chiarelli DA, Martín-Blanco E, 2007. Extrinsic and intrinsic mechanisms directing epithelial cell sheet replacement during *Drosophila* metamorphosis. *Development*. 134(2), 367-79.
- Ohshiro, T., Emori, Y., Saigo, K., 2002. Ligand-dependent activation of breathless FGF receptor gene in *Drosophila* developing trachea. *Mech. Dev.* 114, 3–11.
- Ohshiro, T., Saigo, K., 1997. Transcriptional regulation of breathless FGF receptor gene by binding of TRACHEALESS/dARNT heterodimers to three central midline elements in *Drosophila* developing trachea. *Development* 124, 3975–3986.
- Ostrowski, S., Dierick, H.A., Bejsovec, A., 2002. Genetic control of cuticle formation during embryonic development of *Drosophila melanogaster*. *Genetics* 161, 171–182.
- Page-McCaw, A., Serano, J., Sante, J.M., Rubin, G.M., 2003. *Drosophila* matrix metalloproteinases are required for tissue remodeling, but not embryonic development. *Devel. Cell* 4, 95–106.
- Page-McCaw A, 2007. Remodeling the model organism: matrix metalloproteinase functions in invertebrates. *Semin Cell Dev Biol*. 19, 14-23.
- Paul, S.M., Ternet, M., Salvaterra, P.M., Beitel, G.J., 2003. The Na<sup>+</sup>/K<sup>+</sup> ATPase is required for septate junction function and epithelial tube-size control in the *Drosophila* tracheal system. *Development* 130, 4963–4974.
- Pellegrini, L., 2001. Role of heparan sulfate in fibroblast growth factor signalling: a structural view. *Curr. Opin. Struct. Biol.* 11, 629–634.
- Perkins, L.A., Johnson, M.R., Melnick, M.B., Perrimon, N., 1996. The nonreceptor protein tyrosine phosphatase corkscrew functions in multiple receptor tyrosine kinase pathways in *Drosophila*. *Devel. Biol.* 180, 63–81.
- Perrimon N, 1998. Creating mosaics in *Drosophila*. *Int. J. Dev. Biol.* 42, 243-247.
- Phelps CB., Brand AH, 1998. Ectopic gene expression in *Drosophila* using GAL4 system. **Methods**. 14, 367-379.
- Poss KD, Wilson LG, Keating MT, 2002. Heart regeneration in zebrafish. *Science*. 298, 2188–2190.
- Raftery, L.A., Sutherland, D.J., 1999. TGF-beta family signal transduction in *Drosophila* development: from Mad to Smads. *Devel. Biol.* 210, 251–268.
- Reich, A., Sapir, A., Shilo, B., 1999. Sprouty is a general inhibitor of receptor tyrosine kinase signaling. *Development* 126, 4139–4147.

Reichman-Fried, M., Dickson, B., Hafen, E., Shilo, B.Z., 1994. Elucidation of the role of *breathless*, a *Drosophila* FGF receptor homolog, in tracheal cell migration. *Genes Dev.* 8, 428–439.

Reichman-Fried, M., Shilo, B.Z., 1995. *breathless*, a *Drosophila* FGF receptor homolog, is required for the onset of tracheal cell migration and tracheole formation. *Mech. Dev.* 52, 265–273.

Ribeiro, C., Ebner, A., Affolter, M., 2002. In vivo imaging reveals different cellular functions for FGF and Dpp signaling in tracheal branching morphogenesis. *Devel. Cell* 2, 677–683.

Ruberte, E., Marty, T., Nellen, D., Affolter, M., Basler, K., 1995. An absolute requirement for both the type II and type I receptors, *punt* and *thick veins*, for Dpp signaling in vivo. *Cell* 80, 889–897.

Samakovlis, C., Hacohen, N., Manning, G., Sutherland, D.C., Guillemin, K., Krasnow, M.A., 1996. Development of the *Drosophila* tracheal system occurs by a series of morphologically distinct but genetically coupled branching events. *Development* 122, 1395–1407.

Samakovlis, C., Manning, G., Steneberg, P., Hacohen, N., Cantera, R., Krasnow, M.A., 1996. Genetic control of epithelial tube fusion during *Drosophila* tracheal development. *Development* 122, 3531–3536.

Sato M, Kornberg TB, 2002. FGF is an essential mitogen and chemoattractant for the air sacs of the *drosophila* tracheal system. *Dev Cell*. 3. 195-207.

Sato M, Kitada Y, Tabata T, 2008. Larval cells become imaginal cells under the control of homothorax prior to metamorphosis in the *Drosophila* tracheal system. *Dev Biol* 318, 247–257.

Schonbaum, C.P., Organ, E.L., Qu, S., Cavener, D.R., 1992. The *Drosophila melanogaster* stranded at second (*sas*) gene encodes a putative epidermal cell surface receptor required for larval development. *Devel. Biol.* 151, 431–445.

Sedaghat, Y., Miranda, W.F., Sonnenfeld, M.J., 2002. The *jing* Zn-finger transcription factor is a mediator of cellular differentiation in the *Drosophila* CNS midline and trachea. *Development* 129, 2591–2606.

Shim, K., Blake, K.J., Jack, J., Krasnow, M.A., 2001. The *Drosophila* *ribbon* gene encodes a nuclear BTB domain protein that promotes epithelial migration and morphogenesis. *Development* 128, 4923–4933.

Smith AV, Orr-Weaver TL, 1991. The regulation of the cell cycle during *Drosophila* embryogenesis: the transition to polyteny. *Development*. 112, 997-1008.

Somogyi K, Rørth P, 2004. Evidence for tension-based regulation of *Drosophila* MAL and SRF during invasive cell migration. *Dev Cell*. 7, 85-93.

Sonnenfeld, M., Ward, M., Nystrom, G., Mosher, J., Stahl, S., Crews, S., 1997. The *Drosophila* tango gene encodes a bHLH-PAS protein that is orthologous to mammalian Arnt and controls CNS midline and tracheal development. *Development* 124, 4571–4582.

Sørensen V, Nilsen T, Wiedłocha A, 2006. Functional diversity of FGF-2 isoforms by intracellular sorting. *Bioessays*. 28, 504-14.

Sprenger, F., Yakubovich, N., O'Farrell, P.H., 1997. S-phase function of *Drosophila* cyclin A and its downregulation in G1 phase. *Curr. Biol*. 7, 488–499.

Stark, K.A., Yee, G.H., Roote, C.E., Williams, E.L., Zusman, S., Hynes, R.O., 1997. A novel alpha integrin subunit associates with betaPS and functions in tissue morphogenesis and movement during *Drosophila* development. *Development* 124, 4583–4594.

Stebbing, L.A., Todman, M.G., Phillips, R., Greer, C.E., Tam, J., Phelan, P., Jacobs, K., Bacon, J.P., Davies, J.A., 2002. Gap junctions in *Drosophila*: developmental expression of the entire innexin gene family. *Mech. Devel*. 113, 197–205.

Steneberg, P., Englund, C., Kronhamn, J., Weaver, T.A., Samakovlis, C., 1998. Translational readthrough in the *hdc* mRNA generates a novel branching inhibitor in the *Drosophila* trachea. *Genes Devel*. 12, 956–967.

Steneberg, P., Hemphala, J., Samakovlis, C., 1999. Dpp and Notch specify the fusion cell fate in the dorsal branches of the *Drosophila* trachea. *Mech. Devel*. 87, 153–163.

St Johnston D, 2002. The art and design of genetic screens: *Drosophila melanogaster*. *Nat Rev Genet*. 3, 176-188.

Sutherland, D., Samakovlis, C., Krasnow, M.A., 1996. *branchless* encodes a *Drosophila* FGF homolog that controls tracheal cell migration and the pattern of branching. *Cell* 87, 1091–1101.

Tanaka-Matakatsu, M., Uemura, T., Oda, H., Takeichi, M., Hayashi, S., 1996. Cadherin-mediated cell adhesion and cell motility in *Drosophila* trachea regulated by the transcription factor Escargot. *Development* 122, 3697–3705.



Tellam, R.L., Vuocolo, T., Johnson, S.E., Jarmey, J., Pearson, R.D., 2000. Insect chitin synthase cDNA sequence, gene organization and expression. *Eur. J. Biochem.* 267, 6025–6043.

Tepass, U., Gruszynski-DeFeo, E., Haag, T.A., Omatyar, L., Torok, T., Hartenstein, V., 1996. *shotgun* encodes *Drosophila* E-cadherin and is preferentially required during cell rearrangement in the neurectoderm and other morphogenetically active epithelia. *Genes Devel.* 10, 672–685.

Tepass, U., Hartenstein, V., 1994. The development of cellular junctions in the *Drosophila* embryo. *Devel. Biol.* 161, 563–596.

Tepass, U., Theres, C., Knust, E., 1990. *crumbs* encodes an EGF-like protein expressed on apical membranes of *Drosophila* epithelial cells and required for organization of epithelia. *Cell* 61, 787–799.

Theodosiou NA, Xu T, 1998. Use of FLP/FRT system to study *Drosophila* development. *Methods.* 14, 355-365.

Treisman, R., 1994. Ternary complex factors: growth factor regulated transcriptional activators. *Curr. Opin. Genet. Devel.* 4, 96–101.

Tsruya, R., Schlesinger, A., Reich, A., Gabay, L., Sapir, A., Shilo, B.Z., 2002. Intracellular trafficking by Star regulates cleavage of the *Drosophila* EGF receptor ligand Spitz. *Genes Devel.* 16, 222–234.

Uv, A., Cantera, R., Samakovlis, C., 2003. *Drosophila* tracheal morphogenesis: intricate cellular solutions to basic plumbing problems. *Trends Cell Biol.* 13, 301–309.

Uv, A.E., Roth, P., Xylourgidis, N., Wickberg, A., Cantera, R., Samakovlis, C., 2000. *members only* encodes a *Drosophila* nucleoporin required for rel protein import and immune response activation. *Genes Devel.* 14, 1945–1957.

Van Doren, M., Mathews, W.R., Samuels, M., Moore, L.A., Broihier, H.T., Lehmann, R., 2003. *fear of intimacy* encodes a novel transmembrane protein required for gonad morphogenesis in *Drosophila*. *Development* 130, 2355–2364.

Vincent, S., Ruberte, E., Grieder, N.C., Chen, C.K., Haerry, T., Schuh, R., Affolter, M., 1997. *Dpp* controls tracheal cell migration along the dorsoventral body axis of the *Drosophila* embryo. *Development* 124, 2741–2750.

Vincent, S., Wilson, R., Coelho, C., Affolter, M., Leptin, M., 1998. The *Drosophila* protein *Dof* is specifically required for FGF signaling. *Mol. Cell* 2, 515–525.

Wappner, P., Gabay, L., Shilo, B.Z., 1997. Interactions between the EGF receptor and Dpp pathways establish distinct cell fates in the tracheal placodes. *Development* 124, 4707–4716.

Weaver M, Krasnow MA, 2008. Dual origin of tissue-specific progenitor cells in *Drosophila* tracheal remodeling. *Science*. 321, 1496-1499.

Wigglesworth, V.B., 1983. The physiology of insect tracheoles. *Adv. Insect. Physiol.* 17, 86–148.

Wilk, R., Reed, B.H., Tepass, U., Lipshitz, H.D., 2000. The hindsight gene is required for epithelial maintenance and differentiation of the tracheal system in *Drosophila*. *Devel. Biol.* 219, 183–196.

Wilk, R., Weizman, I., Shilo, B.Z., 1996. trachealess encodes a bHLH-PAS protein that is an inducer of tracheal cell fates in *Drosophila*. *Genes Devel.* 10, 93–102.

Wilkin, M.B., Becker, M.N., Mulvey, D., Phan, I., Chao, A., Cooper, K., Chung, H.J., Campbell, I.D., Baron, M., MacIntyre, R., 2000. *Drosophila* dumpy is a gigantic extracellular protein required to maintain tension at epidermal–cuticle attachment sites. *Curr. Biol.* 10, 559–567.

Wodarz, A., Hinz, U., Engelbert, M., Knust, E., 1995. Expression of crumbs confers apical character on plasma membrane domains of ectodermal epithelia of *Drosophila*. *Cell* 82, 67–76.

Wolf, C., Gerlach, N., Schuh, R., 2002. *Drosophila* tracheal system formation involves FGF-dependent cell extensions contacting bridge-cells. *EMBO Rep.* 3, 563–568.

Wolf, C., Schuh, R., 2000. Single mesodermal cells guide outgrowth of ectodermal tubular structures in *Drosophila*. *Genes Devel.* 14, 2140–2145.

Wolff, J.R., Bar, T., 1972. ‘Seamless’ endothelia in brain capillaries during development of the rat’s cerebral cortex. *Brain Res.* 41, 17–24.

Wolpert L. et al. *Principles of Development*, second edition.

Zallen JA, Cohen Y, Hudson AM, Cooley L, Wieschaus E, Schejter ED, 2002. SCAR is a primary regulator of Arp2/3-dependent morphological events in *Drosophila*. *J Cell Biol.* 156, 689-701.

Zallen JA, 2007. Planar polarity and tissue morphogenesis. *Cell.* 129, 1051-1063.

Zelzer, E., Wappner, P., Shilo, B.Z., 1997. The PAS domain confers target gene specificity of *Drosophila* bHLH/PAS proteins. *Genes Devel.* 11, 2079–2089.

# Curriculum Vitae

## Contact Information

Grosssachsener Strasse 39  
69493 Hirschberg  
Deutschland  
Email: [li.lin@unibas.ch](mailto:li.lin@unibas.ch)

## Personal Information

Name: Li Lin  
Date of Birth: October 29, 1978  
Gender: Female  
Citizenship: Chinese

## Education

2009 PH.D University of Basel, Switzerland  
Developmental Biology, Cell Biology

2004 MSC. University of Heidelberg, Germany  
Molecular and Cellular Biology

2002 EQUIVALENT OF A BACHELOR IN MEDICINE University of Heidelberg, Germany &  
Tongji Medical University, China  
General Medicine

## Working Experiences

2006 – 2008 Junior Specialist, Dr. Thomas Kornberg's lab ([tkornberg@ucsf.edu](mailto:tkornberg@ucsf.edu)), University of California, San Francisco, U.S.A.

2004 – 2006 Ph.D student, Dr. Markus Affolter's lab ([markus.affolter@unibas.ch](mailto:markus.affolter@unibas.ch)), Basel University, Switzerland

2003 – 2004 Short-term Scholar, Dr. Bingwei Lu's lab ([bingwei@stanford.edu](mailto:bingwei@stanford.edu)), Rockefeller University & Stanford University, U.S.A.

2001 – 2002 Trainee, Dr. Pernille Rorth's lab, EMBL (European Molecular Biology Laboratory), Heidelberg, Germany

1999 – 2001 Part-time nurse, St. Vincentius Hospital, Heidelberg, Germany

## Publications

\*Guha A, \*Lin L, Kornberg TB. Organ renewal and cell divisions by differentiated cells in *Drosophila*. *Proc Natl Acad Sci U S A*. 2008 Aug 5;105(31):10832-6.

\*Chanut-Delalande H, \*Jung AC, \*Lin L, Baer MM, Bilstein A, Cabernard C, Leptin M, Affolter M. A genetic mosaic analysis with a repressible cell marker screen to identify genes involved in tracheal cell migration during *Drosophila* air sac morphogenesis. *Genetics*. 2007 Aug;176(4):2177-87.

Pacquelet A, Lin L, Rorth P. Binding site for p120/delta-catenin is not required for *Drosophila* E-cadherin function in vivo. *J Cell Biol*. 2003 Feb 3;160(3):313-9.

(\* These authors contribute equally to the work.)